Universidad Politécnica de Cartagena

Department of Information and Communication Technologies

Ph.D. Thesis

Analysis and Evaluation of In-home Networks Based on HomePlug-AV Power Line Communications

Pedro José Piñero Escuer

2014

Universidad Politécnica de Cartagena

Department of Information and Communication Technologies

Ph.D. Thesis

Analysis and Evaluation of In-home Networks Based on HomePlug-AV Power Line Communications

Author

Pedro José Piñero Escuer

Supervisors

Josemaría Malgosa Sanahuja
Pilar Manzanares López

Cartagena, 2014

DT-17

CONFORMIDAD DE DEPÓSITO DE TESIS DOCTORAL POR LA COMISIÓN ACADÉMICA DEL PROGRAMA

D. Fernando Daniel Quesada Pereira, Presidente/a de la Comisión Académica del Programa de Doctorado en Tecnologías de la Información y Comunicaciones.

INFORMA:

Que la Tesis Doctoral titulada “Analysis and Evaluation of In-home Networks Based on HomePlug-AV Power Line Communications” ha sido realizada, dentro del mencionado programa de doctorado, por D. Pedro José Piñero Escuer, bajo la dirección y supervisión del Dr. Josemaría Malgosa Sanahuja y de la Dra. Pilar Manzanares López.

En reunión de la Comisión Académica de fecha 05/03/2014, visto que en la misma se acreditan los indicios de calidad correspondientes y la autorización del Director de la misma, se acordó dar la conformidad, con la finalidad de que sea autorizado su depósito por la Comisión de Doctorado.

La Rama de conocimiento por la que esta tesis ha sido desarrollada es:

□ Ciencias
□ Ciencias Sociales y Jurídicas
X Ingeniería y Arquitectura

En Cartagena, a 5 de Marzo de 2014

EL PRESIDENTE DE LA COMISIÓN ACADÉMICA DEL PROGRAMA

UNIVERSIDAD POLITÉCNICA DE CARTAGENA
COORDINACIÓN POSGRADO TIC

Fdo: Fernando Daniel Quesada Pereira

COMISIÓN DE DOCTORADO

Universidad
Politécnica
de Cartagena

DT-16

CONFORMIDAD DE SOLICITUD DEAUTORIZACIÓN DE DEPÓSITO DE TESIS DOCTORAL POR EL/LA DIRECTOR/A DE LA TESIS

D. Josemaría Malgosa Sanahuja y Dª Pilar Manzanares López, Directores de la Tesis doctoral "Analysis and Evaluation of In-home Networks Based on HomePlug-AV Power Line Communications".

INFORMA:

Que la referida Tesis Doctoral, ha sido realizada por D. Pedro José Piñero Escuer, dentro del programa de doctorado en Tecnologías de la Información y Comunicaciones, dando nuestra conformidad para que sea presentada ante la Comisión de Doctorado para ser autorizado su depósito.

La rama de conocimiento en la que esta tesis ha sido desarrollada es:

□ Ciencias
□ Ciencias Sociales y Jurídicas
X Ingeniería y Arquitectura

En Cartagena, a 5 de Marzo de 2014

EL DIRECTOR DE LA TESIS	LA DIRECTORA DE LA TESIS
Fdo.: Josemaría Malgosa Sanahuja	Fdo. Pilar Manzanares López

COMISIÓN DE DOCTORADO

A Natalia y a mis padres,
por su apoyo durante estos años

Abstract

Not very long time ago, in-home networks (also called domestic networks) were only used to share a printer between a number of computers. Nowadays, however, due to the huge amount of devices present at home with communication capabilities, this definition has become much wider. In a current in-home network we can find, from mobile phones with wireless connectivity, or NAS (*Network Attached Storage*) devices sharing multimedia content with high-definition televisions or computers.

When installing a communications network in a home, two objectives are mainly pursued: Reducing cost and high flexibility in supporting future network requirements. A network based on Power Line Communications (PLC) technology is able to fulfill these objectives, since as it uses the low voltage wiring already available at home, it is very easy to install and expand, providing a cost-effective solution for home environments. There are different PLC standards, being HomePlug-AV (HomePlug Audio-Video, or simply HPAV) the most widely used nowadays. This standard is able to achieve transmission rates up to 200 Mpbs through the electrical wiring of a typical home.

The main objective of this thesis is to provide new ideas to improve the performance of PLC technology based in-home networks, using as starting point the HPAV standard. A network based on this technology uses a centralized architecture, in which the most important part of the network intelligence is concentrated in a single device, the Central Coordinator (CCo). Hence, most of the modifications proposed in this work will try to improve this particular device, which can even become a multi-technology central manager, able to combine interfaces of different technologies to improve the network performance.

Initially, it is presented a detailed analysis of HPAV performance in some scenarios typically found in a home environment. It was done through simulation and by experimentation using real devices. To obtain the former results, it was designed a HPAV simulator which implements the physical (PHY) and medium access control (MAC) layers of the standard, together with a traffic modeling module which implements the services most commonly found in a home network. This simulation tool was used both in these initial measurements and to evaluate the standard modifications that are proposed in this work.

This analysis provides two main results. Firstly, it was found that when a real PHY model is used together with the CSMA/CA MAC protocol the simulation results were very different to those obtained with previously presented mathematical models of this protocol. Hence, it was proposed a new model that considers these effects. Next, some areas of the technology which could be improved were identified. The rest of the thesis was then centered around proposing solutions to these weaknesses.

The first weakness solved is related to unicast data transmission. PLC medium is frequency selective and time variant, and it presents a remarkable variation among locations or depending on the connected loads. Even in a single link, the channel capacities between transmitter and receiver can be very asymmetric. In such environments, the use of TCP as transport protocol presents serious problems, since it defines some of its parameters according to the Round Trip Time (RTT). Alternatively, the use of Fountain codes for reliable data transmission in these environments was proposed. These codes allow to transmit information without a feedback channel, overcoming in this way the problems related to the variability of the channel. Different experiments were performed comparing both solutions, concluding that in PLC based networks the performance achieved by Fountain codes outperforms the results obtained with a TCP-based application.

In addition, Fountain codes were also used for another application. In home environments, it is very common to find more than one available technology to deploy a network (*Wi-Fi*, *Ethernet*, PLC, etc). Therefore, an application that makes possible the aggregation of different interfaces would be very useful, as it will provide higher bandwidth, fault tolerance and load balancing. The Linux Kernel contains a driver (*Bonding*) which allows Ethernet interfaces aggregation. However, it is not prepared for asymmetric interfaces aggregation and even less for variable capacity technologies like PLC or Wi-Fi. In this work, it is presented a modification of this driver which uses Fountain codes to solve the problems that may arise when asymmetric interfaces are aggregated.

On another note, multicast communications in the actual HPAV standard versions presents serious problems. This is because, although PLC medium is broadcast by nature, the Orthogonal Frequency Division Multiplexing (OFDM) modulation used at PHY layer is always point to point.Therefore, multicast communications are carried out as successive point-to-point transmissions to the different members of the group. This technique clearly degrades the performance of multicast services as the number of receivers increases. In this work, they have been proposed two alternative algorithms. The first one consists of using a common tone map for all the multicast group members. This tone map corresponds to the modulation parameters obtained for the client with the worst channel conditions. This algorithm has been traditionally discarded in OFDM systems because of its poor performance. However, in contrast to other technologies (like wireless for example), channel responses in a given PLC network exhibit significant correlation among them. This reduces the differences among the users, improving the performance of this algorithm. In addition, another technique which uses an optimization algorithm to maximize the multicast bit rate is also evaluated, obtaining that its use can be suitable when the number of multicast clients is high.

Finally, due to the properties of PLC medium, cross-layer technique are eliciting a big interest. These algorithms are based in the information sharing between adjacent layers in the OSI model to improve the system behavior. In this work, it has been proposed an extension of the HPAV CSMA/CA algorithm which modifies the protocol parameters using PHY layer information and the QoS requirements of the upper-layer services. In this way, priority access to the channel can be provided to the nodes with QoS problems, improving the whole network performance. This algorithm has been evaluated through simulation in a typical home environment with very promising results.

Resumen

No hace mucho tiempo, las redes in-home (también denominadas redes domésticas) únicamente se utilizaban para interconectar los diferentes ordenadores de una vivienda, de manera que pudieran compartir una impresora entre ellos. Hoy en día, sin embargo, esta definición es mucho más amplia debido a la gran cantidad de dispositivos existentes en la vivienda con capacidad de conectarse a una red para transmitir y recibir información. En una red *in-home* actual, podemos encontrar desde teléfonos móviles equipados con conectividad WI-FI a dispositivos NAS (*Network Attached Storage*), utilizados para almacenar información, imágenes o videos en red, que a su vez pueden ser transferidos a televisiones de alta definición u ordenadores.

A la hora de instalar una red de comunicaciones en una vivienda, se persiguen principalmente dos objetivos, reducir el coste de instalación y conseguir una gran flexibilidad de cara a futuras ampliaciones. Una red basada en tecnología PLC (*Power Line Communications*) cumple estos requisitos ya que, al utilizar la infraestructura de cableado eléctrico existente en la vivienda, es muy sencilla y económica de instalar y ampliar. Dentro de la tecnología PLC existen diferentes estándares, siendo HomePlug-AV (HomePlug Audio-Video o símplemente HPAV) el más extendido en la actualidad para la instalación de redes domésticas. Este estándar permite alcanzar velocidades de transmisión de hasta 200 Mbps a través de los cables de baja tensión de una vivienda convencional.

El objetivo principal de esta tesis doctoral es aportar nuevas ideas que mejoren las prestaciones de las redes *in-home* basadas en la tecnología PLC, utilizando como base el estándar Homeplug-AV. Estas redes utilizan una arquitectura centralizada, en la que la mayor parte de la inteligencia de red está concentrada en un coordinador central (CCo, por sus siglas en inglés). Por lo tanto, la mayor parte de las modificaciones propuestas irán encaminadas a mejorar dicho dispositivo, que podrá llegar a convertirse en un gestor de red capaz de manejar conjuntamente interfaces de diferentes tecnologías.

En primer lugar, se presenta un análisis detallado del comportamiento del estándar en diferentes situaciones que se pueden producir de manera común en una red doméstica. Este análisis se realizó tanto con dispositivos reales como mediante simulación. Para el segundo tipo de medidas, se diseñó un simulador de la tecnología HomePlug que implementa el nivel físico y el nivel MAC de la misma, junto con modelos de los servicios más utilizados en entornos domésticos. Este simulador se utilizó tanto para estas medidas iniciales como para evaluar las diferentes modificaciones del estándar propuestas posteriormente en este trabajo.

Este análisis proporcionó dos resultados significativos. En primer lugar, se comprobó que al introducir un modelo real de nivel físico al protocolo CSMA/CA utilizado a nivel MAC se producían resultados muy diferentes a los presentados en los modelos publicados hasta ese momento. Por ello, se propuso un modelo matemático que incorporaba dichos efectos. En segundo lugar, se identificaron diferentes áreas de la tecnología que eran susceptibles de mejora. El resto de la tesis se centró entonces en la mejora de dichos punto débiles

El primero de estos puntos débiles está relacionado con las transmisión de datos *unicast*. El medio PLC es selectivo en frecuencia y muy dependiente del tiempo y de la localización de las estaciones. Incluso es posible que, en un mismo enlace, la capacidad de los enlaces ascendente y descendente sea distinta. En estos entornos, la utilización del protocolo de transporte TCP presenta serios problemas, ya que define gran parte de sus parámetros en función del *Round Trip time* (RTT) del enlace. Como alternativa se pensó en los códigos *Fountain*. Este tipo de codificación de fuente permite realizar transmisiones fiables de datos sin necesidad de utilizar un canal de retorno, evitando de esta forma los problemas derivados de las asimetrías de la red. Se realizaron varios experimentos comparando ambas soluciones, y se comprobó que las prestaciones de este tipo de codificaciones superan al protocolo TCP a la hora de transmitir ficheros de manera fiable a través de las redes PLC.

Además, los códigos *Fountain* también se utilizaron para el diseño de otra aplicación. Es muy común que en un escenario doméstico haya disponible más de una tecnología (*Wi-Fi*, *Ethernet*, PLC, etc). Tenemos por tanto que una aplicación capaz de integrar interfaces de diferentes tecnologías podría ser muy útil en estos entornos, ya que se podría conseguir un mayor ancho de banda, mayor tolerancia a errores, balanceo de carga, etc. El *kernel* de Linux dispone de un módulo denominado *Bonding* que permite agrupar diferentes interfaces *Ethernet*. Sin embargo, no está preparado para agrupar interfaces de diferentes tecnologías, y mucho menos para tecnologás de capacidad variable como es el caso de PLC o de las comunicaciones inalámbricas. Por ello, se realizó una modificación de dicho driver utilizando para ello los códigos *Fountain*, que solucionan los problemas que se pueden producir debido a las variaciones de capacidad.

Por otra parte, con la actual versión del estándar HomePlug AV, las comunicaciones *multicast* presentan unas prestaciones muy pobres. Esto es debido a que, a pesar de que el canal PLC es *broadcast*, la naturaleza de la modulación OFDM (*Ortogonal Frequency Division Multiplexing*) que se utiliza a nivel físico es punto a punto. Esto hace que las transmisiones simultáneas a un grupo de receptores se traduzcan automáticamente en sucesivas transmisiones punto a punto a los diferentes miembros del grupo. Con esta técnica, la capacidad efectiva de transmisión *multicast* disminuye de manera muy importante a medida que aumenta el número de receptores. En este trabajo se han propuesto dos técnicas alternativas. La primera consiste en la utilización de un mapa de tonos común para todos los miembros del grupo *multicast*, asignado a estas comunicaciones los parámetros de modulación del cliente con las peores condiciones de canal. Este algoritmo ha sido tradicionalmente descartado en los sistemas OFDM por sus bajas prestaciones. Sin embargo, la correlación existente entre los diferentes canales de una red PLC hace que su comportamiento sea mucho mejor. Además, se propuso un segundo algoritmo que utilizaba técnicas de optimización para maximizar la tasa de comunicación *multicast*, obteniendo

un mejor comportamiento cuando el número de clientes es elevado.

Por último, en redes de capacidad física variable, como es el caso de las redes PLC, las técnicas *cross-layer* están despertando un gran interés. Este tipo de algoritmos están basado en la compartición de información entre diferentes capas de la estructura OSI para mejorar el comportamiento del sistema. En este trabajo se ha propuesto un algoritmo que modifica los parámetros del protocolo CSMA/CA de nivel MAC utilizando información de nivel físico y los requerimientos de QoS del servicio de niveles superiores. De esta forma se consigue dar prioridad en el acceso al medio a los clientes con problemas de QoS, mejorando de esta forma del comportamiento de la red. Este algoritmo ha sido evaluado mediante simulación en un escenario doméstico típico, comprobando que ofrece unos resultados muy prometedores.

Agradecimientos

Esta tesis doctoral es el resultado de casi cinco años de trabajo. El camino hasta finalizarla ha sido largo, con muchos altibajos. Si todo ha terminado bien, ha sido sin duda por la inestimable ayuda de mucha gente, a la que me gustaría dedicar estas líneas.

La primera parte de estos agradecimientos es sin lugar a dudas para mis directores de tesis, Josemaría y Pilar. Muchas gracias por vuestro apoyo durante estos años y por vuestra confianza en mi. También quiero dar las gracias a Juan Pedro, por su colaboración en este trabajo.

De igual forma, muchas gracias a todos los compañeros, becarios y profesores, de la Universidad Politécnica de Cartagena con los que he compartido estos años y que me han hecho muy grata mi etapa allí.

También quiero dar las gracias a los miembros del grupo de trabajo en PLC de la Universidad de Málaga por sus aportaciones y por su ayuda durante mi estancia en tierras andaluzas.

En el ámbito personal, quiero dar las gracias a mi familia, porque sin su apoyo en los momentos difíciles me hubiera sido imposible acabar este trabajo.

Muchas gracias también a mis amigos, tanto a los de toda la vida como a los de mi etapa en Cartagena, a los que tengo que agradecer su apoyo y el aportarme esos momentos de desconexión que algunas veces me hacían tanta falta.

Por último, muchas gracias a Natalia por estar a mi lado todos estos años. Por compartir conmigo los momentos buenos e intentar alegrarme siempre en los malos.

Esta tesis no hubiera sido posible sin todos vosotros.

This Ph.D. Thesis has been supported by the Fundación Séneca, Agencia de Ciencia y Tecnología de la Región de Murcia, with the FPI pre-doctoral fellowship 13251/FPI/09 (from January 2009 to May 2011). It has also been supported by the MINECO/FEDER Project Grant TEC2010-21405-C02-02/TCM (CALM) and also by the framework of "Programa de Ayudas a Grupos de Excelencia de la Región de Murcia", funded by Fundación Séneca (Plan Regional de Ciencia y Tecnología 2007/2010).

Contents

List of Figures

List of Tables

Chapter 1

Introduction

Abstract- This chapter provides an overview of the basic concepts that will be covered in this thesis. First of all, home networks will be defined and the main technologies that can be used to deploy them will be detailed. After that, as this work is centered on Power Line Communications, the characteristics of most popular standards for this technology will be addressed. Finally, the objectives of this thesis and its structure are summarized.

1.1 Home networks

Nowadays, there is an increasing number of devices at home equipped with communication capabilities. From computers and mobile phones to traditional home appliances, all of them can be interconnected to share information or simply can be connected to the Internet through the home access point. For these reasons, home networks (also called in-home networks) are growing in complexity and scalability and, correspondingly, in their implementation challenges, eliciting a significant interest in both the industry and the scientific community.

According to the Consumer Electronics Association (CEA), an in-home network can be defined as follows: “A home network interconnects electronic products and systems, enabling remote access to, and control of those products and systems, as well as any other available content such as music, video or data”. This definition is quite tied to residential services but in fact, in-home networks can be easily extended to other similar scenarios like Small-Medium Enterprises (SME), for example. As can be seen, these networks can be used for a wide range of applications, which include [Zahariadis, 2003]:

- *Home Communication Services*. They will permit the Internet access sharing from multiple home PCs and Internet appliances, and the use of voice and video communication systems, like Voice Over IP (VoIP) or video-conference.

- *Home Entertainment Services*. The popularity of entertainment services, such as music and video streaming, and even online computer gaming is growing exponentially in the last years. These services will benefit from a good in-home network, causing the users to improve their quality of experience.

- *Home Automation*. In-home networks will be key for the development of smart homes. It will be possible, for example, to turn on the house heating system or to start the oven to cook the food before arriving home.
- *Home Security*. Security and anti-theft systems are also a very interesting application, since the technologies used to deploy these networks facilitate the implementation of security services. The users will be able, for example, to monitor their homes remotely or receive an automatic e-mail if something happens. Moreover, they could also install babysitting or health-care services.

By enabling all these possibilities, in-home networks are likely to play a highly important role in what is being called the Internet of Things (IoT). This new paradigm is based precisely in the interaction and cooperation of the different devices around us every day to achieve common goals [Atzori et al., 2010]. Therefore, the advances in home networking technologies will be key for the adequate development of this Future Internet.

1.2 Technologies

Several technologies can be used to deploy a home network. Traditional approaches, like wired and wireless technologies, are the most used nowadays. However, the recently introduced *no-new-wires* solutions, which use existing infrastructures at homes to lay out the network, are capturing a significant market share. In this section, the main characteristics of these technologies are described.

1.2.1 Wired solutions

The main standard in this category is Ethernet, which predominant form is Fast-Ethernet (IEEE 802.3u) or even Giga-Ethernet (802.3ab). It offers bit-rates up to 1 Gbps while guaranteeing the stability and security of the network. However, the use of this technology often requires the installation of a structured wiring infrastructure, which may be costly in most cases.

1.2.2 Wireless solutions

The most interesting technologies in this category are the 802.11x family. From 802.11b, which operates in the 2.4 GHz band and provides a maximum data rate of 11 Mbps, to the recently introduced 802.11n, that offers bit-rates up to 300Mbps by using Multiple Input Multiple Output (MIMO) and interface aggregation technologies at physical layer.

The best benefit of using wireless networks is the freedom to move around while maintaining network connectivity. However, although these solutions are the most extended nowadays, they are not free of some problems:

- *Range*. The typical range of a common 802.11 network is on the order of tens of meters. This can be enough for small houses, but may be insufficient in larger residences. To obtain additional range, repeaters or additional access points are needed.

- *Security*. Wireless networks require very tight security to avoid unauthorized access to the information. Most of these networks already use very complex secure encryption techniques, but some others still use algorithms with recognized weaknesses.

- *Reliability*. Like any radio frequency transmission, wireless networking signals are subject to a wide variety of complex propagation effects. Moreover, as the number of wireless networks increases, the frequency band is more saturated and some interference effects may appear.

1.2.3 *No-New-Wires* solutions

No-new-wires technologies are those that make use of existing wiring infrastructures in a building to lay out the network. This category includes technologies that use the telephone line, the CATV operators coaxial cable or the low voltage power grid to exchange data. Below, the most representative solutions in this category are detailed.

Power line communications

Power line communications (PLC) have become one of the most interesting alternatives for home networking. Networks based on this technology are easy to install and expand as they use the low-voltage wiring installed in the building (220 volts in Europe, 120 volts in America). Therefore, they provide a cost-effective solution for home communications.

PLC market solutions can be divided into two categories: Narrowband and Broadband [Ferreira et al., 2011]. Usually, Narrowband PLC (NB-PLC) refers to low bandwidth communication. This technology uses the frequency band below 500kHz and it provides data rates of tens of kpbs. Meanwhile, Broadband PLC (BPL) utilizes a much wider frequency band, typically between 2MHz and 30MHz, and it allows data rates of hundreds of Mbps. BPL technologies are mainly used today for home networking, as this application requires high speed data rates. On the other hand, NB-PLC technology is used in control and monitoring markets, like smart metering, street lighting, renewable energy generation, etc.

It is necessary to take into account that there are several aspects of the PLC medium that make it difficult to share resources fairly. The main problems that PLC systems face are:

- *Channel distortion*. PLC channel is frequency selective and time variant, and exhibits a remarkable variation among locations, according to the network topology, the type of wires, and connected loads. Even in a specific in-home network, different characteristics can be found depending on the selected transmission path or the status of the electrical appliances.

- *Noise*. This technology suffers from high levels of noise that come from many sources, like light dimmers, motors, power supplies, etc. Because many of these noise sources are tied to human activity, the amount of noise on the power line will vary by time of day.

- *Interference*. Electromagnetic compatibility (EMC) with existing services is also an important problem in PLC. Power lines were not designed for carrying high frequency signals like the used for home networking. They behave as more or less efficient antennas for signals around 30MHz, causing interference with other services that share the same frequency band. Therefore, very low power signals should be used at these frequencies.

Because of all these problems, the implementation of a powerline communications standard has proven to be a very difficult task. Different solutions have been released in the last years, each of them with advantages and disadvantages. The main characteristics of the most extended specifications for BPL based home networking will be described in the next section.

CATV coaxial communications

The most extended standard for home networking through the coaxial lines installed at home is the one developed by the Multimedia over Coax Alliance (MoCA) [Moc, 2014]. MoCA is an association which include important telecommunication companies like Intel, Cisco Systems or Samsung. Its first specification was released in 2006 and only few months later the first compliant device was brought onto the market.

The last version of the standard, MoCA 2.0, was released in 2010. It achieves a maximum physical bitrate of 1.4 Gbps, which means a MAC throughput of around 700 Mbps, by using RF signals with an operating frequency range from 500 to 1.650 MHz. This high capacity, together with its low latency (around 5 milliseconds under good channel conditions), make this technology a very promising alternative for home networks deployment. Moreover, in contrast to other technologies like PLC, it is free of noise and interference thanks to the coaxial cable shield.

However, this technology has two important drawbacks. Firstly, at least in the majority of European countries, the number of points of connection with the cable network in a house is very limited. Even in USA, although MoCA ensure that 90% of houses have a CATV infrastructure, recent studies show that, in fact, this percentage hardly reach the 30%. Moreover, most of CATV installations include amplification devices that are not designed for MoCA frequencies. In these cases, the devices should be replaced or avoided through different RF components like splitters and mixers.

Phone line communications

As in the previous case, the most extended standard in this area was developed by an association of companies. It is named Home Phoneline Networking Alliance (HPNA) [Hpn, 2014]. They release the first version of the HPNA standard for home networking over phoneline infrastructure in 1998.

The last version of this specification, HPNA 3.1 (also known as G.9954), was released by the International Telecommunication Union (ITU) in 2007. The main improvement of this version is the use of the coaxial infrastructure together with the phoneline in order to achieve better communication rates. Although according to the standard it offers physical data rates up to 320 Mbps, the real field tests have shown that its rate is near 100 Mbps.

This capacity fall is mainly caused by the poor state of the phoneline infrastructure. This fact, but above all the limited number of connection points, have supposed an important limitation for the expansion of this technology.

1.3 Power line communications standards

Although broadband power line communications have proven to be a very interesting alternative for home networks deployment, there is an important factor that is delaying the wider adoption of this technology: the slow development of standards. The standardization process was initially carried out by groups of companies, which created incompatible specifications that usually cannot coexist in the same area. However, by the end of 2011, the IEEE1901 universal standard for broadband over power line was released and, nowadays, many of these companies are bringing to market products compatible with this specification. The main characteristics of the most extended standard for BPL are described below.

1.3.1 HomePlug-AV

HomePlug Audio-Video (HPAV) is a specification developed by the HomePlug Powerline Alliance [Hpa, 2014], which was released in 2005. It is an evolution of the HomePlug 1.0, the first specification on the alliance which was presented in 2001.

The HPAV Physical (PHY) layer operates in the frequency range of 2 - 28 MHz and provides a 200 Mbps channel rate and a 150 Mbps information rate. It uses Orthogonal Frequency Division Multiplexing (OFDM) modulation and a powerful Turbo Convolutional Coding (TCC).

At Medium Access Control (MAC) layer, it provides two kinds of communication services: Carrier Sense Multiple Access/Collision Avoidance (CSMA/CA) and Time Division Multiple Access (TDMA). The former provides a contention-free service for applications with high Quality of Service (QoS) requirements, while the CSMA/CA service provides a connectionless, prioritized contention service for best-effort applications.

To efficiently provide both kinds of communication service, HPAV implements a flexible, centrally-managed architecture. The central manager is called Central Coordinator (CCo). The CCo establishes a beacon period and accommodates both the contention free and the contention-based periods (see Figure 1.1. Note that, for better adaptation to the channel, the CCo fits these periods inside a 50 Hz AC period). The CCo broadcasts a beacon frame at the beginning of each beacon period, which is used to communicate the scheduling within the beacon period.

HPAV is the most extended standard nowadays, with over 180 certified Homeplug products on the market at this time [Pro, 2014]. Moreover, the Homeplug Powerline Alliance has recently release an evolution of this standard, Homeplug-AV2 [Yonge, 2013], that extends the channel data rate up to 1Gbps by extending the used frequency band while being compatible with HPAV and IEEE 1901. Since this thesis is mainly focused on this standard, it will be explained in depth in the next chapter.

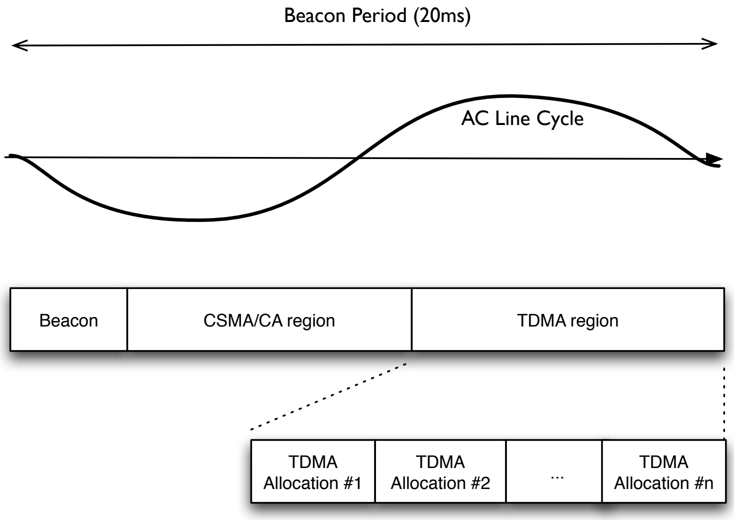

Figure 1.1: HPAV beacon period structure.

1.3.2 DS2/UPA

This standard was presented by the Universal Powerline Alliance (UPA), a company alliance founded by the Spanish company DS2, in 2005. It uses a FFT-based OFDM scheme as modulation technique in the frequency band 2-33MHz, providing a physical rate of 240Mbps, which turns into an information rate of 160Mbps. Moreover, DS2/UPA standard uses Trellis Coded Modulation (TCM) and Red-Solomon forward error correction to avoid the harsh conditions of the PLC channel.

At MAC layer, this standard uses an Advanced Dynamic Time Division Multiplexing (ADTDM) scheme, which basically consist in a centralized protocol that avoid collisions by using a token-ring approximation. An UPA device can play three roles: Head End (HE), repeater or Customer Premise Equipment (CPE). There is only one HE in the network, which controls the channel access of the other nodes through a token packet. Moreover, a repeater can be placed in the network to forward the signal if the HE cannot reach all the CPE.

However, DS2 had financial problems in 2010, and it was acquired by Marvell Technology Group in 2011. Although Marvell continued providing UPA specifications compliant devices, the UPA suspended activities in November 2010. Nowadays, the UPA market is maintained by Marvell and its partners.

1.3.3 HD-PLC

This standard has been developed by the HD-PLC Alliance [HDP, 2014], founded by Panasonic in 2007. Its physical layer is different to the previous specifications, as it uses Wavelet transform based OFDM modulation. This modulation is an evolution of FFT-based OFDM that requires less overhead. In fact, this technology is able to provide information rates up to 210 Mbps in the frequency range of 2-28 MHz. In addition, like HPAV, this standard also uses a hybrid media access protocol with a TDMA zone and a

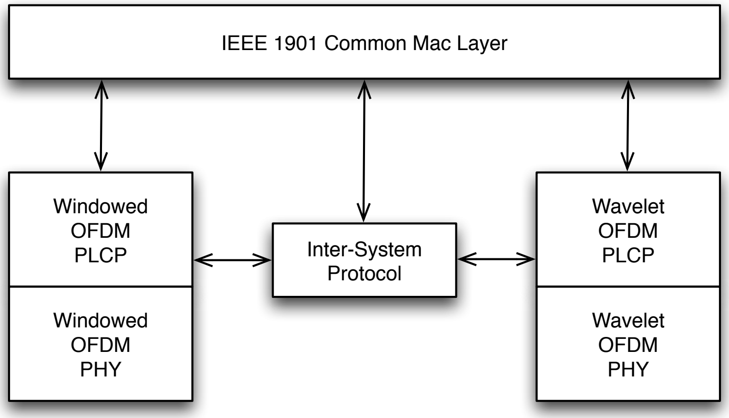

Figure 1.2: IEEE 1901 standard architecture.

CSMA/CA zone in each frame, which are regulated by a central coordination node.

1.3.4 IEEE 1901

The IEEE 1901 working group was created in 2005 with the objective of creating an universal standard for BPL, which should be compatible with previous technologies. The resulting specifications was released at the end of 2011. It uses transmission frequencies below 100 MHz, offering a physical bitrate up to 500 Mbps.

The architecture of this standard can be seen in Figure 1.2. The compatibility objective was achieved through the use of two different PHY layer technologies: Windowed OFDM and Wavelet OFDM. The former facilitates the backward compatibility with HPAV devices, while the second do the same with HD-PLC compliant devices. On top of these physical layers, a common MAC layer was defined, which handles the different PHY technologies though an intermediate layer called Physical Layer Convergence Protocol (PLCP). Finally, it was introduced an Inter-System Protocol (ISP), which allow the interaction of devices based on different PHY layer technologies by using a TDMA approximation.

From its part, the Common MAC layer uses an hybrid access control, based on TDMA and CSMA/CA, and a master/slave architecture. In this case, the master node acts as a QoS controller, regulating the access to the different frame areas depending on the requirements of each service.

At present, the companies which have developed HomePlug and HD-PLC modems are starting to bring to market IEEE1901 compatible devices. It is expected that in few years this standard becomes widely expanded.

1.4 Objectives

Once seen the main technologies to deploy in-home networks, it is time to focus on the motivations and the objectives of this research work. The main objective of this thesis is the improvement of the weak aspects of home networks based on HPAV technology. This standard uses a centralized network architecture, in which the main aspects of network intelligence are managed by the CCo. Therefore, the proposed changes mainly affect to this device, that can even become a multi-technology central manager, able to combine interfaces of different technologies to improve the communications. To this end, our first task was to perform a detailed analysis of the technology, accomplishing the following partial aims:

- *PLC Channel characterization*. The first step of this work was the characterization of the PLC channel. This study was mainly focused on the effects caused by different home appliances in the communications performance.

- *HPAV network simulator*. To better evaluate the different proposals made in this thesis, it was needed a HPAV network simulator. After the channel characterization, it was developed an accurate tool that simulate both the physical and the mac layers of this technology. This tool was the result of a collaborative effort with the PLC working group of the University of Malaga.

- *Network analysis*. The next step was the performance evaluation of HPAV technology in a domestic scenario. This evaluation includes unicast and multicast communications and it was made through simulation and real measurements. In this part, the main issues related to the use of this technology to deploy a home network were identified. The rest of the thesis was focused on implementing solutions to these problems.

As said before, different weaknesses of this technology were identified in the experiments performed to evaluate the PLC technology in a domestic scenario. In order to solve them, we have proposed some improvements for the HPAV standard which will significantly increase the whole network performance. These improvements can be divided into three different groups:

- *Fountain codes*. There are several aspects of the PLC channel that make difficult the communications, such as time-varying behavior or the broadcast nature of the channel. In this environment, Fountain codes [MacKay, 2005] can provide important advantages that worth to be studied. In addition, these codes can be used to transmit information through asymmetric interfaces. This feature is very interesting, since eventually would allow the CCo to use interfaces of different technologies together as a single logical link to improve the network performance. An important objective of this thesis has been to propose and evaluate different uses of Fountain codes in home networking.

- *Multicast communications*. Many of the services traditionally used in home networks require multicast communications, e.g. music and video streaming, online computer gaming, gaming consoles, or even video conferencing. However, OFDM based technologies do not implement real multicast data transmission due to the modulation properties. In this thesis some new ways of implementing multicast communications over these networks are presented and evaluated.

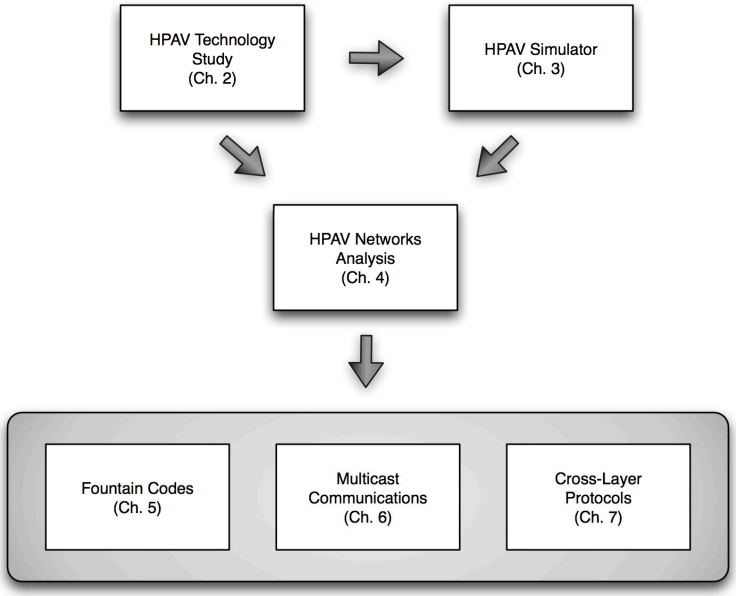
HPAV Technology Study (Ch. 2)
HPAV Simulator (Ch. 3)
HPAV Networks Analysis (Ch. 4)
Fountain Codes (Ch. 5)
Multicast Communications (Ch. 6)
Cross-Layer Protocols (Ch. 7)

Figure 1.3: Thesis structure.

- *Cross-layer*. Finally, in these environments, cross-layer techniques have recently elicited much interest in the scientific community. These techniques allow the use of information from different layers (physical layer or upper layers) at MAC layer to improve the network performance. Traditionally, these techniques have been applied to TDMA services [Papaioannou and Pavlidou, 2008]. However, in this work a cross layer optimization of the CSMA/CA algorithm has been proposed with promising results.

1.5 Structure and main contributions of this thesis

As described in the previous section, this work follows the strucutre shown in Figure 1.3. Chapter 2 presents the main characteristics of HPAV standard, carefully analyzing the different layers. This analysis is key for the later development of a simulator tool that replicate the behaviour of a home network based on this technology. This tool is addressed in chapter 3, where its different parts are explained in detail. It has been published in [Pinero et al., 2011a]:

- *A Realistic HomePlug-AV Simulator for In-Home Network Services Planning*, IEEE Global Telecommunications Conference (GLOBECOM 2011)

Then, chapter 4 provides a description of the different experiments performed to adequately characterize a HPAV based home network. In this point, some problems inherent to the architecture (OFDM at PHY layer and shared medium at MAC layer) were identified. Moreover, from the results of this chapter, it was proposed a mathematical model for HPAV CSMA/CA protocol, which was published in [Pinero et al., 2011b]:

- *Homeplug-AV CSMA/CA Evaluation in a Real In-Building Scenario*, IEEE Communications Letters, 2011

In order to solve the problems found in the previous chapter analysis, different improvements of the HPAV standard are proposed along the rest of chapters of the thesis. All of them are easy to implement and they only require small modifications of the current technology version. These changes have been divided into three different areas: Fountain codes, multicast communications and cross-layer techniques.

The use of Fountain Codes in HPAV networks is addressed in chapter 5. They are used to increase the data throughput in highly disturbed environments and to aggregate asymmetric interfaces. This chapter is mainly supported by the following publications [Muñoz et al., 2011][Piñero et al., 2011][Montoro et al., 2011]:

- *Rateless Codes for Reliable Data Transmission over HomePlug AV Based In-Home Networks*, International Conference on Software and Data Technologies (ICSOFT 2009, Revised Selected Papers published in Communications in Computer and Information Science series)

- *Rateless codes for heterogeneous in-home interfaces aggregation*, IEEE International Symposium on Power Line Communications and Its Applications (ISPLC 2011)

- *An Implementation of a Highly Accurate Timestamping System Embedded in the Linux Kernel and its Application to Capacity Estimation*, International Conference on Software and Data Technologies (ICSOFT 2011)

Multicast communications experiments are presented in chapter 6, where the multicast problem is carefully described and different solutions are compared through simulation. This work has been published in [Piñero et al., 2014][Piñero et al., 2012]:

- *Analysis and improvement of multicast communications in HomePlug-AV based in-home networks*, Computer Networks, 2014

- *Evaluation of a New Proposal for Efficient Multicast Transmission in HomePlug-AV Based In-Home Networks*, Lecture Notes of the Institute for Computer Sciences, Social Informatics and Telecommunications Engineering, 2012.

Next, the use of cross-layer techniques to improve the HPAV CSMA/CA algorithm is evaluated in chapter 7, being the obtained results published in [Pinero et al., 2014]:

- *Homeplug-AV CSMA/CA Cross-layer Extension for QoS Improvement of Multimedia Services*, IEEE Communications Letters, 2014

Finally, the main conclusions derived from the work are summarized in chapter 8, where future works are also discussed.

Chapter 2

HomePlug-AV Standard

Abstract- In this chapter, the main features of the HomePlug-AV standard for broadband power line communications are described. It is given an introduction to the different elements of the system architecture, describing the solutions adopted in each one to overcome the problems generated by the harsh conditions of PLC channel.

2.1 Introduction

HomePlug-AV [Hpa, 2007] is a standard developed by the Homeplug Powerline Alliance with the purpose of providing enough capacity to support broadband Internet access and the distribution of high-quality audio and video contents [Afkhamie et al., 2005a]. It is an evolution of its predecessor, HomePlug 1.0, which was released by the alliance in 2003.

The system architecture is shown in Figure 2.1. As can be seen, the system is divided into two clearly differentiated parts: Data Plane and Control Plane. The former is related to data management and it provides the traditional layered approach, with a PHY layer, a MAC layer and a Convergence Layer (CL). On the other hand, the specification has chosen to define the control plane as a monolithic entity, called Connection Manager (CM), since its primary function is the management of the different connections from higher layer applications. Although in the figure appears a Central Coordinator module, this entity only will be active in one -and only one- station in a single HPAV network.

2.2 Data plane

2.2.1 PHY layer

The PHY layer operates in the frequency range of 2-28 MHz. It uses OFDM modulation, which is based on simultaneous transmission of a large number of orthogonal carriers with a very narrow bandwidth. Specifically, 1.155 carriers from 1.8Mhz to 30Mhz are used in HPAV, so the separation between carriers is approximately 24.4KHz. However, some of these carriers coincide with radio amateur emission bands and cannot be used, which brings the total of usable carriers down to 917. Figure 2.2 shows the attenuation

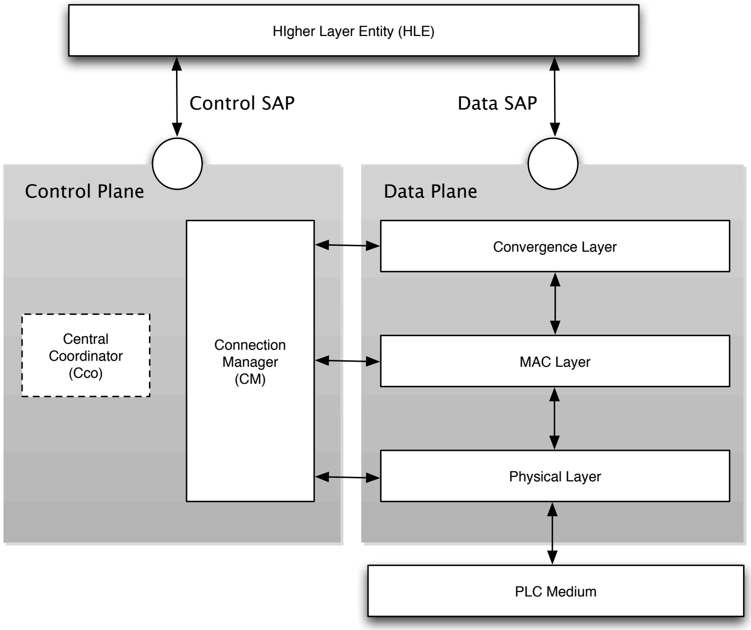

Figure 2.1: HomePlug-AV system architecture

mask that has to be used on HPAV transmissions to eliminate unavailable frequencies in the 1.8-30 Mhz range. As the figure also shows, the transmission power of the usable carriers is limited to -50dBm/Hz. The main advantages provided by this modulation technique are:

- Robustness against noise and narrow band interferences, since these perturbations only affect to a portion of carriers.

- The information is transmitted using a high number of orthogonal carriers. Therefore, OFDM system are able to use longer symbol periods. This modulation technique is very efficient dealing with multipath fading channels and with impulsive noise, as they will only affect to a part of the symbol.

- Each carrier can be independently modulated, depending on the channel conditions. This modulation may be anything from simple BPSK (1 bit of information per carrier) when the Signal-To-Noise Ratio (SNR) at the carrier frequency is low, to 1024 QAM (10 bits of information per carrier) when the SNR is very high. In this way, a better adaptation to the channel response is achieved. The CM is in charge of periodically checking the channel in order to choose the more adequate modulation scheme for each of the 917 carriers.

Each modem connected to the network has a Tone Map (TM) to communicate with the others, which indicates the type of modulation that each carrier must use. It is important to remark that, due to the properties of the PLC channel, the frequency response for each transmitting-receiving pair will be different, and as a consequence, the TM will

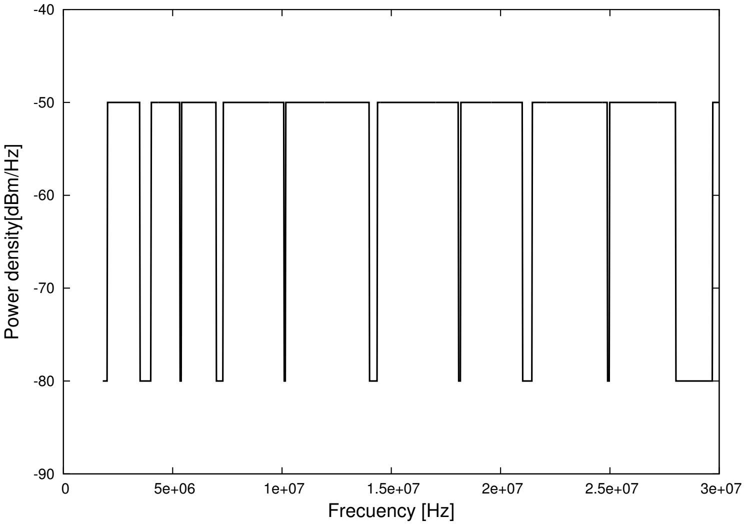

Figure 2.2: HomePlug-AV transmission mask

be different too. Therefore, although the PLC channel is broadcast, OFDM communications are always point-to-point and each transmitting-receiving pair will have a different transmission rate.

To improve the system performance, OFDM modulation is used together with a Forward Error Correction (FEC) code. In this case, Turbo Convolutional Coding technique [Berrou and Glavieux, 1996] is used. This codification is widely known as it provides additional resilience to noisy environments, with a performance close to theoretical channel throughput limits and manageable complexity. The coding rate used by HPAV is 16/21 (although a 1/2 rate coding can be used under certain conditions described below), which limits the maximum information rate provided by the standard to approximately 150 Mbps.

An scheme of the HPAV transceiver can be seen in Figure 2.3. On the transmitter side, the inputs from the MAC layer follow a processing chain depending on their type. HPAV control packets are processed by a FEC encoder block and a diversity copier, which replicates the frame in order to increase robustness. On the other hand, HPAV data packets pass through a scrambler, a FEC encoder and an interleaver. HomePlug 1.0 frames use a different transmission chain, since they use a different type of FEC encoder and interleaver. The outputs of these blocks are passed to the modulation block, which consists of a mapper, an IFFT processor (which is the OFDM modulator) and a cyclic prefix insertion, and finally they are transmitted to the PLC medium through the Analog Front End (AFE). Meanwhile, in the receiver side, these steps are performed in reverse order to recover the information. The only differences are the Automatic Gain Control (AGC) and a time synchronization element to allow the correct reception of the transmitted frames.

Attending to the segmentation procedure, the MAC layer sends to the PHY layer a MAC Protocol Data Unit (MPDU), which consists of a header and one or more Physical Block (PB)s. The size of these PBs is 520 or 136 bytes long depending on if they are used to transmit data or control information respectively, and they are independently encrypted and included in a FEC block. A PHY Protocol Data Unit (PPDU) consists of a frame

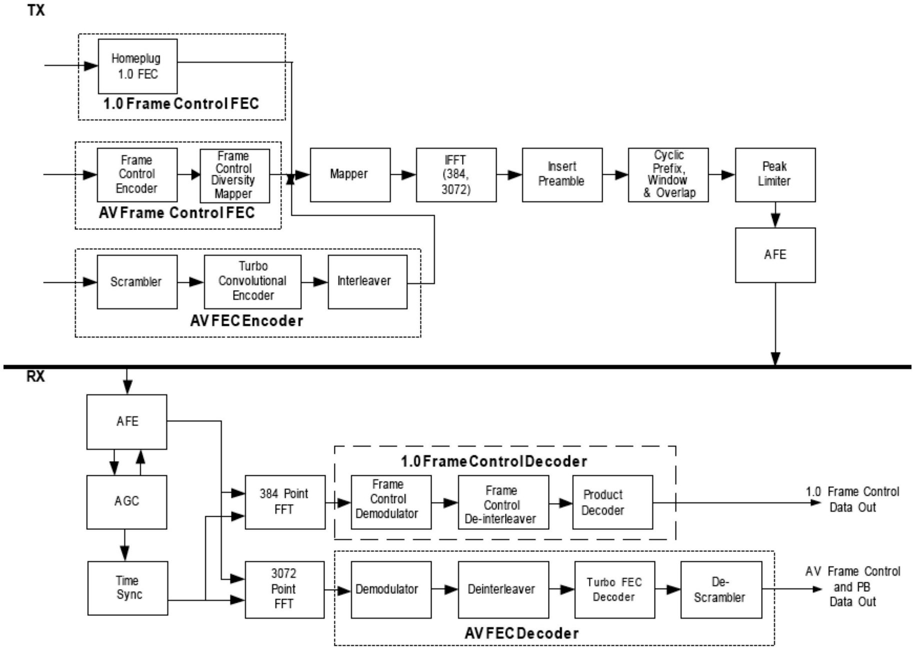

Figure 2.3: HomePlug-AV transceiver

Table 2.1: ROBO Modes

Mode Name	PB size (bytes)	Redundancy (N_{copies})	PHY rate (Mbps)
MINI_ROBO_AV	136	5	3.77
STD_ROBO_AV	520	4	4.92
HS_ROBO_AV	520	2	9.84

delimiter and a certain number of FEC blocks depending on the modulation.

Finally, HPAV standard also includes three robust modulation schemes, called Robust Modulation (ROBO), that are understood by all nodes. They are used for control frames, and for multicast and broadcast communications. These ROBO modes use QPSK modulation along with a Turbo Convolutional Codes with rate 1/2. Moreover, they achieve an additional robustness by replicating each FEC block. The characteristics of each ROBO mode are shown in Table 2.1.

STD_ROBO_AV is the mode normally used in HPAV networks. However, a node can choose to use the HS_ROBO_AV mode if it determines that the channel conditions are good enough to transmit with a lower number of repetitions. This can be done, for example, for multicast transmissions with very good channel conditions between the transmitter and the receivers. Finally, the MINI_ROBO_AV mode is used when a high robustness is needed. For example, Beacon frames are transmitted using this mode.

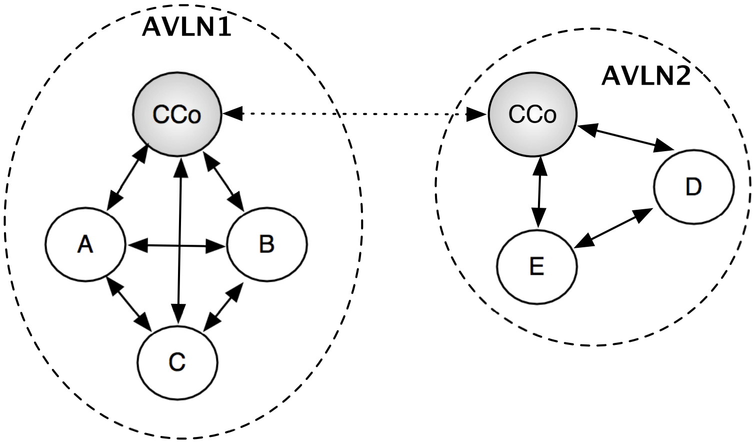

Figure 2.4: HomePlug-AV network structure. No communication between AVLN1 (A,B,C) and AVLN2 (D,E) nodes, but CCos work in coordinated mode to avoid interference.

2.2.2 MAC layer

A HPAV network consists of a set of stations connected to the power line network that is identified by the same Network Identifier (NID). The network is logically isolated by an encryption mechanism based in 128-bit AES by using a Network Encryption Key (NEK). These networks are called In-home AV Logical Network (AVLN).

Each AVLN is managed by a CCo, which periodically transmit a beacon frame at the start of each beacon period. With this frame, the CCo inform the other nodes about the beacon period structure, which include the two kinds of communication services provided by HPAV:

- Connection-oriented contention free service, based on periodic TDMA allocations of adequate duration, to support the QoS requirements of demanding applications.
- Connectionless, prioritized contention service, based on CSMA/CA, to support both best-effort applications and applications that rely on prioritized QoS.

In addition, the CCo can communicate with other CCos of neighbour AVLN (see Figure 2.4). In this way, an AVLN can work in two modes: Uncoordinated and Coordinated mode. In the former case, the network CCo generates its own timing and transmits its own beacon independently of other networks. In the second, the interfering networks shall share the bandwidth. In this situation, the QoS is guaranteed by using reserved TDMA regions, while the CSMA/CA area is shared by all nodes in both networks.

The CSMA/CA protocol used in HPAV employs priority resolution and random backoff mechanisms in order to resolve collisions efficiently and to provide QoS. Each transmission is preceded by two Priority Resolution Slot (PRS) called PRS0 and PRS1. There are also two gaps, one after a successful transmission and another before the reception of the response, called Contention InterFrame Space (CIFS) and Response InterFrame Space (RIFS) respectively. The complete timing sequence for the transmission of frames on the medium is shown in Figure 2.5.

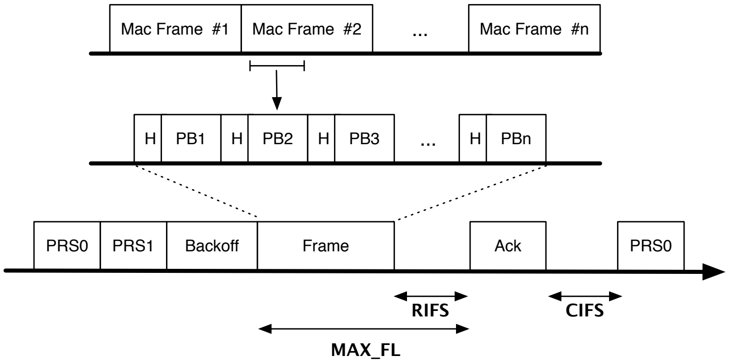

Figure 2.5: Timing sequence for the transmission of MAC frames

The protocol defines four priority levels, from CA3 (the highest) to CA0 (the lowest). Stations having frames for transmission are required to send a control packet in the priority resolution slots depending on their priority level. Stations with CA0 priority do not send any signal in PRS0 or PRS1. Those with CA1 priority send a signal only in PRS1. Stations with CA2 priority send a signal only in PRS0, and just stations with CA3 priority send signals in both PRS0 and PRS1 slots. The control packets sent in the priority resolution slots can be sensed by the stations. Depending on the state of the medium, the low priority stations will defer their transmission.

Regarding the backoff algorithm, it is an extension of the traditional IEEE 802.11 implementation. It uses two counters called Backoff Procedure Counter (BPC) and Backoff Counter (BC), which are equivalent to IEEE 802.11 Backoff Stage Counter (BSC) and Backoff Time Counter (BTC), that represent the number of retransmissions and the random backoff time respectively. In addition, HPAV adds a third counter, Deferral Counter (DC), which is used to roughly estimate the number of contending stations. The algorithm uses a variable contention window size, depending on the values of BPC and DC (see Table 2.2). In this way, the backoff is adapted to the network status.

When a node is ready to send a frame, it initializes the BPC counter to zero and the BC counter to a number between 0 and W-1, where W is the window size. The BC value is decremented by one every time slot, and when it becomes zero, the station transmits. If a collision is detected, the BPC counter is increased and both the BC and DC are updated to the new corresponding value (see Table 2.2). On the other hand, the DC counter is decremented each time a busy slot is detected and, if it reaches zero, the station infers that there is a high probability of collision and delays the frame transmission by reinitializing again the backoff procedure.

On the other hand, the TDMA service allocates stations with high QoS requirements in the contention free zone of the beacon period. These allocations can be either on a per-beacon basis (i.e. once per beacon period) or multiple times within each beacon period. Contention free sessions are assigned during the admission control procedure, which is controlled by the CCo. However, the TDMA service is an optional feature that is not available in most commercial modems. In this case, HPAV modems act in *CSMA/CA Only Mode*.

As said before, in both services the information is fragmented into MPDU, which

Table 2.2: HPAV CSMA parameters as functions of Priority

	Priorities CA3,CA2		Priorities CA1,CA0	
BPC=0	DC=0	W=7	DC=0	W=7
BPC=1	DC=1	W=15	DC=1	W=15
BPC=2	DC=3	W=15	DC=3	W=31
BPC>2	DC=15	W=31	DC=15	W=63

are composed of a header and one or more PBs. In all cases, the receiver selectively acknowledges the PBs. Those that are not positively acknowledged are retransmitted during the next channel access of the station. A MAC frame is not considered as received until all of its PBs have been received correctly.

2.2.3 Convergence layer

The CL acts as a interface between the applications in the Higher Layer Entity (HLE) and the HPAV stack. It receives data frames from the Data Service Access Point (SAP), applies the required format changes, and redirects them to the appropriate destination in the MAC layer. In addition, it performs the functions described below:

- *Classification*. The CL take incoming frames from the application and determines the connection which they are associated to. This step is done by using a rules set generated when the connection is created.

- *QoS Monitoring*. The CL gathers statistics about each application performance and passes them to the CM. In this way, the CM is able to verify if the system satisfy the QoS requirements required by service level.

- *Auto-Connect Service*. This optional service provides support for applications that start transmission without specifying QoS parameters. In this case, the connection is automatically established with specific QoS parameters based on the recognition of the data stream characteristics.

- *Smoothing*. The last optional feature in the CL is a point-to-point smoothing of the data stream. This service consist in a delay compensation and jitter control of the data packets before sending them to the corresponding application. In this way, a better user experience is achieved.

2.3 Control plane

2.3.1 Connection Manager

The main part of the control plane is the Connection Manager, which main function is the management of the different connections from the HLE. When an application opens a connection, it provides a Connection Specification (CSPEC), that details its QoS requirements. The CM is responsible for evaluating that CSPEC and setting up the appropriate connection in conjunction with the CM in the station at the other end of the connection and with the CCo. It is Connection Manager's responsibility to ensure that the appropriate mechanisms are used in order to provide to the application the required QoS parameters.

Another important task performed by the CM is the estimation and maintenance of the Tone Map. To this end, the CM invokes a procedure that is divided into two phases: Initial channel estimation and Dynamic channel estimation.

The initial channel estimation is invoked by the transmitter when there is data to transmit and it does not have any valid tone map. During this procedure the transmitter sends one or more frames to the receiver, who uses them to estimate the channel characteristics and designate a default tone map. This tone map may be used by the transmitter anywhere in the AC line cycle. Then, the receiver sends this tone map back to the transmitter. Once the transmitter have a valid tone map, it starts the transmission of data frames to the receiver. Using these data frames, the receiver is able to obtain updates to the default tone map or to generate new tone maps. These new tone maps are usually only valid at specific intervals of the AC line cycle. This procedure is called Dynamic Channel Estimation.

2.3.2 Central Coordinator

When a HPAV station is powered on, it performs a Power-on Discovery procedure. If it hears an existing AVLN, it attempts to join it. If it does not hear an existing AVLN, it will form its own network by becoming the CCo and broadcasting a beacon with a specific NID. In this case, the station activates the CCo module in its control plane.

After that, the CCo attempts to learn the topology of its AVLN and of any neighboring AVLNs. To achieve this, it starts a Discover Beacon procedure, which consist in periodically sending a frame with information about the station itself and the AVLN to which it belongs. Each station that hears these frames adds the contained information to the Discovered Stations List (DSL). However, if the information is related to a different AVLN, the station adds the information about the other network to the Discovered Networks List (DNL). The CCo periodically asks each station about its DSL and DNL and uses the information to create a topology map. If during this procedure a station that would be a better CCo is discovered, the handover of CCo functions to that station is negotiated.

Besides transmitting the beacon frame, the CCo also performs bandwidth management functions. It receives connection requests from the stations, which are scheduled depending on the QoS parameters and the network status. Moreover, when a connection cannot be allocated because of bandwidth limitations, the CCo rejects it to avoid compromising the QoS of existing connections.

Finally, the last subject controlled by the CCo is the network security. It controls the access to the AVLN and ensures the privacy of the data exchanged between the stations. The security is provided by means of a single encryption algorithm (128-bit AES) and a single hash function (SHA-256).

2.4 MediaXtreme Extension

In order to achieve better performance, an extension of the HPAV standard has been proposed by BroadCom corporation [bro, 2014]. It consist in two technologies called MediaXtreme and Xtendnet. The former is used to achieve up to 882 Mbps PHY rate and with the second the nodes can act as repeaters, increasing the network coverage and the throughput between distant devices.

MediaXtream technology basically consists in extending the operation band of HPAV up to 300MHz. However, because of EMC regulations, very low power levels should be used, causing the MediaXtreme band to rapidly vanish in long distances. Modems implementing this technology are completely interoperable with traditional HPAV devices, since this new band is only used if both, transmitter and receiver modems, have this capability.

To deal with the coverage problem, it is proposed an intelligent routing technology, known as Xtendnet. This technology monitors the QoS and the link rates to determine the best options for information delivery, and to try to ensure that each node is reachable. For each node in a network, Xtendnet can decide if it acts as a normal node or as a repeating node or as both. If a node is configured as a repeating node, it will regenerate and reamplify received signals for improved signal coverage.

Chapter 3

HomePlug-AV Networks Simulator

Abstract- In this chapter, a network simulator for power line communications based in Homeplug-AV technology is presented. The simulator implements both the PHY and the MAC layers, along with a traffic generator which emulates the behavior of most frequently used services in home networks. Therefore, this simulator is a very powerful tool for the analysis of HPAV home networks and the evaluation of the improvements of the standard proposed in this thesis.

3.1 Overview

The particular characteristics of the PLC channel make very difficult the development of a PLC network simulator. In fact, nowadays, there are no simulators that implement both the physical and the MAC layers of the HPAV standard. Because of that, the evaluation of HPAV protocols in the literature is usually performed by the simplification of the physical layer [Yoon et al., 2008][Kim et al., 2008].

The development of an accurate HPAV simulator was a key aspect to reach the different objectives of this thesis. Firstly, it was needed a tool to analyze the performance of an HPAV in-home network in order to obtain the main limitations of the technology. Then, it was also used to implement the proposed enhancements of the standard and to assess how much improved its performance.

In this chapter, it is presented a PLC network simulator based in the HPAV technology, which is the result of a collaboration with the PLC research group of the University of Málaga [PLC, 2014]. The simulator implements both, the PHY and the MAC layer, and also a traffic generator which includes the services most used in home networks. It uses the channel model proposed in [Canete et al., 2011] and the OFDM system described in [Afkhamie et al., 2005b][Latchman et al., 2005]. The MAC layer implementation is based in the CSMA/CA protocol detailed in [Chung et al., 2006]. Although, according to the standard, HPAV also provides a TDMA service, it is not available in most commercial modems. Therefore, in this first version of the simulator, only CSMA/CA contention service is implemented. However, as detailed below, the modular design of the simulator facilitates the later addition of the TDMA service.

The structure of the simulator is shown in Figure 3.1. As seen, the simulator consists

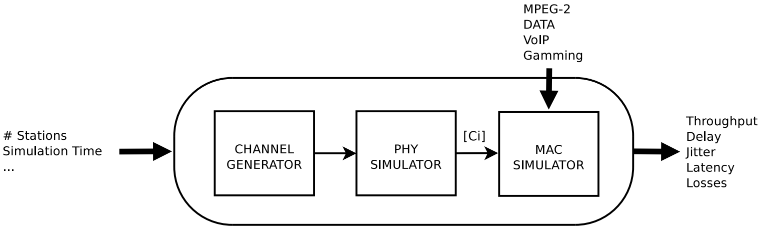

Figure 3.1: Simulator structure

of three different blocks. The first block generates the noise and the channel response associated to each station of the network. Then, the PHY layer simulator computes the bit rate, C_i, for each generated channel. Using these values, the MAC layer block simulates the Homeplug AV CSMA/CA protocol with the indicated configuration.

Input parameters

To configure a simulation, the user should indicate the following configuration parameters:

- *Stations list*. It should be indicated, through an XML file, the number of stations in the simulation and their upper-layer traffic pattern. The available traffic patterns will be described below in this chapter.

- *Number of simulations*. In order to obtain statistically representative results, the simulator allows the user to perform a number of simulations with different seeds. The results of each one is saved in a different file and they can be combined to obtain statistical estimators through simple scripts.

- *Transition times*. As it will be explained later, two versions of the channel generator are provided. The first one allows the user to generate long-term changes in the physical capacity to simulate the connection/disconnection of a home appliance in the PLC network. This configuration parameter is associated to these long-time variations.

- *Simulation time*. The total simulation time in seconds.

Output parameters

As a result, the simulator provides, for each station, the following results:

- *Throughput*. Amount of useful data successfully received by the destination station in a given time period.

- *MAC delay*. Time spent by the CSMA/CA protocol to successfully transmit a frame.

- *Jitter*. Variability over time of the MAC delay. It has been computed according to the definition given in RFC 3550 [Schulzrinne et al., 2003]:

$$J(i) = J(i-1) + \frac{1}{16}\left(|D(i) - D(i-1)| - J(i-1)\right). \tag{3.1}$$

- *Latency*. Time spent by a frame to cross the whole system, from its arrival to the transmitter station buffer to its fully reception at the destination.
- *Frame Errors*. Frame losses caused by a transmitter station buffer overflow (buffer size is limited to 1 MB).

Simulation modes

To complete the different objectives of this thesis, the simulator has been coded to offer three different working modes:

- *Normal*. In the normal mode, the output parameters are calculated in a per-second scale. The results provided in each case are averaged within that second.
- *Instantaneous values*. In this case, the instantaneous latency, delay and jitter for each transmitted frame are saved. This mode is off by default due to the huge size of the output files.
- *Multicast p-to-p*. When this mode is on, the first station acts as a multicast server, sending data to the other stations. The data is sent as described in the HPAV standard, i.e. data is sent to each client sequentially using point to point transmissions. This mode can be used together with any of the previously presented ones.

3.2 Channel Generator

The channel response generator is based on the simplified bottom-up model proposed in [Canete et al., 2011]. It considers the indoor power grid as a set of multiple transmission lines interconnected and ended in different impedance values. The link between each pair of stations is represented by a simplified structure consisting of a main path from which three stubs are deployed, as shown in Figure 3.2. Similarly, a reduced set of impedance values is considered. This simplified topology is not intended to model the whole layout of the indoor grid, but only the equivalent network seen from the transmitter to the receiver. This model, although simple, is very realistic.

Two versions of this channel generator has been implemented within this thesis. The former, which was presented in [Pinero et al., 2011a], was able to generate long-term variations in the generated channels. It is achieved by changing the impedance function connected to a randomly selected socket at the instants indicated in the simulation configuration. Moreover, each time a long-term variation in the impedance is generated, the noise can be changed too. In this way, a connection/disconnection of a home appliance in the network can be simulated. Figure 3.3 represents a channel response with five long-term

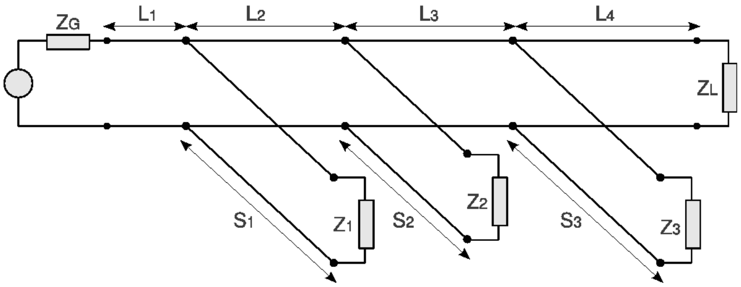

Figure 3.2: Simplified network topology used by the channel generator

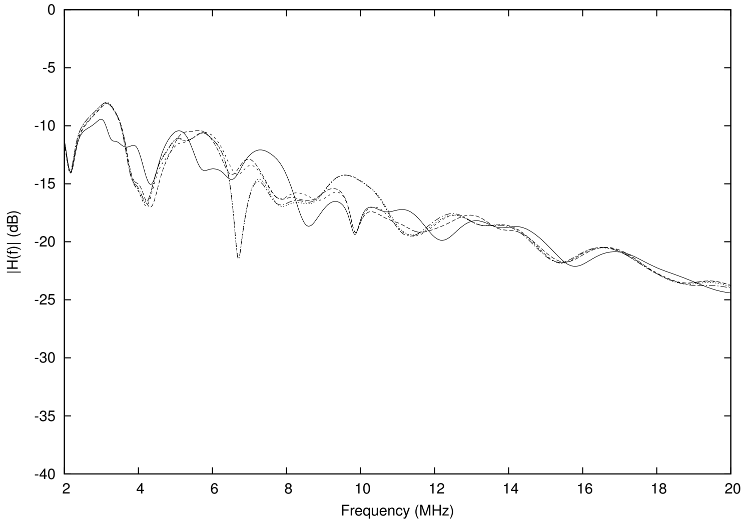

Figure 3.3: PLC Channel response long-term variations

variations generated with the simulator. As can be seen, the impedance changes do not significantly affect to the attenuation Therefore, the noise is the main limiting factor of the PHY layer capacity.

The second channel generator allows to model the correlation among the channels established in a given in-home power grid. This is done using the following procedure: The first time the channel response generator is called, it works as in the previous case, i.e., the main path and the length and ending load of the three stubs are randomly selected. Then, in successive calls, channels are generated by randomly changing the length and the impedance value of only one of the three stubs. The changed stub is also randomly selected. Thus, the length of the main path is common for all the channels of an in-home network.

The correlation among channels generated with this procedure has proven to be similar to the one exhibited by actual channels measured in 22 indoor networks [Cortes et al., 2014]. As an example, Figure 3.4 (a) depicts the real response of four channels measured in an apartment, Figure 3.4 (b) shows four channels obtained with a generator that does not take into account the correlation among the channels established in a given in-home network, and Figure 3.4 (c) shows four channels obtained with the correlated generator. As

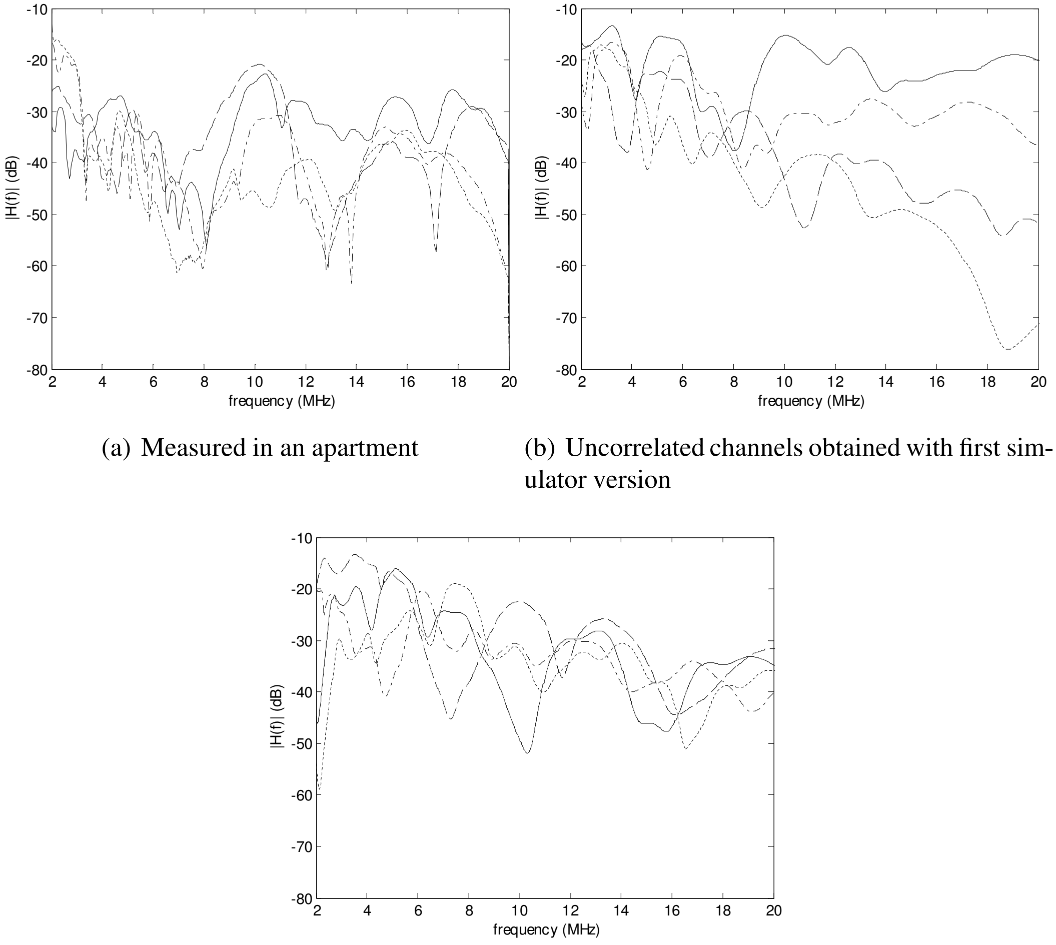

(a) Measured in an apartment

(b) Uncorrelated channels obtained with first simulator version

(c) Correlated channels obtained with the proposed channel generator

Figure 3.4: Example of measured and generated channels

seen, differences among the channels in Figure 3.4 (c) are more realistic than among the channels in Figure 3.4 (b). This correlation cannot be achieved by means of any of the statistical channel models proposed in the literature, which generate uncorrelated channels. Compared to other bottom-up models, in which correlation among channels is the natural result of the grid layout, this strategy releases the user from the burden task of defining the in-home grid for each considered network.

Regarding the Noise Generator, noise at each communication end is composed of three terms that are assumed to be stationary: background noise, a set of narrowband interferences affecting to a set of carriers in the HPAV band and two periodic asynchronous impulsive noise components with frequencies 26.3 kHz and 48.9 kHz, respectively. Three noise scenarios, which differ in the power of the different noise terms, have been defined: heavily, medium and weakly disturbed. Each time the channel generator is called, it randomly selects one of these scenarios. In this way, it is achieved a variability in the channel capacity that is observed in real scenarios.

Table 3.1: HPAV MAC layer parameters.

Parameter	Value	Parameter	Value
max_FL	2501.12 μs	Response Timeout	140.48 μs
CIFS	100 μs	RIFS	30.72 μs
PRS0	35.84 μs	PRS1	35.84 μs
PB Payload	512 bytes	PB Head	8 bytes
Frame Payload	1500 bytes	Frame Head	26 bytes

3.3 PHY layer

The physical layer simulates a pulse-shaped and windowed OFDM system as the one defined in the Homeplug-AV standard. The system parameters have been drawn from [Afkhamie et al., 2005b][Latchman et al., 2005]. To speed up simulations, the channel coding block has been substituted by a constant coding gain. This substitution is widely accepted in the related bibliography. The value of that gain is selected depending of the coding block type and the characteristics of the system noise. In this case, a gain of 12 dB has been selected (nevertheless, the $16/21$ code rate is taken into account). The number of bits per carrier is computed using the expression given in [Chung and Goldsmith, 2001], which implicitly assumes that both the noise and distortion are Gaussian. To compensate for the two aforementioned approximations, a 3 dB system margin has been included. The Bit Error Rate (BER) is fixed to 10^{-5}.

3.4 MAC layer

As said before, the present version of the simulator only implements the contention service based on CSMA/CA. For this layer, it has been developed a custom event-driven simulator of this protocol that uses the parameter values shown in Table 3.1.

Figure 2.5, shown in chapter 2, depicts an example of the timing sequence for the transmission of frames on the medium. An important restriction on the sequence is the maximum frame transmission time in each channel access (MAX_FL), which cannot exceed 2501.12 μs, including the RIFS. Therefore, the amount of bytes transmitted by a station depends on its PHY layer rate. Each time a node gets the channel for transmission, it gets its instantaneous channel capacity from the data generated by the PHY layer simulator to calculate the number of PBs it can transmit. These PB can independently fail due to the existing BER, and in this case, they are retransmitted in the next channel access. A MAC frame is not considered as received until all of its PBs have been acknowledged. Therefore, the lost of a PB turns into a delay growth.

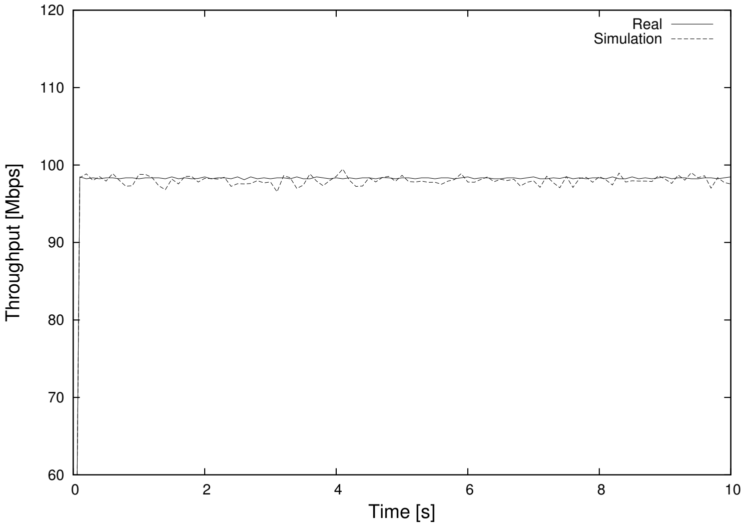

Figure 3.5: ON/OFF model comparison with real traces

3.5 Upper-layer services

In order to provide an accurate performance evaluation of a home network, the simulator includes traffic models for the services that are commonly used in such environments: data transfer, video streaming, video-conference, VoIP and network gaming. The following subsections provide a brief description of their main characteristics.

3.5.1 Data Transfer

An ON/OFF model has been used to emulate the bursty nature of the TCP-based data transmission. This model uses only two states, namely ON and OFF. The time spent in these states follows an exponential distribution and the stations only transmit data frames during the ON period.

To determine the model parameters for this service, different TCP files transmissions between two isolated computers were carried out. The sniffers where carefully analyzed, obtaining a mean value of $8.32 \cdot 10^{-4}$ and $1.4 \cdot 10^{-4}$ seconds for the ON and OFF periods respectively. In addition, to adequately genererate the input traffic, the mean separation between the data frames inside the ON period was also obtained, being $1.03 \cdot 10^{-4}$ seconds.

To evaluate the proposed model, the throughput evolution corresponding to a sniffered transmission and to a simulated one were compared. The results are shown in Figure 3.5. The traffic generated with the simulator perfectly fits the real behavior, validating the proposed model.

3.5.2 Video Streaming

In this service, frames to be transmitted are generated according to an MPEG-2 codec model. A typical MPEG-2 encoded video consists of three types of frames, namely I (intraframe-coded), P (predictive-coded) or B (bidirectionally-predictive-coded) frames.

An I-frame is made up of a single uncompressed video frame, and its content is unrelated to the preceding and the following frames. On the other hand, P-frames and B-frames use motion-compensated prediction. P-frames are based on the previous frame and B-frames are based on previous and future frames. A group of coded frames is called a Group-of-Pictures, or GOP in short. The GOP structure defines the number and the temporal order of P and B frames between two successive I frames.

The MPEG-2 model implemented in this work [Krunz and Hughes, 1995] suggests the following GOP structure: IBBPBBPBBPBBPBB. In addition, the size of the different frame types follows a Lognormal distribution (eq. 3.2) with the parameters shown in table 3.2. A film is divided into a set of scenes, and each scene has a number of GOPs that is exponentially distributed with mean 10. Consecutive I frames in the same scene have exactly the same size of the first I frame. The transmission rate is set to 30 fps.

$$f\left(x\right) = \frac{1}{x\sigma\sqrt{2\cdot\pi}}e^{-(lnx-\mu)^2/2\sigma^2} \tag{3.2}$$

Table 3.2: MPEG-2 model Lognormal distribution parameters

Frame type	SDTV Rate	HDTV Rate
I-frame	μ = 800 Kbits σ = 240 Kbits	μ = 3.2 Mbits σ = 960 Kbits
P-frame	μ = 240 Kbits σ = 160 Kbits	μ = 960 Kbits σ = 640 Kbits
B-frame	μ = 80 Kbits σ = 24 Kbits	μ = 24 Kbits σ = 96 Kbits

3.5.3 Video-conference

Video-conference service is based on the MPEG-4 video codec, which model is proposed in [Koumaras et al., 2005]. This codec uses a GoP composed of I, B and P frames, with 30 fps and the following structure: IPBPBPBPBPBPB. In this case, the size of the frames is shorter than in MPEG-2 codec due to the improved compressing process. In MPEG-4 model, the frame size distribution fits to a Gamma distribution:

$$f\left(x\right) = \begin{cases} x^{k-1}\cdot\frac{e^{-x/\theta}}{\theta^k\cdot\Gamma(k)} & x > 0 \\ 0 & otherwise \end{cases} \tag{3.3}$$

where Γ represents the Gamma function. Finally, Table 3.3 shows the Gamma distribution parameters depending on the video quality.

3.5.4 VoIP

VoIP service has been implemented using the G729 codec based model proposed in [Hassan H., 2005]. This model characterizes the VoIP traffic as an ON/OFF model, where

Table 3.3: MPEG-4 model Gamma distribution parameters

Frame type	SDTV Rate	HDTV Rate
I-frame	θ = 9.013 k = 12240	θ = 45.06 k = 12240
P-frame	θ = 2.812 k = 11880	θ = 14.06 k = 11880
B-frame	θ = 1.665 k = 9660	θ = 8.325 k = 9660

Table 3.4: Gaming traffic parameters

Parameter	Server (per client)	Client
Interarrival time	Extreme (a=55, b=6)	Deterministic (40 ms)
Packet Size	Extreme (a=120, b=36)	Extreme (a=80, b=5.7)

both, the active period (talk spurt) and the inactive period (silence) are exponentially distributed with mean values of 0.35 and 0.65 seconds respectively. During the ON period, the source sends 70 bytes frames at regular intervals of 30 ms.

3.5.5 Network Gaming

Network gaming traffic is becoming one of the most used multimedia services in home networks. The analysis of this traffic is also very interesting because of its restrictive time constraints. A traffic model for this service is proposed in [Färber, 2002]. This model is based on a client-server architecture, where the server traffic increases with the number of clients. The Extreme probability distribution (shown in eq. 3.4) is used to generate both client and server traffics. The parameters of the distribution are shown in table 3.4.

$$f\left(x\right)=\frac{1}{b}e^{-\frac{x-a}{b}}\cdot e^{-e^{-\frac{x-a}{b}}} \tag{3.4}$$

3.6 Statistical Analysis

As explained above, the simulation tool generates a random topology (i.e. attenuation and noise) each time it is executed. In addition, in a single realization, the results are averaged during the simulation time. Hence, it is important to obtain how many different simulations and how long they should be to obtain reliable statistical results.

To obtain the required simulation time, a realization with three stations (each of them with a different channel capacity) was performed for a long time. It was analyzed the time required by the averaged throughput to become stable (with an statistical error less than 1%). The obtained results are shown in Figure 3.6. As can be seen, this time is very similar in all the stations, being approximately 200 seconds.

Then, the required number of simulations was obtained by studying the mean PHY bitrate of a station versus the number of simulations. Figure 3.7 shows five different

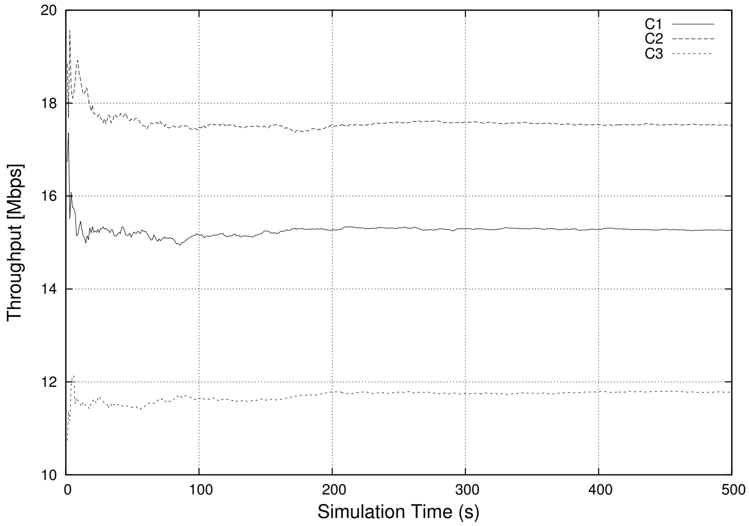

Figure 3.6: Average throughput evolution versus the simulation time

realizations of the described experiment. From these results, it can be extracted that 50 simulations seems to be an appropriate value to obtain a good estimate of any output parameter, since for a higher number of simulations the PHY bitrate of a station hardly varies.

With all this information, it can be concluded that 50 simulations of 200 seconds are enough to obtain statistically representative results. Unless otherwise stated, all the simulations carried out in this thesis have been performed with these parameters.

3.7 Validation

The simulator validation comprises two steps: validation of each layer and validation of the overall simulator. The procedure to validate each layer depends on the layer to be tested:

- Channel Generator. The channel response generator is validated by comparing its results with measurements accomplished in a large number of real indoor power line networks. Two issues are checked: the distribution of the main channel response parameter and the correlation among channels that correspond to the same indoor network. The results of the former are thoroughly presented in [Canete et al., 2011], while the latter is illustrated in Figure 3.4.

- Physical layer. Paradoxically, this is the most difficult layer to be validated because, to the authors' knowledge, there are not available papers in the literature which assess only the performance of this layer. In addition, the physical layer cannot be directly accessed in real modems. Since the MAC and the upper layer effects cannot be isolated, a direct comparison between simulated and real results is not possible. Hence, only the sanity check of its performance in an scenario with Additive White Gaussian Noise (AWGN) has been accomplished.

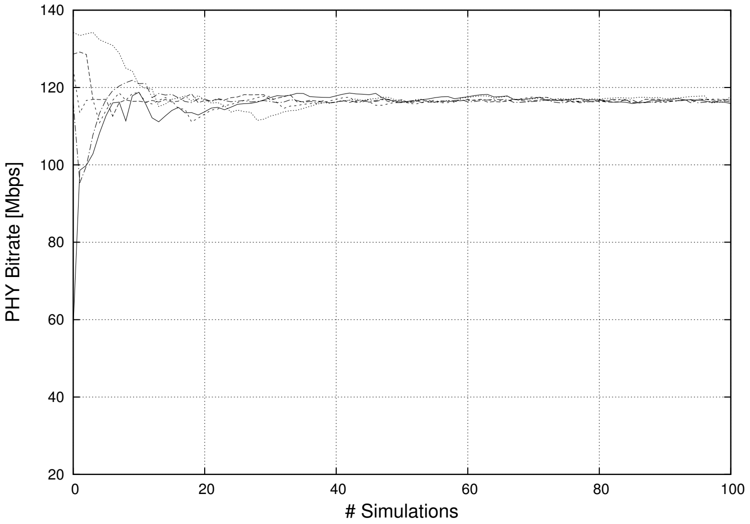

Figure 3.7: Average PHY bitrate evolution analysis

- MAC layer. It has been validated by comparing the simulated results with those given by the analytical expressions presented in [Chung et al., 2006].

- Upper layers. Since this module implements traffic models proposed in the literature, the validation has been restricted to check that the generated traffic has the statistics of the reference models.

The validation of the overall simulator is done by comparing the simulator outputs with tests accomplished using real HomePlug AV modems. Regarding to that, it is important to highlight two issues. The first one is that it must be done over a large number of indoor networks in order to verify the ability of the Channel Generator to produce statistically representative channels. However, since this capacity has already been thoroughly assessed in [Canete et al., 2011], only one scenario might be considered. The second is that, when selecting a validation scenario, it must be taken into account that modems made by different manufacturers perform almost equally in high SNR scenarios, differences among them appear in bad channel conditions. This pitfall can be avoided by using a network with very low attenuated channels.

An scenario which fulfil this requirement was obtained by connecting up to six commercial HomePlug AV modems (Linksys PLE200) quite close to each other. In the simulator, the scenario was replicated by adjusting the configuration parameters of the Channel Generator. One of the modems acts as a server, receiving the transmission from the clients. Each of them is connected through its Fast-Ethernet interface to a PC. The latter generates UDP traffic at a rate high enough to saturate the interface. Therefore, it can be assumed that the input rate to each modem is approximately 100 Mbps. The UDP throughput of the first client has been measured while the other modems are sequentially connected. This experiment has been repeated five times. The average values with their respective 95% confidence intervals, along with the simulated ones, are shown in Figure 3.8. As seen, there is an excellent match between them.

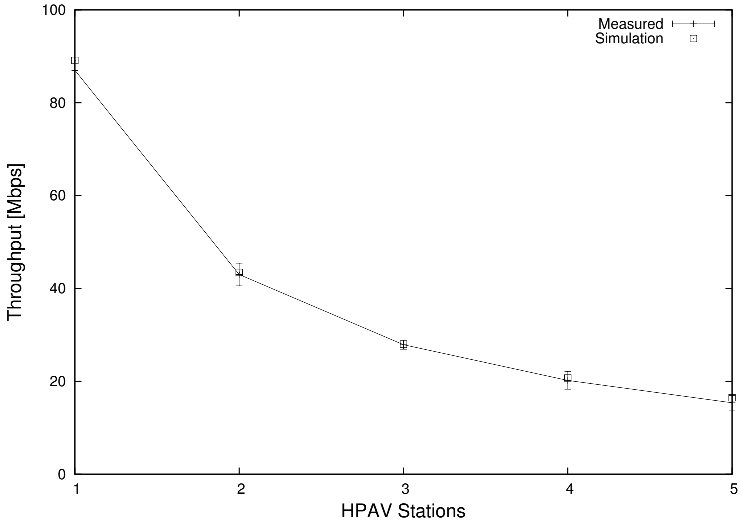

Figure 3.8: Overall simulator validation results

3.8 Publications

The work developed in this chapter has been partially published in the following references:

- Piñero, P., Cortés, J., Cañete, F., Díez, L., Manzanares, P., and Malgosa, J., *A realistic HomePlug-AV simulator for in-home network services planning*, Global Telecommunications Conference (GLOBECOM 2011), IEEE, pages 1-5, 2011.

Chapter 4

HomePlug AV Networks Analysis

Abstract- In this chapter, the experiments made to analyze the HPAV based in-home networks are detailed. These tests are mainly divided into two groups: real measurements and simulations. Through the first set of measurements, the particularities of HPAV in unicast and multicast communications will be evaluated. Simulation has been used to test some aspects of the standard that cannot be checked from real measurements and also to validate the simulator itself. In addition, from the results obtained in both cases, it is proposed a model that emulates the influence of the PHY layer in the CSMA/CA protocol behavior. Finally, the conclusions of the experiments are listed, identifying some aspects of the standard that could be improved, which will be addressed in the remaining chapters of this thesis.

4.1 Real measurements

In this section, the laboratory tests performed to analyze the PLC communication channels will be described. This set of experiments was divided into two groups: Unicast and Multicast. In each case, different experiments were performed to help us to understand the particularities of the medium.

All the presented experiments have been made using a laboratory test-bed, which has been designed to be quite similar to a real in-home scenario. It consists of 15 computers divided into 5 groups as shown in Figure 4.1. The groups are connected to different electrical phases, which are isolated enough to assume that an in-building environment is emulated (each group represents a different home). Moreover, the computers of the same phase are separated by different distances, emulating in this way the different link lengths of a typical home.

To perform the tests, PLE200 HomePlug AV Ethernet adapters of Linksys has been used (see Figure 4.2 (a)). These adapters connect the Ethernet device of a computer to the 220 V power line. The HPAV implementation details in these devices are not known, but from our characterization measurements, it can be extracted that they work in CSMA/CA-only mode, not implementing the TDMA service.

In addition, some experiments were performed to test the MediaXtream extension described in chapter 2. In this case, two F5D4076 Belkin modems, which implement

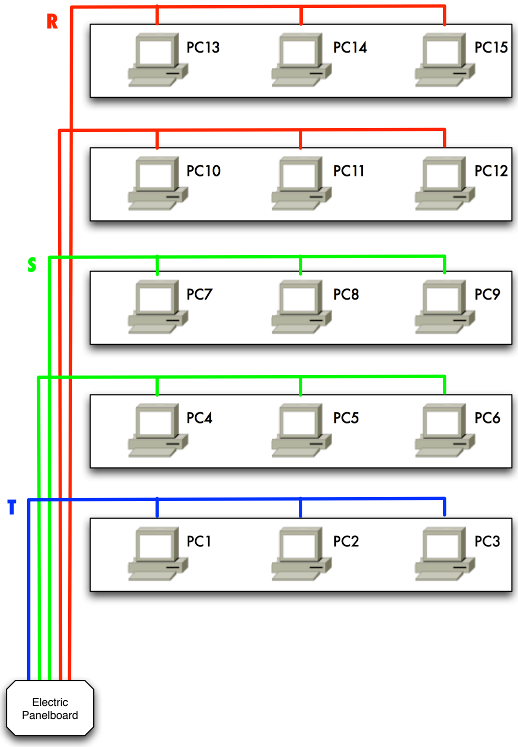

Figure 4.1: Laboratory test-bed schematic. R, S and T represent the three different electrical phases respectively.

MediaXtream and Xtendnet technologies, were used (see Figure 4.2 (b)).

4.1.1 Unicast communications

To characterize the unicast communications in a HPAV network, four aspects were evaluated: First, the variable capacity model of the physical layer; second, the possible asymmetries of the network; and third, the packet losses. Furthermore, the behavior of the MediaXtream extension is also tested.

The first objective was the evaluation of the data rate adaptation according to the noise level or the impedance mismatch. For this aim, we use two computers (PC13 and PC15) connected to the HomePlug AV network using the corresponding Ethernet adapters. To avoid interferences, their power suppliers are connected to another electrical phase of the laboratory, different from the one used to implement the HomePlug AV network. Therefore, initially, the PLC network is free of noise sources.

In order to measure the capacity of each link, it was used a UDP traffic generator which transmits traffic to the maximum capacity allowed by the physical network. The achieved results are presented in Figure 4.3(a). In particular, it can be observed that the modem is able to achieve a maximum capacity around 87 Mbps. After 8 seconds, a mobile phone charger was connected to the same electrical phase, causing a reduction of the link capacity to 60 Mbps. After 12 seconds, the charger was disconnected from the electrical line and the transmission rate slowly increased up to 87 Mbps again. Note that, for a

(a) Linksys PLE200 HPAV device (b) Belkin F5D4076 MediaXtream device

Figure 4.2: Modems used in the experiments

complete capacity restoration, the modem needs about 5 minutes, because of that, it is not shown in the figure. The connection of the mobile charger causes a descend in the SNR in that link. Specifically, the rectifier included in this device causes a periodic impulsive noise each time the electrical signal reach zero. Therefore, HPAV devices should adapt their TM to reduce the packet losses. After the disconnection of the charger, the channel adaptation procedure is able to modify the TM again to recover the maximum data rate but, according to the HPAV standard, this increment is slow to achieve a better adaptation to the network conditions.

This experiment has been repeated with other electronic devices. Table 4.1 represents the link capacity obtained for each one. Among the most usual devices, the mobile charger and energy efficient light bulb are the noisiest. The former because of the reason described above, and the efficient light bulb because of it uses a switched-mode power supply that causes harmonics in the HPAV frequency band. On the other hand, a simple extension lead (without any connected devices) reduces the capacity to 72 Mbps, not because of the noise but the impedance mismatch effect caused by the new branch.

Effects of the simultaneous combination of several devices were also evaluated (see Table 4.1). Firstly, it can be concluded that several devices of the same type do not reduce the SNR more than one of them. On the other hand, the combination of different devices generates different effects in function of how they are mixed. The reason of that is strictly related to the frequencies affected by the devices.

Next, the objective of the following experiments is to prove that the connection of a noise source does not affect in the same way to all the stations in the HPAV network, causing assimetries in the communications. The experiments were made in a HPAV network with three computers (PC15, PC13 and PC12). Firstly, the transmission capacities between the three HPAV modems, were measured in a noise-free scenario, being close to 87 Mbps. Later, a device that is known to cause a high performance degradation (a mobile phone charger) was connected next to PC12, and the capacities of the links were measured again. The results are graphically represented in Figure 4.3(b). It can be observed that the

Table 4.1: Channel capacity with different electrical devices connected to the power line. 95% confidence intervals

Device	Channel capacity [Mbps]
Without noise	86.921 ± 0.131
Mobile phone charger	60.600 ± 0.458
Laptop	84.045 ± 0.253
Wishk	82.236 ± 0.824
Heater	83.884 ± 0.142
Multimedia hard disk	86.379 ± 0.229
PC screen	76.303 ± 0.141
Electric heater	59.061 ± 0.780
Reading lamp	79.519 ± 0.118
Extension lead	72.106 ± 0.125
Energy efficient light bulb	57.058 ± 0.726
Charger + Reading lamp + Electric heater	40.654 ± 0.448
Charger + Reading lamp	54.310 ± 0.473
Charger + Electric heater	43.155 ± 0.724
Reading lamp + Electric heater	57.694 ± 0.476
Reading lamp + Reading lamp	74.552 ± 0.285
Charger + Charger	57.092 ± 1.252

connection of the new device at second 6 causes a very important reduction of the PC15-PC12 transmission rate but it does not affect the capacity of the PC15-PC13 connection. When the device is disconnected at second 12, the capacity of the link increases and it will reach its initial value. It is important to remark that the two transmission represented in the figure are not simultaneous, although in both cases the noise pattern is the same. Therefore, it has been proved that HPAV networks have several effects of asymmetries: whereas some HPAV devices have a correct operation, others can suffer a reduction in their transmission capacities. These asymmetries can even affect to a single link. For example, in this case, the transmission rate of the PC12-PC15 link remains close to 87 Mbps when the mobile phone charger is connected.

It is important to remark that, in all the described experiments, the packet losses are close to zero. This is because the modem implements a flow control mechanism to limit the traffic from the PC under bad PLC channel conditions. To check this, a sniffer capture was performed in the transmitter PC, obtaining that the modem is sending MAC Pause frames [IEE, 1997] to indicate the Ethernet interface not to send more frames to avoid buffer overflow.

The last set of experiments have the purpose of evaluating the HPAV MediaXtream extension (named Gigabit PLC modems), in particular the distance in which this technology is useful. To evaluate the variation of the UDP throughput with the distance, two F5D4076 modems were connected in an isolated scenario by wires of different lengths. The same experiments were performed with two PLE200 HPAV modems. Figure 4.4 shows the obtained results. As can be seen, a strong dependence on distance is observed

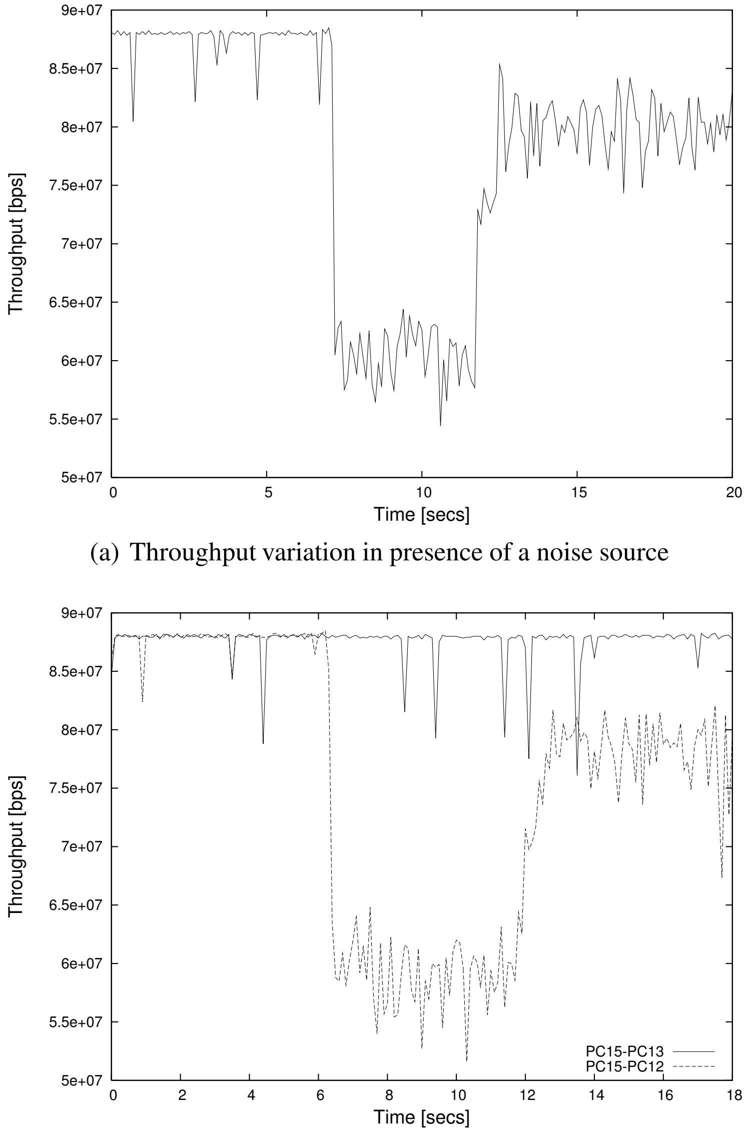

(a) Throughput variation in presence of a noise source

(b) Throughput asymmetry

Figure 4.3: Variable channel capacity analysis

for Gigabit modems while, for HPAV modems, the throughput remains constant. Belkin modems achieve a 300Mbps UDP throughput for short distances, but if the distance is longer than 40m, MediaXtreme band vanishes completely and the modems act like traditional HPAV modems. However, it is important to take into account that when several MediaXtream modems work together, some of them can act as repeaters, increasing the distance with maximum throughput.

4.1.2 Multicast communications

The next set of experiments has the objective of evaluating the performance of multicast communications in a real HPAV network. To this end, a socket program was coded to

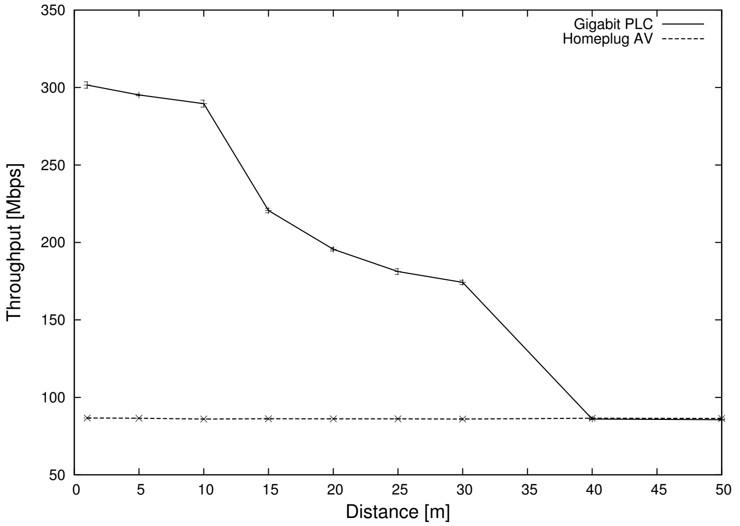

Figure 4.4: Throughput for different distances using Gigabit PLC and HPAV (95% confidence intervals)

select the data rate required by the multicast server. Moreover, the frames where numbered in ascending order, so each client was able to estimate the percentage of lost frames during the communication.

In these experiments, PC15 was set as multicast server, and PC13, PC12, PC9 and PC3 where set as multicast clients. A mobile phone charger was connected near to PC3 to achieve asymmetric communications channels between the server and the clients. In each case, the maximum unicast data rate was measured, obtaining the following results:

- PC15 - PC13: 87 Mbps
- PC15 - PC12: 50.4 Mbps
- PC15 - PC9: 39.3 Mbps
- PC15 - PC3: 29.5 Mbps

After that, several multicast transmissions with different data rates were initiated, obtaining the results shown in Figure 4.5. Figure 4.5(a) shows the evolution of the lost packets and Figure 4.5(b) shows the data rates received by each client as a function of the server data rate. As can be seen, an asymmetric multicast communication is obtained, where the clients with best channel conditions receive more data. The reason for these results is that, according to the standard, multicast transmissions in HPAV are implemented as a set of consecutive point-to-point transmissions that are carried out in a transparent way to end users. Consequently, assuming that the server must transmit the information to each of the four clients, their received multicast data rate should be a quarter of their unicast data rate. These values are 21.75, 12.6, 9.83 and 7.38 respectively, which are very similar to the obtained results. Therefore, it seems that the modems work according to the standard.

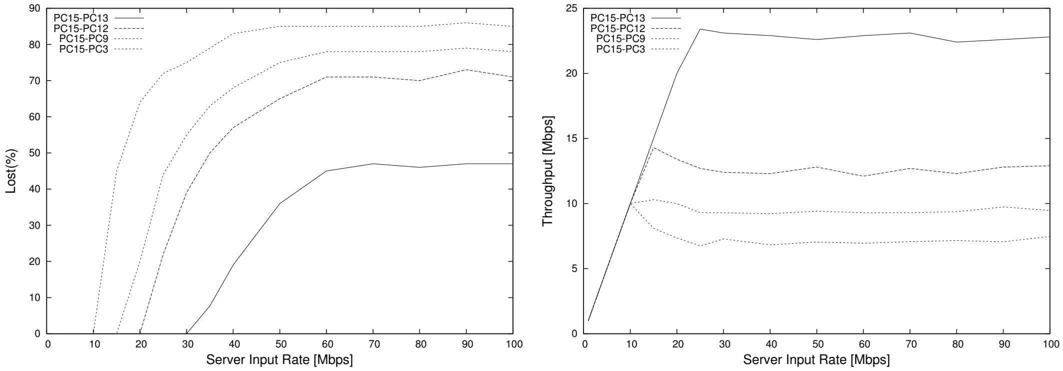

(a) Lost packets

(b) Throughput

Figure 4.5: Multicast transmission results in a real scenario

But, what does it happen with the losses? In this case, the transmitting station should have a different buffer for each client. These buffers should have the same input rate, but a different output one, so the losses suffered by each client are different. Theoretically, in such situations, the MAC pause flow control should limit the input rate from the PC, but it does not work properly in this environment. This is probably because only one buffer is used for multicast communications, causing problems in the flow control.

4.2 Simulation

To complete the analysis of HPAV networks, other characteristics of the standard that are difficult to test in real environments will be tested through simulation. They are mainly related with the behavior of the CSMA/CA protocol in different network configurations.

Firstly, the evolution of the throughput, the MAC delay, the jitter and the latency as the number of active stations increases is obtained. As said before, the results have been computed by averaging 50 in-home networks corresponding to a simulation time of 200 seconds. In these simulations, the frame arrival rate is high enough to assume saturation conditions, i.e. all the stations have frames to transmit in every access to the channel. Figure 4.6 shows both the throughput of a single station and the total network throughput as function of the number of active stations. Two situations are displayed. HP results correspond to the case in which all the stations have the highest priority. LP results correspond to the case in which all the stations have the lowest priority. It can be observed that the stations priority has a relative impact in the total network throughput, about a 12% of throughput loss for 10 active stations. Similarly, it can be observed that the throughput achieved by each active station is almost inversely proportional to the total number of active stations. This result indicates that the protocol is well designed, as the overall network throughput loss caused by the contention is almost independent of the number of active stations.

However, there is an interesting result in such experiments. It seems that HP stations perform worse than LP stations. Does this result have any sense? The answer is yes. According to Table 2.2, the contention window size of a HP station is smaller for high

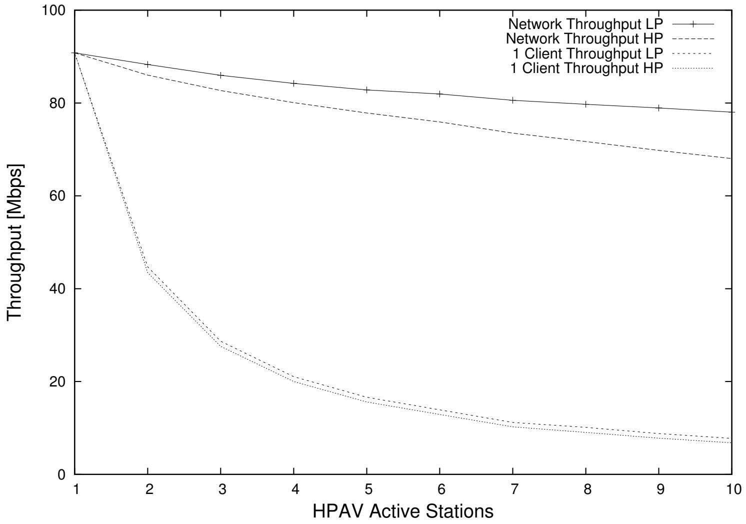

Figure 4.6: Total network throughput and one client throughput versus the number HPAV active stations

BPC values. This configuration gives certain "priority" in the channel access to these stations in highly saturated environments. However, in scenarios where all stations are HP this contention window configuration causes more collisions and the resulting decrease in the network throughput.

To evaluate the impact of the collisions in the total network throughput, it is also interesting to represent the normalized throughput as the number of active stations increases, and the number of collisions per second that each station suffers. These results are shown in Figure 4.7. It can be seen that, for ten active stations, the collisions produce a 22% throughput reduction for the high priority case and a 10% for the low priority one. The representation of the collisions per second for each client shows a maximum value when there are three active stations in the network. From that value on, although the total network collisions increase, the number of collisions per active station decreases. The reason of this decreasing behavior is that the backoff procedure uniformly distributes the channel accesses among the contending stations. Therefore, as the number of active stations increases, the number of channel accesses per station decreases, causing a reduction in the number of collisions that each station suffers. Finally, the average MAC delay, jitter and latency are also represented in Figure 4.8.

4.2.1 Network service planning

Another interesting test consists in the use of the HPAV simulator for network services planning. In this experiment, the video-conference service is taken as an example. Active stations want to start a video session using a HDTV MPEG-4 codec. In video-conferences, the QoS is mainly defined by the latency, which cannot be higher than 150 ms, and jitter, which should be limited to 30 ms. In our scenario, the most limiting parameter is the latency. The CDF of MAC frames latency as function of the number of active stations is shown in Fig. 4.9. This figure can be used to determine the probability that a frame

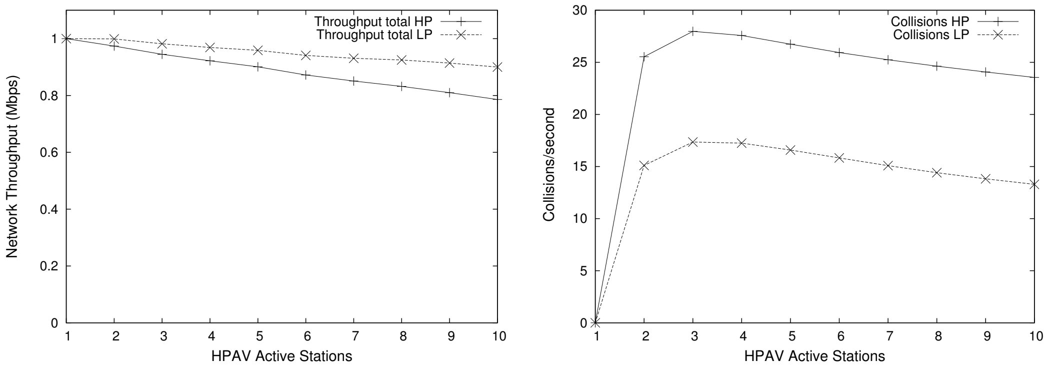

(a) Normalized throughput

(b) Number of collisions per station

Figure 4.7: Normalized throughput and number of collisions versus the number of HPAV stations

exceeds the maximum latency requirement. Results are shown in table 4.2. Assuming that in higher layers the frames that exceed the maximum delay restriction will be discarded, these latency exceeding probabilities can be considered as losses. According to [Miras, 2002] the maximum Packet Loss Ratio (PLR) for a good quality video reception is 10^{-2}. Hence, a maximum of seven HDTV video- conference services can be carried out at the same time in a HPAV network.

Table 4.2: Probability of exceeding maximum frame latency requirements for different number of active stations

# stations	Probability	# stations	Probability
1	0	6	$2.711 \cdot 10^{-4}$
2	0	7	$1.935 \cdot 10^{-3}$
3	0	8	$1.225 \cdot 10^{-2}$
4	$5.9 \cdot 10^{-7}$	9	$4.959 \cdot 10^{-2}$
5	$2.08 \cdot 10^{-5}$	10	$1.440 \cdot 10^{-1}$

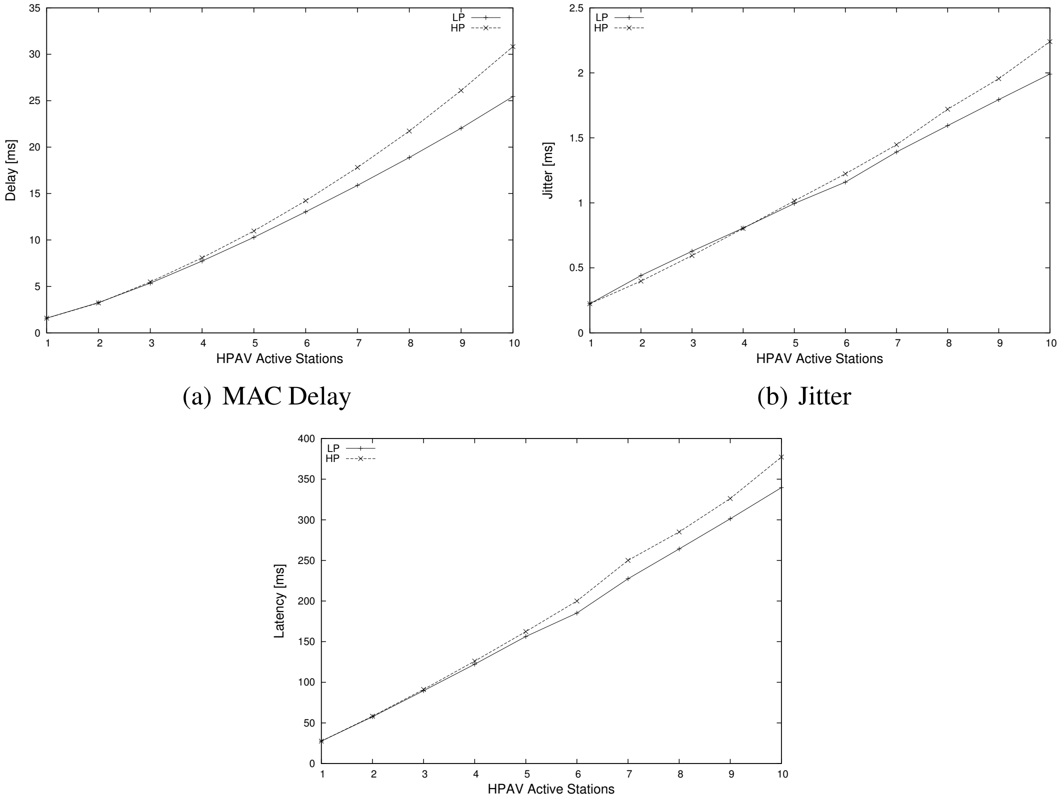

(a) MAC Delay

(b) Jitter

(c) Latency

Figure 4.8: Delay, Jitter and Latency evolution versus the number of HPAV stations

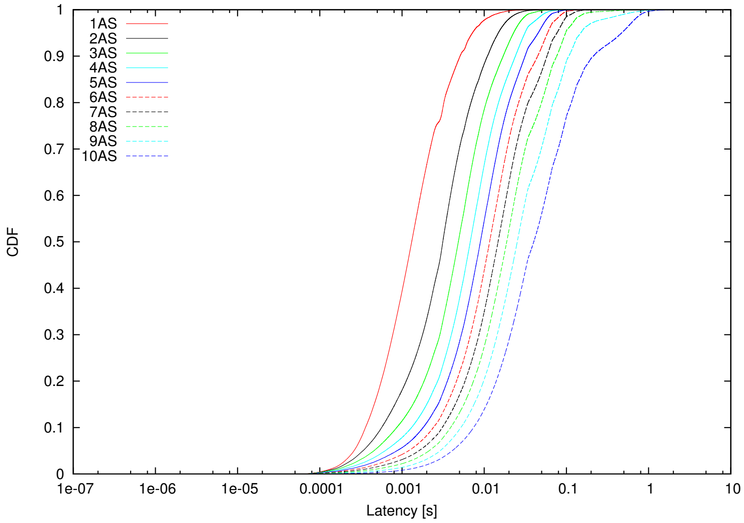

Figure 4.9: MAC latency CDF versus the number of HPAV active stations (AS)

4.3 Mathematical Modeling

After analyzing the behavior of the CSMA/CA protocol used in HPAV, the results were compared with [Yoon et al., 2008][Chung et al., 2006], which are two of the most relevant previous works in this area. It was found that the existing mathematical models for this protocol do not consider the variable physical layer capacity of this kind of networks. In them, it is assumed that the physical transmission rate of all the pairs is equal to the maximum transmission rate allowed by the medium. As can be extracted from the previous results, the PHY rate has an important impact in the CSMA/CA performance that worth to be studied. To this end, it was decided to use the developed simulator to extend the existing models.

The starting point in this study is [Chung et al., 2006], where the CSMA/CA backoff procedure under saturated conditions (all the stations have frames for transmitting immediately after a successful frame transmission) is mathematically modeled as a tridimensional Markov chain (see Figure 4.10). The state is defined by the following tuple (BPC(t),DC(t),BC(t)), where each variable denotes the stochastic process representing the values of the corresponding counter at the beginning of the slot t. Moreover, p_b and p are the probabilities of sense the medium busy and the probability of a collision respectively. It is assumed that the network is composed of n stations. In this case, these probabilities have the same value, which can be expressed as follows:

$$p_b = p = 1 - (1-\tau)^{n-1} \tag{4.1}$$

where τ is the probability that a station transmits a frame in a slot. In this algorithm, all the station transmits when BC counter reaches 0. Therefore τ can be calculated by using the following expression:

$$\tau = \sum_{i=1}^{m} \sum_{j=0}^{M_{i-1}} P_{i,j,0} \tag{4.2}$$

where m and M_{i-1} are the maximum values of BPC and DC respectively and $P_{i,j,k}$ is the steady state probability for the Markov chain, which solution is presented in the referenced paper.

Using these expressions, the throughput under saturated conditions can be expressed as:

$$S_{sat} = \frac{P_{tr}P_sE[N_{Payload}]}{(1-P_{tr})\sigma + P_{tr}(P_sT_s + (1-P_s)T_c)} \tag{4.3}$$

where P_{tr} is the probability that at least one station transmits a frame, P_s is the probability that a station successfully transmits a frame, $E[N_{payload}]$ is the average payload size, σ is the duration of an idle slot and T_s and T_c are the average times that the medium is busy due to a successful frame transmission and due to a collision, respectively. The P_{tr} and P_s values are shown below:

$$\begin{aligned} P_{tr} &= 1 - (1-\tau)^n \\ P_s &= \tfrac{n\tau(1-\tau)^{n-1}}{P_{tr}} \end{aligned} \tag{4.4}$$

In addition, taking into account that a collision is detected when the sending station does not receive an acknowledgment (ACK):

$$\begin{aligned} T_s &= PRS0 + PRS1 + HEAD + T_{frasuc} + RIFS + T_{res} + CIFS \\ T_c &= PRS0 + PRS1 + HEAD + T_{fracol} + CIFS \end{aligned} \tag{4.5}$$

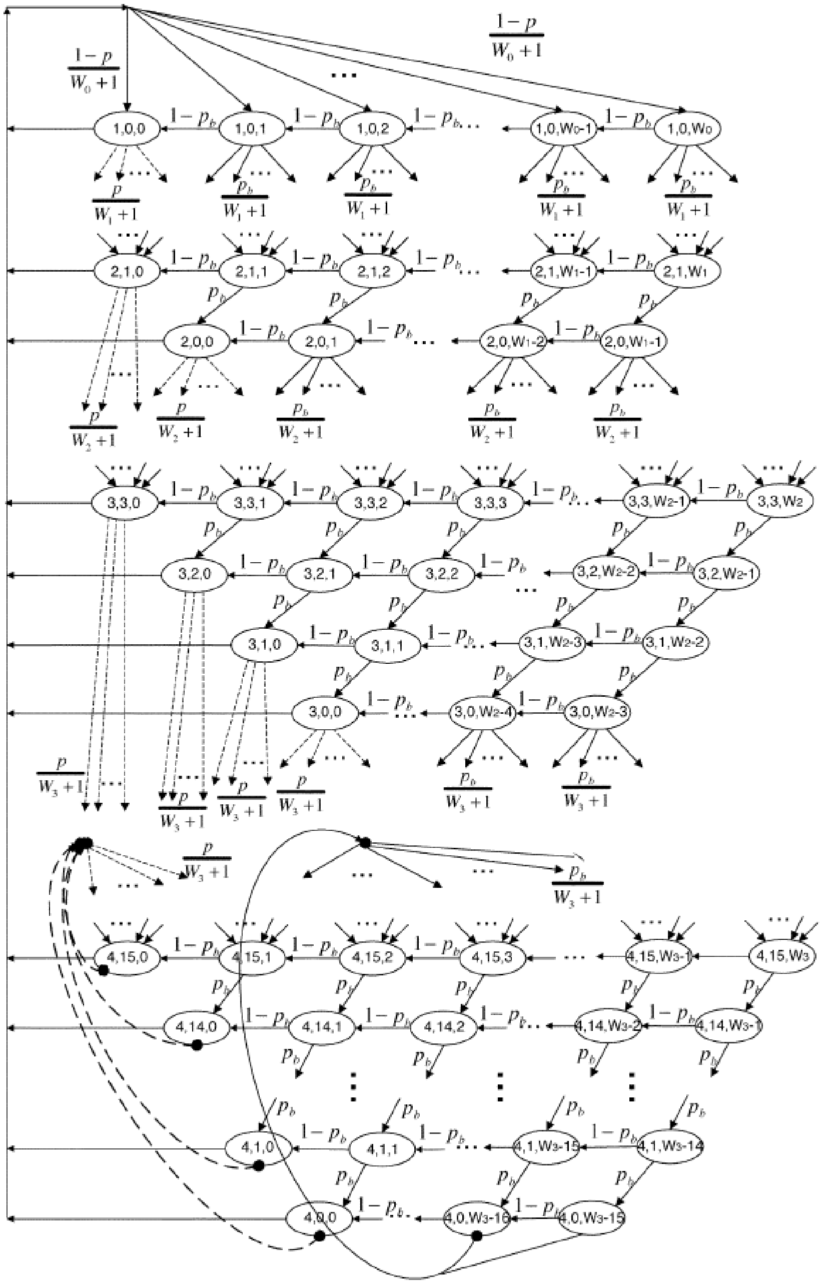

Figure 4.10: State transition diagram of HPAV CSMA/CA backoff procedure under saturated conditions. Extracted from [Chung et al., 2006]

where T_{frasuc} and T_{fracol} indicate the mean frame transmission time in a successful transmission and in a collision, respectively, T_{res} indicates the acknowledgment frame duration and HEAD denotes the HPAV head time, whose duration is independent of the transmission rate.

Proposed extension

Authors of [Chung et al., 2006] assume that the physical transmission rate of the contending stations is constant and equal to the maximum rate allowed by the medium (i.e. 150.19 Mbps). Therefore, T_{frasuc}, T_{fracol} and $E[N_{payload}]$ are constant too. However, in the real world the physical transmission rates of the contending station are usually different and lower than 150.19 Mbps. Therefore, these parameters are not constant. In this case, the values of these parameters can be obtained using the following expressions:

$$E[N_{Payload}] = \frac{1}{N}\sum_{i=1}^{N} L_i =$$

$$= \frac{1}{N}\sum_{i=1}^{N} \lfloor \frac{C_i(Max\_FL - RIFS)}{PBsize} \rfloor \cdot PBsize \tag{4.6}$$

where L_i is the amount of bits that the station i transmits each time it can access to the shared channel, N is the number of contending stations, C_i is the physical rate from the station i to the destination and $PBsize$ is the physical block size.

$$T_{frasuc} = \sum_{i=1}^{N} \frac{p_t(i)L_i}{C_i} = \frac{1}{N}\sum_{i=1}^{N} \frac{L_i}{C_i} \tag{4.7}$$

where $p_t(i)$ represents the transmission probability of station i. Note that, under saturated conditions, all the contending stations have the same opportunities to access the channel.

Finally, T_{fracol} is determined by the worst of each two stations which are colliding. Without lost of generality, the collision of only two stations has been considered (a higher order collision is quite unlikely). Thus,

$$T_{fracol} = \sum_{i=1}^{N}\sum_{j=1}^{N} p_c(i,j) \cdot max(\frac{L_i}{C_i}, \frac{L_j}{C_j}) \tag{4.8}$$

where $p_c(i,j)$ represents the collision probability between stations i and j. Since the collision procedure is memoryless, its probability is given by:

$$p_c(i,j) = \begin{cases} \frac{1}{\binom{N}{2}} & \text{if } i \neq j \\ 0 & \text{if } i = j \end{cases} \tag{4.9}$$

The proposed model can be simplified (with a minimum loss of accuracy) assuming that the transmitted information is a multiple of the $PBsize$. In this case, the parameters T_{fracol} and T_{frasuc} remain constant, being $E[N_{Payload}]$ the only variable parameter:

$$T_{fracol} = T_{frasuc} = Max\_FL - RIFS$$

Table 4.3: Physical transmission rates for CSMA/CA mathematical model evaluation

Station	C_{PHY} (Mbps)
1	100.029
2	109.629
3	108.771
4	100.781
5	95.668
6	118.415
7	82.264
8	98.756
9	114.359
10	113.634

$$E[N_{Payload}] = \frac{(Max\_FL - RIFS)}{N} \sum_{i=1}^{N} C_i \tag{4.10}$$

In the same way, [Chung et al., 2006] also provides a procedure to obtain the throughput under unsaturated conditions. It is assumed that the arrival of frames to each station follows a Poisson process with arrival rate λ. In this case, the throughput under unsaturated conditions is obtained through numerical methods which use the same parameters than in the saturation analysis. Therefore, the proposed extension can also be applied to this scenario.

The proposed model has been validated and compared to the original one using the simulator described in the previous chapter. The simulation scenario is composed of ten HPAV stations. Table 4.3 shows the physical transmission rates of the transmitter-receiver pairs. These values have been obtained using the uncorrelated channel generator and no long term variations in the channel response have been simulated.

In a first experiment, the frame arrival rate is high enough to assume saturation conditions. Figure 4.11 shows the total network throughput values when clients join the network in the order indicated in Table 4.3. As can be seen, the obtained throughput values are rather worse when real physical transmission rates are considered. As said before, in the original model all the stations are considered to achieve the maximum physical transmission rate, and as consequence they transmit the maximum amount of bits in each channel access. However, when real physical rates are considered, less bits are transmitted in each access. This fact causes the total MAC throughput to be lower than in the original model. The proposed model is also validated since analytical and simulation results are quite similar.

Note that the arrival of a new station does not necessarily involve a reduction of the total MAC throughput. In fact, it can even produce a throughput improvement. This is due to a pair of facts. First of all, the frame transmission time is fixed by the HPAV standard, and therefore, the faster stations can transmit more bits in each access than the slower ones. On the other hand, due to the CSMA/CA medium access control, under saturated conditions all the stations have the same opportunities to access the channel. As a consequence, when a fast station is connected, it can turn into a total network throughput

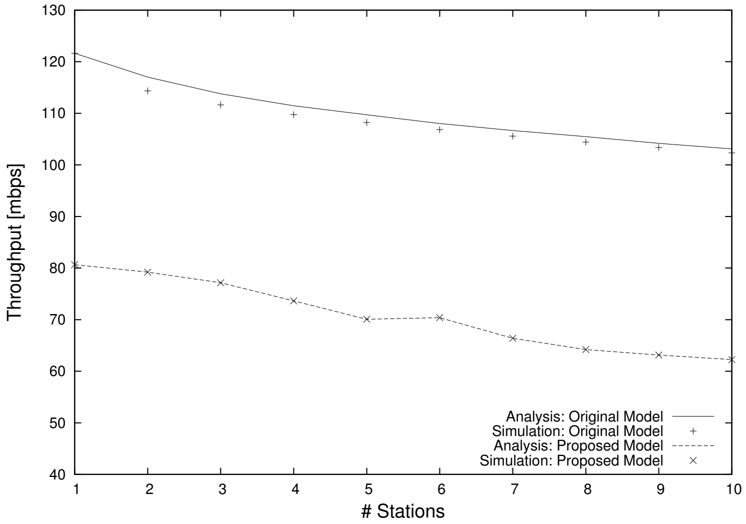

Figure 4.11: Throughput under saturated conditions

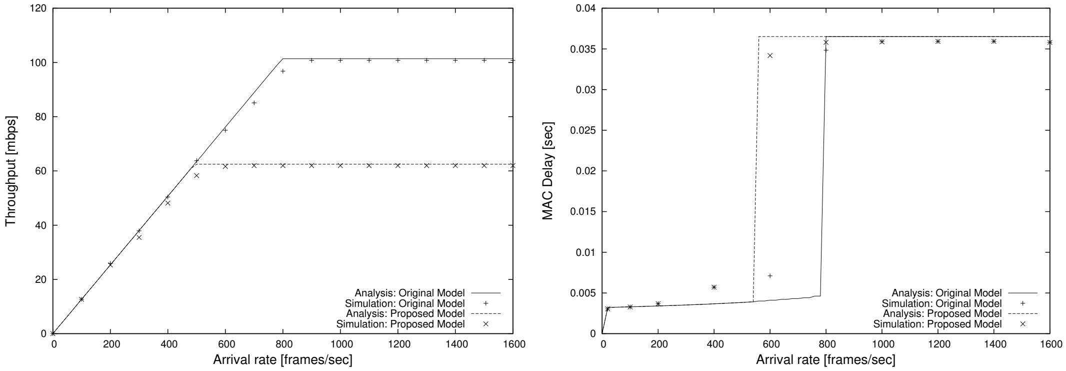

(a) Throughput

(b) MAC Delay

Figure 4.12: Throughput and Delay under unsaturated conditions for 10 contending stations

increase. This fact can be easily observed when station 6 is connected to the network.

Next, the model was also evaluated under unsaturated conditions. To this end, a Poisson arrival pattern with variable rate and frames of 1500 bytes were chosen for the stations. Figure 4.12(a) shows the throughput results when the ten stations are connected to the network. It can be seen that the throughput values are similar to the original model until the saturation condition is achieved, which happens for a lower arrival rate when real capacities are considered. Moreover, when saturation is reached, the throughput value coincide with the value showed in Figure 4.11 for ten contending stations (approximately 62 Mbps).

In addition, [Chung et al., 2006] also detailes a procedure to calculate the MAC delay in both cases, under saturated and unsaturated conditions. The proposed extension can also be used to calculate this parameter. The obtained results show that the MAC delay under saturation conditions is not affected by the physical bitrate of the involved stations. This is a logical result, since all the stations have frames to transmit after a successful transmission and will always compete for the channel. Hence, the time delay between two channel accesses experienced by a station will not depend on the number frames transmitted by a station in a single channel access but on the number of contending stations.

In the unsaturated scenario, the results obtained for the MAC delay are different. As shown in Figure 4.12(b), the delay experiences a big increment when the saturation is achieved, being the value in this point similar to that obtained in the saturated model.

4.4 Analysis conclusions

From all the experiments performed in this chapter, several conclusions can be extracted. Regarding the real measurements, it can be inferred that:

- HPAV PHY layer exhibits a remarkable variation, which depends on the network topology, the type of wires and the devices connected to the electrical network. This variability can cause very important changes in the MAC layer throughput, which can experience a reduction of 30% with the only connection of a home appliance to the grid. Moreover, these changes can only affect to a part of the network, obtaining important asymmetries even in a simple link. However, these effects do not cause an increase in the packet losses, since the MAC flow control algorithm implemented in the modems limits the traffic from the PC under bad PLC channel conditions.

- Multicast communications are implemented as consecutive point-to-point transmissions, done in a way transparent to the end user. With this technique, the effective multicast capacity is significantly reduced when number of clients is high. Moreover, the MAC flow control does not work properly in this situation, causing a high number of packet losses.

In addition, from the simulations results, it can be concluded that:

- It has been proved that the simulator is a very powerful tool to evaluate the performance of services with QoS requirements and to implement cross-layer solutions, since it implements both PHY and MAC layers of HPAV standard.

- It has been proposed a model that is able to emulate the effects of the variations at PHY layer in the CSMA/CA protocol. The model accuracy has been evaluated with the simulator, obtaining good results.

With these results, it was decided that there were three areas that worth a detailed study: The use of Fountain codes for reliable data transmission, the proposal of solutions to improve the multicast communications and the implementation of cross-layer protocols to build a “PHY-aware” MAC. By including these enhancements in the HPAV CCo, the whole HPAV system performance can be significantly improved. Some of these functionalities can be directly tested in the real test-bed. However, others require modifications in the standard, so they must be evaluated by simulation.

4.5 Publications

The work developed in this chapter has been partially published in the following references:

- P.J. Piñero, J. Malgosa, P. Manzanares, J.P. Muñoz, *Homeplug-AV CSMA/CA Evaluation in a Real In-Building Scenario*, IEEE Communications Letters, Vol 15, No. 6, pp. 683-685, 2011

Chapter 5

Fountain Codes

Abstract- Fountain codes are a class of source codes which are able to provide reliable communications without a feedback channel. Because of the properties of the PLC channel, these codes can be very useful in networks based on this technology. Concretely, two different applications will be presented, one for reliable data transmission and another for aggregation of asymmetric interfaces. In the first case, they could be used to overcome the limitations of TCP in shared mediums, and in the second, the use of this codification technique will allow the combination of interfaces of different technologies to improve the whole home network performance.

5.1 Introduction

The main idea behind Fountain codes (also known as rateless codes) [MacKay, 2005] is that the transmitter acts like a fountain of water, which is able to produce an infinite number of water drops (coded packets). The receiver represents a bucket that needs to collect a certain number of these water drops to be able to decode the information. The main advantage of these codes is that the receiver can obtain the information regardless of which coded packets it has collected. Therefore, Fountain codes should have the following properties:

- A transmitter can generate a potentially infinite amount of encoded packets from the original data.
- A receiver can decode a message that would require K packets from any set of K' encoded packets, for K' slightly larger than K.

The most important implementations of Fountain codes are LT codes, Raptor codes and Online Codes. LT codes were the first practical realization of a fountain code. The only drawback of these codes is that their encoding and decoding costs scale as $Klog_eK$, where K is the file size. Raptor codes are an evolution of LT that achieve linear cost for encoding and decoding. Finally, Online Codes are a free-software alternative to Raptor codes that also achieve linear cost for both operations.

There are lots of application of Fountain codes in digital communications although the most important are:

- *Multicast*. In multicast communications, each receiver experiences losses independently to the others'. Therefore, the number of control packets to recover all these lost packets can be very high. Through the use of Fountain codes this problem is solved, even allowing a receiver to start the reception of a message with a certain delay.

- *Parallel download*. Fountain codes can also be very useful in a scenario where a receiver downloads a file from various sources at the same time (for example in P2P networks). Through them, each source can generate a stream of coded packets independently, and the receiver only needs a number of packets without care of their origin.

- *Video streaming*. One of the most common problems in video streaming is the delay caused by retransmissions. Through the use of Fountain codes this problem is solved since the receiver only needs to wait for the needed number of packets to recover the image, without being aware of losses. In fact, Raptor codes has been adopted as encoding technique for Digital Video Broadcasting (DVB) in IPTV services [Stockhammer et al., 2011].

In this chapter, two different uses of these codes in PLC networks will be evaluated: Reliable data transmission and aggregation of asymmetric interfaces. The first one makes use of these codes to overcome the limitations of TCP protocol in PLC networks, in which the variable capacity and the shared medium access cause a reduction in TCP performance. In the second set of experiments, it will be shown that the use of this codification technique allows the combination of interfaces of different technologies to improve the in-home network performance.

5.2 Description

5.2.1 Random Linear Codes

Random Linear Codes (RLC) are the most simple implementation of a Fountain Code. The procedure to transmit a message composed of k packets is as follows:

1. In each clock cycle (called *n*), the transmitter generates an array with k random bits (G_{nk}).

2. The coded packet (t_n) is obtained by XOR-ing the source packets for which G_{nk} is 1.

3. The generated bit array for each packet is saved, creating a binary generator matrix (G).

By using this procedure, the receiver is able to obtain the source packets by inverting the generator matrix:

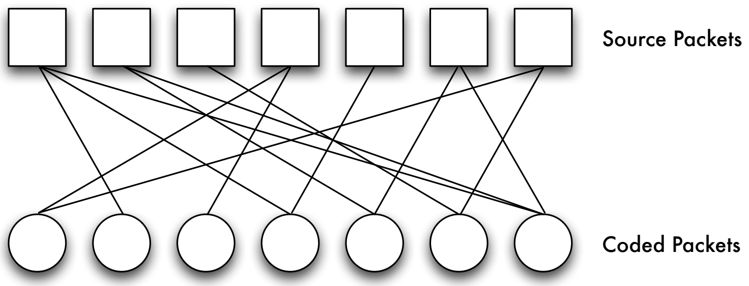

Figure 5.1: LT codes codification graph

$$s_k = \sum_{k=1}^{N} t_n \cdot G_{nk}^{-1} \tag{5.1}$$

As can be seen, the receiver needs the generator matrix to perform the information decoding. Therefore, a procedure to send it from the transmitter to the receiver must be implemented. The decoding procedure needs a number of packets $N \geq k$ to start, and its failure probability coincides with the probability that the matrix G is not invertible. It can be shown that the process will be successful with a probability $1 - \delta$ if the number of coded packets received is $N = K + log_2(1/\delta)$.

The main problem of these codes is their computational load, since the cost of inverting the matrix is $O(k^3)$. In addition, due to a mean of $k/2$ operations is needed to code each packet, the coding process requires $k^2/2$ operations. Therefore, this codification technique would be appropriate only for short messages.

5.2.2 LT Codes

LT Codes were created by M.Luby in 1998 and firstly published in 2002 [Luby, 2002]. They were the first implementable solution of a Fountain code. LT codes retain the good performance of RLC codes, while drastically reducing the encoding and decoding complexity.

If this coding technique is used to transmit a message composed of k source packets, $O(ln(k/\delta))$ operations are needed to generate a coded packet. At the receiver side, the original message can be recovered with a probability $1 - \delta$ from $k + O(ln^2(k/\delta) \cdot \sqrt{k})$ coded packets through $O(k \cdot ln(k/\delta))$ operations.

To create a coded packet, the first step is the random selection of its degree (d). To this end, it is used a particular statistical distribution, which design and analysis will be shown later in this section. Then, the coded packet is the result of the XOR operation of d randomly selected source packets. Like in RLC codes, the codification procedure of a LT code can be expressed as a graph, where it is shown the source packets from which each coded packet is composed (see Figure 5.1).

To correctly decode the source packets, the decoder should know the degree of each coded packet. Therefore, it should be sent together with the coded information (for example in the packet header). Then, the original message can be obtained by using the next

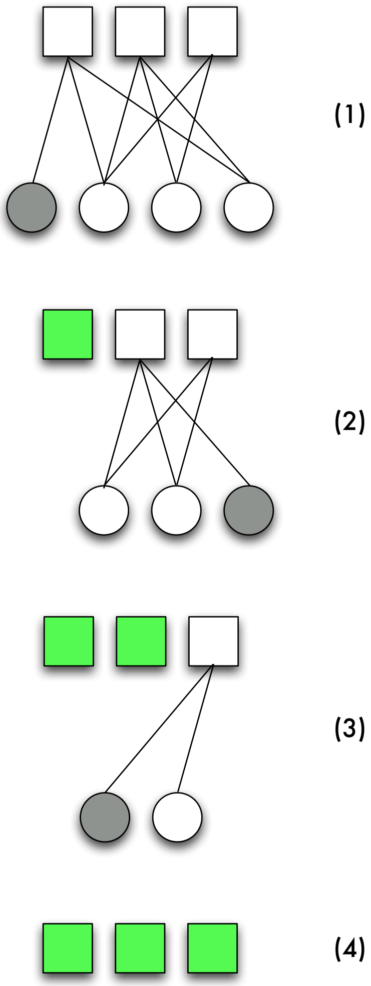

Figure 5.2: LT decoding procedure

procedure:

1. Search for a coded packet generated from only one source packet (i.e. with degree 1).

2. Remove this source packet from the rest of coded packets which include it. This can be done simply by XOR-ing both the source and the coded packet, reducing the degree of these coded packets by one. In this way, new degree-1 packets are generated. The group of degree-1 coded packets in a particular instant is called $Ripple$.

3. Repeat this operation till all the source packets are recovered. Note that the decoding process will fail in any step if the $Ripple$ group is empty. This fact can be minimized by selecting an appropriate degree distribution. A graphical example of this decoding process is shown in Figure 5.2.

An adequate degree distribution would allow an adequate $Ripple$ size during the decoding process. If the $Ripple$ size is too long, there is a high redundancy, and if it is too short, it can disappear and cause a fail in the decoding process. Ideally, a good solution to this problem is that the $Ripple$ is only composed of one packet at each iteration. Using this condition, Luby proposes the *Ideal Soliton Distribution* ($\rho(.)$) shown below:

$$\rho\left(d\right)=\begin{cases}\frac{1}{k} & d=1\\ \frac{1}{d(d-1)} & d=2,...,k\end{cases} \tag{5.2}$$

However, this distribution does not work properly in real scenarios, since the mean value of the $Ripple$ size is one, and a small variance can cause the failure of the decoding process. To solve this problem, the ***Robust Soliton Distribution*** ($\mu(.)$) is proposed. To obtain this distribution, it is defined $R = c \cdot ln(k/\delta) \cdot \sqrt{k}$, where δ is the decoding process failure probability, c is a positive constant, and $\tau\left(d\right)$ is defined as:

$$\tau\left(d\right)=\begin{cases}\frac{R}{dk} & d=1,...,\frac{k}{R}-1\\ \frac{R\cdot ln(R/\delta)}{k} & d=\frac{k}{R}\\ 0 & d=\frac{k}{R}+1,...,k\end{cases} \tag{5.3}$$

With all these parameters, $\mu(.)$ is obtained as follows:

$$\beta=\sum_{\forall d}\tau(d)+\rho(d) \tag{5.4}$$

$$\mu(d)=\frac{\tau(d)+\rho(d)}{\beta} \quad \forall d \in 1...k \tag{5.5}$$

Using this degree distribution, only $k{\cdot}\beta$ coded packets are needed in order to guarantee a successful decoding probability of $1-\delta$. It can be also shown that this distribution fulfill all the conditions that have been detailed for LT codes. In addition, the c parameter can be adjusted to modify the behavior of the process. A high c value decreases the mean degree of the coded packets, increasing the probability of successful decoding but also increasing the number of packets needed to start this process. If c value is low, the opposite behavior is achieved.

5.2.3 Raptor Codes

As seen before, LT codes has non-linear decoding time. Raptor codes [Shokrollahi, 2006] are a extension of LT codes which achieve linear coding/decoding times. This codification technique is able to recover a message composed of k source packets from $k(1-\epsilon)$ coded packets with a probability of $1-\delta$, where $\epsilon = 4\delta(1-4\delta)$. Each coded packet is generated through $O(ln(1/\epsilon))$ mathematical operations while the whole source message is recovered with $O(k \cdot ln(1/\epsilon))$ operations.

The main idea behind this technique is the concatenation of a traditional FEC code (Reed-Solomon, Turbo-Codes, Tornado, etc) with a "*weak*" LT code. The "*weak*" LT code does not allow the recovering of all source packets, which should be recovered through the concatenated FEC decoding. Assuming that a message composed of k source packets is transmitted with a Raptor encoder, the first step is the use of a FEC encoder, to generate n intermediate packets. Then, these n packets are the input of the LT encoder, that generates a infinite amount of coded packets. Meanwhile, in the receiver side, these steps are performed in reverse order to recover the information.

To design a Raptor code, the first step is to choose the degree distribution of the LT encoder. To this end, the author proposes a variation of the *Soliton Distribution* ($\Omega(.)$):

$$\Omega_D(x) = \frac{1}{\mu+1}\left[\mu x + \sum_{i=2}^{D} \frac{x^i}{i(i-1)} + \frac{x^{D+1}}{D}\right] \tag{5.6}$$

The next step is the selection of a FEC code. In [Shokrollahi, 2006] the author shows that this outer code should fulfill the following conditions:

- Its information rate should be $R = (1-\epsilon/2)/(1+\epsilon)$.
- The number of intermediate packets generated should be $n = [k/(1-R)]$.

The most used FEC encoders are Low Density Parity Check (LDPC) and Tornado codes, or even a combination of them.

5.2.4 Online Codes

Online Codes [Maymounkov and Mazieres, 2003] are characterized by two parameters ε and q. The receiver can recover the original message from any $(1+3\varepsilon)K$ coded blocks (also called *check blocks*) with a success probability determined by of $1-(\varepsilon/2)^{q+1}$.

The structure of Online Codes is depicted in Figure 5.3. The encoding process is divided into two layers, the inner code and the outer code. The inner code is in charge of generating the *check blocks*. Every check block is computed as the XOR operation of d blocks uniformly chosen from the message (d represents the degree of the check block). The probability that $d = i$ is given by a specific probability distribution ρ_i:

$$\rho_1 = 1 - \frac{(1+1/F)}{(1+\epsilon)} \tag{5.7}$$

$$\rho_i = \frac{(1+\rho_1)F}{(F-1)i(i-1)} \quad i = 2, 3, ..., F \tag{5.8}$$

where F is given by

$$F = \frac{ln(\epsilon^2/4)}{ln(1-\epsilon/2)} \tag{5.9}$$

However, due to the random selection of the message blocks, some of them may not be selected in the inner coding process, for example the third input block in Figure 5.3. One solution to this problem is to add a preliminary coding process (called outer coding) which generates $0.55q\epsilon K$ *auxiliary blocks* from the original message. The message blocks that

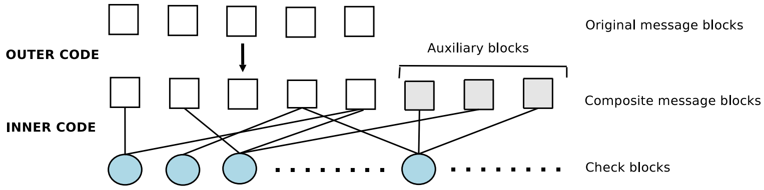

Figure 5.3: Online codes structure

do not participate in the inner process will be able to be decoded thanks to this redundancy. In fact, the input blocks of the inner coder are the union of the original message blocks and the auxiliary blocks. All this set is called *composite message*.

From all the available procedures to generate redundancy (Reed-Solomon, Cyclic Redundancy Check, Parity Bits, etc.), Online Codes uses one of the simplest: for each block of the original message, q auxiliary blocks are chosen. Each auxiliary block is computed as the XOR operation of the original message blocks assigned to it.

The original message can be decoded from the check blocks, with the success probability showed before. The decoding process is also divided into two steps. In the first step a $1 - \epsilon/2$ fraction of composite message blocks should be recovered. The knowledge of this fraction of blocks is enough to decode the original message: the composite message has such a property thanks to the redundancy added by the outer code. In the second step, the original message is recovered from the composite message blocks obtained in the first step.

In order to successfully recover the needed fraction of composite message blocks, it is necessary to know the degree of each check block and the composite message blocks from which it is made up (also called *adjacent blocks*). How to send this information to the receiver must be implemented on the transmitter side. However, if the receiver uses the same random number generation algorithm as the transmitter, it will only be necessary to send the seed to reach this objective. Next, the decoding process can start, following these steps:

1. Find a check block with only one adjacent block ($d = 1$) and recover this composite message block.

2. Remove this recovered block from other check blocks that also have this recovered block as adjacent (by simple subtracting it; that is, computing the XOR again). After this, some check blocks can become degree-one blocks.

3. Continue with this process until a $1 - \epsilon/2$ fraction of composite message blocks is recovered. The process fails if, in some of these steps, there are no degree-one blocks.

When all the necessary composite message blocks are recovered, the same process can be used to obtain the original message blocks. In this case the success probability is close to one because only the auxiliary blocks have a degree higher than one.

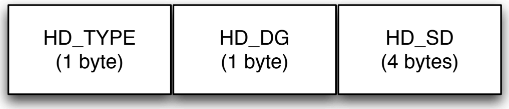

Figure 5.4: Online codes protocol header

5.3 Implementation details

Among the different implementations of Fountain Codes described in the previous section, Online codes were selected for the different experiments performed in this chapter. These codes present a linear encoding/decoding cost, and moreover, they are not protected by patent like Raptor and LT codes.

In order to develop an application based on Online codes, the implementation available in [imp, 2014] was used. However, that software only allows the coding and decoding of a local file. Therefore, UDP transmission capability has to be added and a very simple protocol was designed. One of the main drawbacks of Online codes (and of Fountain codes in general) is that the receiver should store a high number of coded packets before starting the decoding process. This number increases as the number of source blocks rises. To solve this problem, the implemented protocol is able to fragment the input file into smaller data chunks, which have a maximum size defined by the user. To this end, this protocol uses the header shown in Figure 5.4 and defines four types of message:

- *OC_FIRST* (HD_TYPE = 5). Message sent by the server at the start of the transmission to notify the clients of the number of chunks in which the input file has been divided. This data is sent in the HD_DG field, while HD_SD is set to 0.

- *OC_START* (HD_TYPE = 3). When the transmission of a new chunk starts, the server sends this message to indicate the number of source blocks which the receivers should recover. This information is enclosed in the HD_DG header field, while the seed used to generate the adjacent blocks of the composite message is sent in the HD_SD field.

- *OC_ACK* (HD_TYPE = 2). This message is used by a receiver to inform the server that its decoding process has finished. When the server receives an OC_ACK from all the clients, it starts the transmission of the next data chunk. Both header fields are set to 0 in this message.

- *OC_DATA* (HD_TYPE = 1). Message used to send a coded packet. The header includes the packet degree (HD_DG) and the seed used to generate the auxiliary blocks (HD_SD).

If no feedback channel is available, the server will not receive OC_ACK packets. In such scenarios, the number of data packets transmitted for each block should be dynamically calculated depending on the channel losses. Luckily, this problem does not appear in HPAV networks.

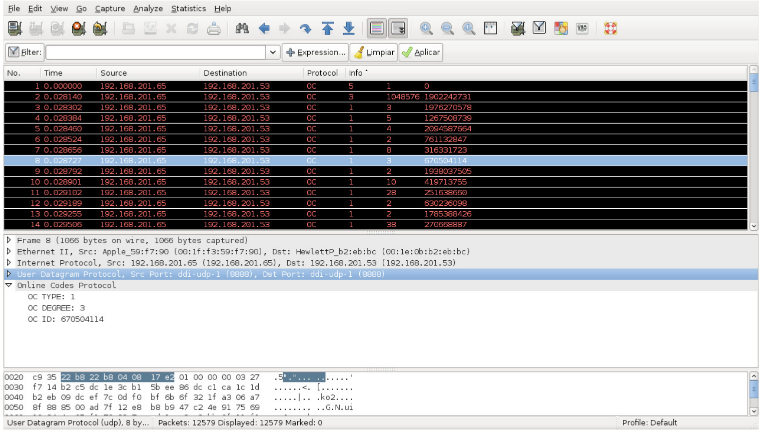

```
No.   Time      Source          Destination     Protocol Info
    1 0.000000  192.168.201.65  192.168.201.53  OC       5    1        0
    2 0.028140  192.168.201.65  192.168.201.53  OC       3    1048576  1902242731
    3 0.028302  192.168.201.65  192.168.201.53  OC       1    3        1976270578
    4 0.028384  192.168.201.65  192.168.201.53  OC       1    5        1267508739
    5 0.028460  192.168.201.65  192.168.201.53  OC       1    4        2094587664
    6 0.028524  192.168.201.65  192.168.201.53  OC       1    2        761132847
    7 0.028656  192.168.201.65  192.168.201.53  OC       1    8        316331723
    8 0.028727  192.168.201.65  192.168.201.53  OC       1    3        670504114
    9 0.028792  192.168.201.65  192.168.201.53  OC       1    2        1938037505
   10 0.028901  192.168.201.65  192.168.201.53  OC       1    10       419713755
   11 0.029102  192.168.201.65  192.168.201.53  OC       1    28       251638660
   12 0.029189  192.168.201.65  192.168.201.53  OC       1    2        630236098
   13 0.029255  192.168.201.65  192.168.201.53  OC       1    2        1785388426
   14 0.029506  192.168.201.65  192.168.201.53  OC       1    38       270668887
```

```
▷ Frame 8 (1066 bytes on wire, 1066 bytes captured)
▷ Ethernet II, Src: Apple_59:f7:90 (00:1f:f3:59:f7:90), Dst: HewlettP_b2:eb:bc (00:1e:0b:b2:eb:bc)
▷ Internet Protocol, Src: 192.168.201.65 (192.168.201.65), Dst: 192.168.201.53 (192.168.201.53)
▷ User Datagram Protocol, Src Port: ddi-udp-1 (8888), Dst Port: ddi-udp-1 (8888)
▽ Online Codes Protocol
    OC TYPE: 1
    OC DEGREE: 3
    OC ID: 670504114
```

```
0020  c9 35 22 b8 22 b8 04 08  17 e2 01 00 00 00 03 27   .5"."... ......'
0030  f7 14 b2 c5 dc 1e 3c b1  5b ee 86 dc c1 ca 1c 1d   ......<. [.......
0040  b2 eb 09 dc ef 7c 0d f0  bf 6b 6f 32 1f a3 06 a7   .....|.. .ko2....
0050  8f 88 85 00 ad 7f 12 e8  b8 b9 47 c2 4e 91 75 69   ........ ..G.N.ui
```

```
User Datagram Protocol (udp), 8 by...   Packets: 12579 Displayed: 12579 Marked: 0   Profile: Default
```

Figure 5.5: Wireshark plugin

Finally, to facilitate the protocol implementation and the results extraction procedure, a Wireshark plugin was created. The plugin (called *dissector*) creation process is well documented in the application website [wir, 2014]. A snapshot of the protocol traffic capture is shown in Figure 5.5. As can be seen, the content of header fields is shown in the protocol info section, to facilitate the post-processing of the results.

5.4 Reliable data transmission

Although in the previous chapter it was said that the flow control implemented in the modems causes packet losses to be close to zero, there are still some situations where the modems lose some frames. Two examples of those situations are highly saturated environments, where the number of collisions can be very high, and environments with high asynchronous impulsive noise conditions. In traditional networks, to overcome these losses, the TCP protocol is used. However, TCP protocol does not perform correctly in PLC networks due to the following reasons [Francis et al., 2012]:

- *Random losses*. TCP was designed for Ethernet networks and it assumes that all packet losses are caused by congestion. Therefore, after a packet loss is detected, the protocol launches the congestion avoiding mechanisms that could considerably reduce the network throughput.
- *Contention*. When TCP protocol is used, the communication is bidirectional. Therefore, transmitter and receiver have to compete for the channel to transmit data and ACK packets respectively. This causes an increment in the number of collision, even increasing the previously described effect.
- *Variable Round Trip Time (RTT)*. Most of TCP timeouts are defined according to the RTT. However, in PLC network this RTT is very time-variant, causing duplicate retransmissions or the assignment of very high timeout values that can affect to the protocol performance.

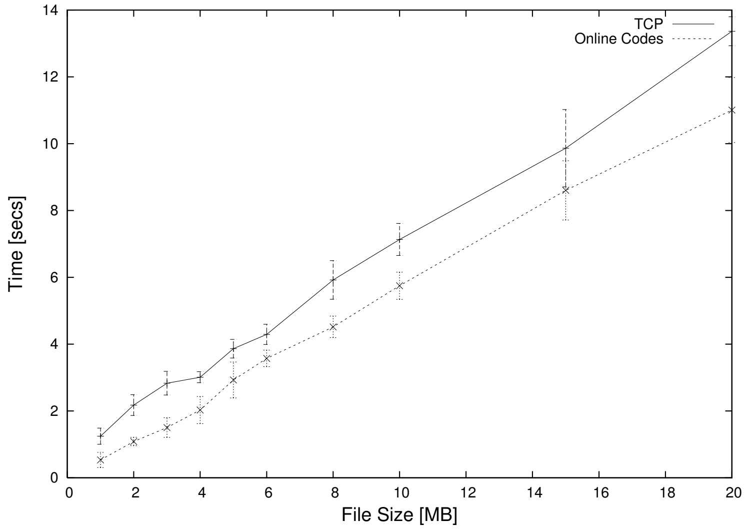

Figure 5.6: Duration of TCP and Online Codes sessions in a scenario with two (background) data flows sharing the channel.

- *Assymetric channel capacities*. In PLC systems it is very common to find different channel capacities for the downlink and the uplink in a communication between two stations. If uplink capacity is lower than downlink, this results in queuing up of ACK messages, becoming the traffic bursty in nature.

Instead of using TCP, we propose in this work the use of an application that implements some kind of forward error correction mechanism, for example, Fountain codes. In the following experiments, we want to compare the performance achieved by both options. To this end, the Online code application described before and a TCP socket will be compared.

The scenario of these experiments is the described in Figure 4.1. There, PC15 and PC9 acts as TCP and Online code server respectively. The other computers are used to generate background traffic that compete for the channel with the evaluated transmission. Firstly, both file transmission applications are evaluated in a scenario with other two simultaneous TCP file transmission connections. The size of the transmitted file varies from 1 up to 20 Mbytes. In this case, both applications are able to receive the full file without errors. Therefore, in the evaluation we are going to compare them taking into account the necessary time to receive the full file. Figure 5.6 shows the average duration of the TCP and Online Code sessions, extracted from 5 different experiments. In addition, the figure also represents the 95% confidence interval. The first result that can be concluded from the previous figure is that the Online code sessions are always faster than the TCP sessions. In addition, the increase of the TCP sessions with respect to the Online code sessions is approximately constant and equal to 1 second, although for large files this increment increases up to 2 seconds. Therefore, it can be drawn that in a contention scenario the performance achieved by an Online Codes-based file transmission application is better than the performance achieved by a TCP-based file transmission application.

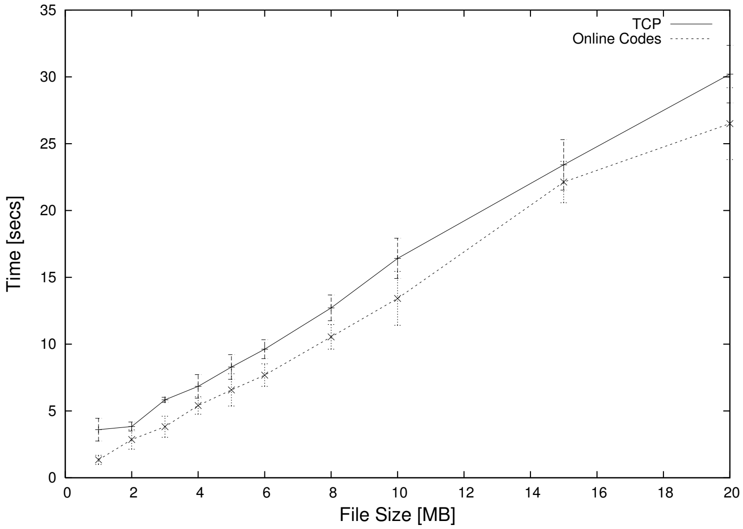

Figure 5.7: Duration of TCP and Online Codes sessions in a scenario with four (background) data flows sharing the channel.

Next, both file transmission applications are evaluated in a contention scenario, but in this case, with four simultaneous file transmission connections. Figure 5.7 shows the average duration of the TCP and Online code sessions, extracted again from 5 different experiments, and the associated 95% confidence interval. In this scenario, the Online Codes sessions are also faster than the TCP sessions. However, in this case the increase of the TCP sessions with respect to the Online Codes sessions is higher than in the previous scenario, ranging from 2 to 4 seconds depending on the size of the file. On the other hand, if these results are compared with those presented in Figure 5.6, we can observe that the increase of simultaneous file transmission connections causes an increase in the length of the sessions. This result is absolutely obvious because in this case the broadcast medium has to be shared by a larger number of users.

As a conclusion, in multiple access networks (like in-home PLC based networks), it has been proven that the performance achieved by a Online codes based application is better than the performance achieved by a TCP-based file transmission application.

5.5 Asymmetric interfaces aggregation

In a building or a house, it is very common to have more than one technology to deploy a home network. Therefore, an application that makes possible the aggregation of different interfaces would be very useful, as it will provide higher bandwidth, fault tolerance and load balancing.

The Linux Kernel contains a driver called Bonding [bon, 2014] that allows the aggregation of Ethernet interfaces. The main problem with this driver is that it is not prepared for asymmetric interfaces and even less for variable capacity technologies like PLC. In this section, an improvement of the bonding module, that works properly in asymmetric scenarios by using Fountain Codes, is presented.

Bonding Driver modification

The Linux bonding driver provides a method for aggregating multiple network interfaces into a single logical *bonded* interface. This driver provides seven different working modes. Among them, the most interesting one is the *Round-Robin* mode, which transmits the packets using the aggregated interfaces in a sequential order. With this mode, load balancing and fault tolerance are achieved. However, when different technology interfaces are aggregated, the module must transmit by all the interfaces at the worst rate (i.e., the minimum rate) in order to avoid packet disordering.

To develop a driver that works properly with asymmetric interfaces a modification of the *Round-Robin* mode is proposed. A new variable is defined within the main structure of the module to store the minimum transmission rate among the aggregated interfaces. This variable is used to determine the amount of packets that each interface will transmit. Concretely, in each turn, the driver will transmit by each interface a number of packets equal to the times that its transmission rate exceeds the minimum transmission rate.

Note that, for variable capacity technologies, it is necessary to periodically measure the channel capacity in order to update the packets distribution (or even to eliminate an interface if it fails). This capacity measurement procedure has to be as fast as possible and it should avoid sending too much information to not affect other stations in shared channels, such as PLC or Wireless. The capacity measurement procedure used in this work is explained below.

However, this packet distribution update only solves the long term capacity variations, and there are other short term problems that can seriously affect to the data transmission when this driver is used:

- Packet losses due to an unpredictable and short-term phenomenon, such as impulsive noise in PLC channels, or due to collisions in the shared channel.

- Packet disordering due to capacity variations between two bandwidth measures.

In order to overcome these problems, the use of fountain codes is proposed in this work.

Bandwidth Measurement Procedure

In order to configure the Round-Robin parameter, a link capacity measurement of the aggregated links is needed. Since some of the technologies that can be aggregated provide variable capacity links, this bandwidth estimation procedure has to be periodically executed. In this work, a completely integrated tool that uses packet dispersion techniques for estimating these capacities has been developed. This tool provides an efficient and accurate capacity measure of each of the aggregated links.

The capacity measurement system lays in packet dispersion concepts. The basics of the packet dispersion techniques were originally proposed in [Jacobson, 1988]. In this paper, it is discussed the feasibility of obtaining the capacity of one link using the information of the interarrival time of two packets sent through that link if they are injected back-to-back, i.e., if there is no time separation within transmissions of the individual

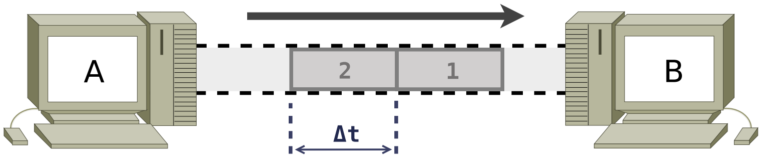

Figure 5.8: Illustration of the packet dispersion technique.

packets. In [Harfoush et al., 2009] this procedure is employed to measure different bandwidth links.

An illustrative scheme of this concept is showed in figure 5.8, where the capacity of the link between *host A* and *host B* is intended to be measured. For that purpose, two packets of size $s(p)$ are injected back-to-back into the link. In this case, the interarrival time of the two packets (Δt) will contain information related to the capacity of the link (see expression (5.10)). Therefore, the link capacity can be obtained by measuring the interarrival time of the packets in *host B* and by using the expression (5.11).

$$\Delta t = \frac{s(p)}{c} \tag{5.10}$$

$$c = \frac{s(p)}{\Delta t} \tag{5.11}$$

However, time measurements in computer systems are limited by clock resolution. Therefore, the accurate measurement of a very small time like Δt would be very difficult. Thus, in order to get better capacity estimations, it is possible to send more than two packets and measure the interarrival time between the first and the last packet ($\Delta t'$). In this case, if n packets of size $s(p)$ are transmitted back-to-back, the link capacity can be obtained by using expression (5.12).

$$c = \frac{s(p) \cdot (n-1)}{\Delta t'} \tag{5.12}$$

The value of n must be chosen to balance the trade off between time accuracy and traffic load. Moreover, in order to guarantee that the n packets are transmitted back-to-back, the proposed asymmetric bonding drive disables the hardware interruptions during the packet transmission.

The measurement system has to be divided into two parts. The first one has been embedded in the bonding system, where the sending capabilities are implemented. The second one has been implemented as a new socket family, which will be responsible of calculating the channel capacity estimations. This new socket family has been developed from the Linux Raw socket family [afp, 2014], and the functionalities for making highly accurate time measurements are implemented using specific kernel function called *ktime* functions [kti, 2014]. Once the capacity is estimated, the socket provides the bonding module with this information via the $/proc$ file-system interface.

At startup, three parameters must be set in the measurement system:

- The number of packets used in each measure (*n*).

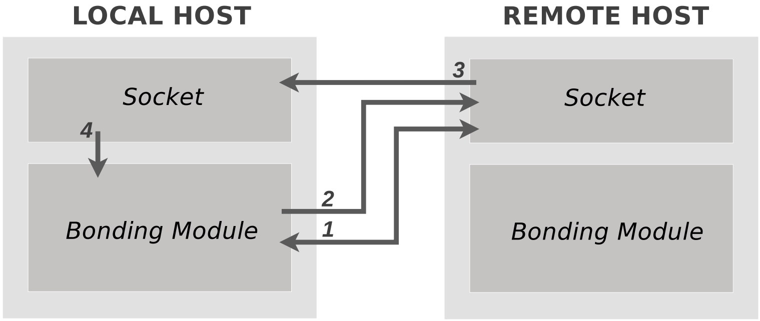

Figure 5.9: Sequential steps of the measurement procedure.

- The number of repetitions of the measurement procedure (*m*).
- The time period between two reconfigurations (*T*).

The possibility of repeating the measure *m* times is implemented to avoid possible errors of a single measure. These errors are quite common in shared medium systems like PLC.

The process used to measure one link is shown in the figure 5.9. In this figure, the host that starts the measurement procedure and the host at the end of the link are labeled as *local host* and *remote host* respectively. Every *T* seconds, the bonding module establishes a connection with the socket in the other host (step 1). By this connection procedure the bonding module tells the socket the procedure parameters (*n*, *m*). After this, the bonding module sends *m* series of *n* packets to the remote socket (step 2). The socket obtains the interarrival time between the first and the last packet of each serie and estimates the values of the link capacity using expression 5.12. With these estimations, the socket computes an histogram and estimates the final capacity for the link as the most repeated value in this histogram. This capacity value is sent back to the local host (step 3) and, once there, it is passed to the bonding module using the $/proc$ file-system interface (step 4).

Using this procedure, the bonding module estimates the capacity of the two aggregated links every *T* seconds and recalculates the round robin parameter to adapt the packet relation to eventual capacity changes. In this work, ten packets ($n = 10$) and five repetitions ($m = 5$) were employed. Under these conditions, the whole measurement and reconfiguration procedure injects approximately 75 *kB* of traffic into each link. The period between reconfigurations has been set to $T = 600$ seconds.

To check the proper functioning of the proposed method of interface aggregation, a test scenario composed by two computers was built. These computers were connected by a Fast-Ethernet link and by two F5D4076 Belkin PLC modems (see Figure 4.2). Fast-Ethernet works at constant rate of 100 Mbps. On the other hand, the PLC modem uses the MediaXtream technology described before, working at a variable capacity but limited up to 1 Gbps (although in fact, the TCP flows are transmitted at around 300 Mbps).

The first step in this experiment was the validation of the proposed capacity measurement procedure. The results are showed in Figure 5.10. As can be seen the Fast-Ethernet measure is very accurate (since it is a constant capacity interface) while the PLC result can

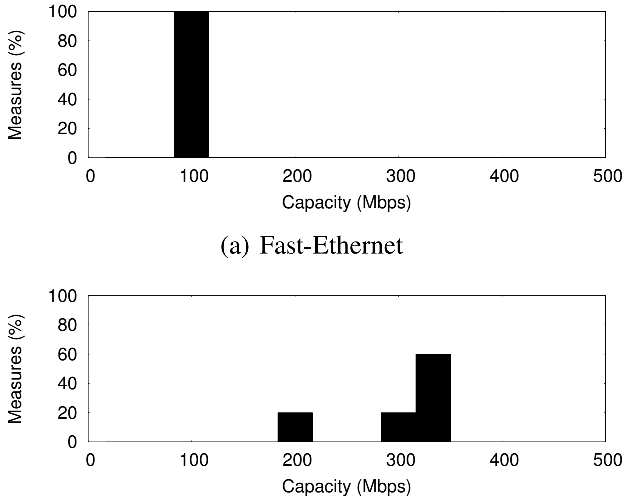

(a) Fast-Ethernet

(b) PLC

Figure 5.10: Bandwidth Estimation Histograms.

present some wrong values. However, by repeating the bandwidth estimation procedure five times the correct bandwidth value can be obtained in a precise way.

A histogram representation was chosen because no much precision is needed. The selected capacity will be the central value of the most repeated histogram column, and the packet distribution is obtained through the following expression:

$$p_i = \left\lfloor \frac{B_i}{W} \right\rfloor \tag{5.13}$$

were B_i is the bandwidth of the ith interface and W is the worst bandwidth value between the considered interfaces. Applying procedure, in the presented experiment the driver will transmit three packets by the PLC interface and one by the Fast-Ethernet interface in each turn.

Once the packet distribution was obtained, the modified bonding driver was evaluated through a Raw Socket. A huge amount of data was transmitted by each interface separately and by the *bonded* interface. In both cases, the data rate at the receiver side was measured using WireShark. In order to obtain more realistic results, a noise source (i.e. a energy-efficient bulb) was connected to an outlet near to the PLC modem to cause a fast transmission rate fading. The results are showed in Fig. 5.11, where it can be seen that the transmission rate achieved by the bonding interface is higher than the rate achieved by the other interfaces separately. The bandwidth obtained with the original bonding driver is also showed. As expected, it transmits by each interface at the lowest rate, achieving a bandwidth rather worse than the obtained with the modified driver. Note that it is not possible to transmit by each interface separately and by the *bonded* interface at the same time. Therefore, the results were obtained at different times but connecting the noise source at the same instant.

The bandwidth estimation procedure is periodically executed. Therefore, some time after the noise source connection, the system is able to check the new PLC capacity

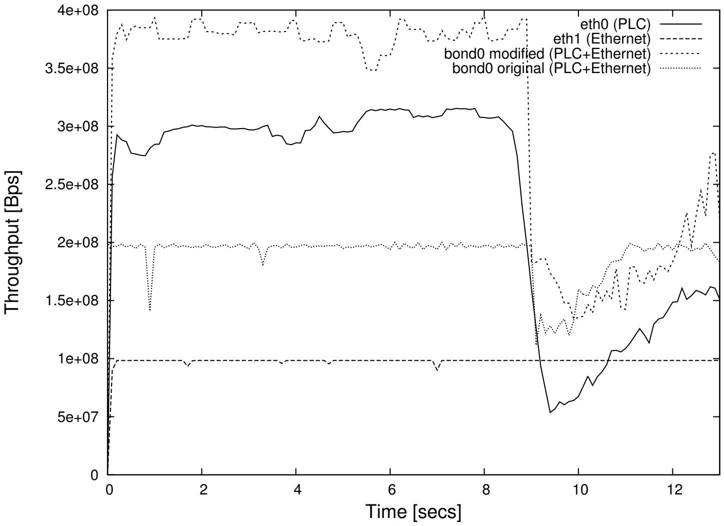

Figure 5.11: MAC layer transmission rate. Energy efficient bulb connected to the low tension network at 8 secs.

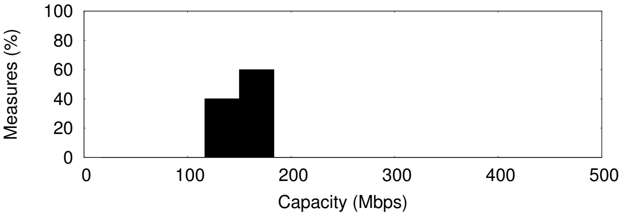

Figure 5.12: Bandwidth Estimation Histogram after noise source connection.

(around 175 Mbps, see figure 5.12) and from this moment, the bonding driver will transmit only one packet by each interface.

It must be taken into account that a little amount of packets transmitted will probably be received out of order. However, the use of Fountain Codes eliminates the necessity to rearrange those packets at the reception side. TCP protocol can also be used to overcome the packet loss and disordering. However, in the previous section it was shown that a Fountain codes based application works better than a TCP based one over PLC networks because TCP defines most of its parameters according to the steady state Round Trip Time (RTT) value. Obviously, the typical rate variations in a PLC channel introduce a dynamism in the RTT that TCP cannot follow.

Finally, files from 1 up to 10 Mbytes were transmitted between the two computers using each interface separately with TCP protocol. Then, these interfaces were aggregated to a logical interface and the transmission of the same files was made but now, using Fountain codes and TCP. Fig 5.13 shows the average duration of each session, from five equivalent experiments. The figure also represents the 95% confidence interval.

The results show that the transmission time obtained with the Fountain codes is always lower than the time obtained by each interface separately and even by the *bonded* interface when TCP is employed. On the other hand, the gain obtained by the online codes

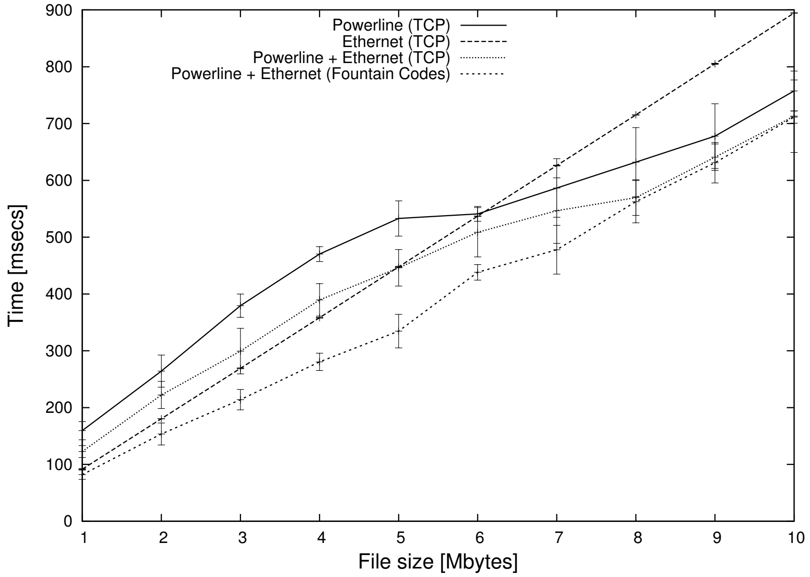

Figure 5.13: Duration of TCP and Fountain Codes sessions. The confidence interval has been set to 95%.

diminishes as the size of the file rises because the high memory consumption. To solve this problem it is enough to conveniently divide the large files into small ones and transmit them separately. It is important to remark that the employed modems are able to work at around 300Mbps, but only if needed. The default rate is approximately 90 Mbps. That is the reason because of the slope of the PLC transmission time curve diminishes when the file size is larger bigger than 5MB.

5.6 Publications

The work developed in this chapter has been partially published in the following references:

- Muñoz, J.P., Piñero, P.J., Malgosa, J., Manzanares, P., Sanchez, J.C., *Rateless Codes for Reliable Data Transmission over HomePlug AV Based In-Home Networks*, International Conference on Software and Data Technologies (ICSOFT 2009, Revised Selected Papers published in Communications in Computer and Information Science series), 2011.

- P.J. Piñero, D. Montoro, J. Malgosa, P. Manzanares, J.P. Muñoz, *Rateless codes for heterogeneous in-home interfaces aggregation*, IEEE International Symposium on Power Line Communications and Its Applications (ISPLC 2011).

- D. Montoro, J. Malgosa, P.J. Piñero, J.P Muñoz, P. Manzanares, *An Implementation of a Highly Accurate Timestamping System Embedded in the Linux Kernel and its Application to Capacity Estimation*, International Conference on Software and Data Technologies (ICSOFT 2011)

Chapter 6

Multicast

Abstract- Homeplug AV implements an inefficient multicast mechanism in which these communications are carried out as successive point-to-point transmissions. In this chapter, the limitations of this approach will be analyzed and new algorithms that improve the multicast performance of the standard will be proposed and evaluated using the previously presented simulator. They are firstly compared in terms of their physical bit rate. Finally, their capacity to deliver a video streaming service is also assessed.

6.1 Introduction

Multicast communications are very important in shared medium networks, like PLC. Thanks to multicast technology it is possible to transmit an information flow to a (probably great) set of receivers using only one transmission flow. Otherwise, collisions and delays would frustrate the provision of the service. There are not a lot of services that are multicast in nature, but most of the used in in-home and in-building scenarios are, like for example IPTV or digital-radio.

As it was previously said and corroborated through real measurements, HPAV does not implement real multicast data transmission. This is because its bit-loaded OFDM physical layer has been designed to exploit the frequency selectivity of the channel, which is a very link dependent feature. Therefore, multicast transmissions in HPAV networks are implemented as a set of consecutive point-to-point transmissions that are carried out in a transparent way to end users.

The multicast problem has been widely explored in wireless scenarios, and some solutions have been recently proposed. They can be divided into two categories: Solutions that try to minimize the total power consumption under the fixed system throughput constraint [Kim et al., 2007][Wu et al., 2010], and solutions that maximize the total system throughput under the power consumption constraint [Suh and Mo, 2008] [Liu et al., 2008] [Bakanoglu et al., 2010]. However, these results cannot be directly applied to PLC, since the maximum Power Spectral Density (PSD) is the most restrictive constraint in this technology. In fact, all carriers are transmitted at the maximum power level allowed by the PSD mask. Hence, decreasing the power level used in one carrier does not allow increasing it in another one. On the other hand, the contributions to this area in PLC networks are very limited. To the our best knowledge, the only relevant contribution related to multicast communications in these networks can be found in [Maiga et al., 2010], where the use of pre-coded OFDM is proposed. This solution improves the multicast throughput but requires significant changes at the physical layer, which discards it as a real alternative for the HPAV standard.

Moreover, these works only evaluate the physical layer transmission rates, but do not consider their implications at higher layer services. A common feature of the aforementioned multicast works is that they have been accomplished in wireless scenarios or using PLC channel models that generate uncorrelated channels. Nevertheless, all the links established in a given in-home PLC network share a common network layout, which causes the channels to exhibit some degree of correlation. This correlation has been traditionally neglected because it has no influence on the physical layer analysis in point-to-point communications. However, it cannot be disregarded when assessing multicast algorithms, since their performance is strongly dependent on the differences among the involved channels. The larger the dissimilarities among them, the poorer the multicast performance.

In this chapter, it will be evaluated the performance of multicast communications in a HPAV network using the previously presented network simulator. It will be shown that it can be significantly improved by means of the classical multicast algorithm in which the number of bits per carrier is determined by the user with the worst SNR. In addition, a more elaborated multicast algorithm is proposed for scenarios with higher number of users. Finally, it will be assessed the performance of a video streaming service using the multicast strategy implemented in the HPAV standard and a modified version that includes the classical multicast algorithm.

6.2 Multicast Communications Algorithms

6.2.1 Multicast communications in the HPAV standard

In order to send a multicast frame to a multicast group, the current version of the HPAV standard sends one point-to-point frame to each member of the multicast group. This technique clearly degrades the performance of multicast services as the number of receivers increases. Its effective multicast transmission bit rate can be calculated by means of expression (6.1). Since transmissions are serially accomplished, the time required to accomplish the multicast transmission, T_M, is the sum of the transmission times of the M multicast clients, t_m, with $m = 1...M$. Therefore, assuming that the transmitted data has size L, and that the channel conditions remain invariable during the transmissions, the inverse of the multicast bit rate, C_M, will be the sum of the inverse of the different clients bit rates, C_m.

$$T_M = \sum_{m=1}^{M} t_m \Rightarrow C_M = \frac{L}{T_M} = \frac{L}{\sum_{m=1}^{M} t_m} \Rightarrow \frac{1}{C_M} = \frac{\sum_{m=1}^{M} t_m}{L} = \sum_{m=1}^{M} \frac{1}{C_m} \tag{6.1}$$

As it will be shown below in this chapter, this poor performance can be improved with a multicast algorithm that selects a common tone map for all the multicast clients.

This is the most straightforward multicast strategy and will be referred to as Greatest Common Tonemap (GCT). Although its performance in PLC networks is much better than in wireless environment, it still decreases rapidly when the number of user increases. Therefore, a new algorithm is proposed to tackle situations with a relatively high number of users, e.g., in a hotel floor. This algorithm will be referred to as Aggregated Multicast Bitrate Maximization (AMBM).

6.2.2 Greatest Common Tonemap (GCT)

In this technique, the constellation used in each carrier will be that of the multicast user with the worst SNR in the corresponding frequency band. Let us denote by $b_{m,k}$ the number of bits per symbol that the mth user would use in carrier k in a single-user scenario. The number of bits per multicast symbol in carrier k, b_k, is computed as

$$b_k = \min_m \left(b_{m,k}\right) \quad \text{for } m = 1...M, \tag{6.2}$$

and the multicast bit rate is

$$C_M = \frac{1}{T}\sum_{k=1}^{N} b_k, \tag{6.3}$$

where T is the OFDM symbol period and N is the number of OFDM carriers (917 in HPAV).

This algorithm is implemented at the physical layer and could be added to the HPAV standard with minimum changes. It is the simplest multicast algorithm and it has been widely evaluated in wireless networks obtaining poor performance [Suh and Mo, 2008]. Because of this fact, it has been traditionally discarded also for PLC. However, in contrast to wireless network, where users experience independent fading, channel responses in a given PLC network exhibit significant correlation among them. This reduces the differences among the SNR experienced by different users in a given sub-band. As a consequence, the performance of the algorithm is significantly better than in scenarios where channels from different users are uncorrelated. To the authors' best knowledge, this fact has not been previously considered in the literature.

6.2.3 Aggregated Multicast Bit rate Maximization (AMBM)

The objective of this algorithm is to maximize the aggregated multicast bit rate at the physical layer. This is done at the expense of achieving different bit rate for each multicast user. Therefore, retrieving information in these circumstances requires the use of some kind of coding in higher layers, which will be discussed at the end of this section. Hence, the suitability of this algorithm for PLC will depend on the trade-off between the gain achieved at the physical layer and the overhead introduced by the selected coding technique. Since the bit rate gain at the physical layer (with respect to the GCT) increases with the number of users, this strategy will be useful in scenarios with high number of users.

The aggregated multicast bit rate can be improved by solving the optimization algorithm shown in expression (6.4). The function $\rho_{m,k}$ indicates whether the mth client will use carrier k, $\rho_{m,k} = 1$, or not, $\rho_{m,k} = 0$, in the multicast transmissions.

$$\begin{aligned} &\max \sum_{m=1}^{M} \sum_{k=1}^{N} b_k \cdot \rho_{m,k} \\ &\text{subject to } \ b_k = \min_{m}(b_{m,k} \cdot \rho_{m,k}) \ \ \forall \rho_{m,k} = 1, m = 1...M. \end{aligned} \tag{6.4}$$

In this case, it is difficult to obtain an unique multicast bit rate value in order to compare it with the previous algorithms, because the algorithm assigns a different bit rate for each multicast user. In this paper, we consider that the multicast bit rate (C_M) can be computed as the average amount of multicast information delivered in a given time period,

$$C_M = \frac{1}{MT} \sum_{m=1}^{M} \sum_{k=1}^{N} b_k \cdot \rho_{m,k}, \tag{6.5}$$

which is larger than (6.1) and (6.3), as it will be shown later in this paper.

It is important to note that the AMBM algorithm is a non-linear integer programming problem, because of the "min" operator. As a consequence, it becomes an NP-hard problem with $(B \cdot M)^N$ possible solutions, where B is the number of different values that b_k might take, i.e. the number of different constellations. In our problem $B = 7$ (HPAV uses constellations with 1, 2, 3, 4, 6, 8 and 10 bits/symbol) and $N = 917$ as detailed in chapter 2. Hence, even for a scenario with only two users, it yields to 14^{917} possible solutions.

It must be also highlighted that, even assuming that the problem might be formulated as an Integer Linear Programming (ILP) problem, the computational complexity would be extremely high because of the large number of carriers. Moreover, the time required to solve an ILP problem does not depend only on the number of variables, but also on the constraints and constants of the problem. Hence, even for a fixed number of clients and carriers, the time needed to solve the problem is not deterministic, but depends on the quality of the involved links. Because of these pitfalls, suboptimal approaches based on Linear Programming (LP) are commonly used. However, while LP has reduced solving times, it leads to non-integer values of that, when rounded, might lead to solutions that are far from the optimum one. Hence, the following greedy algorithm is proposed to solve it:

For $k = 1...N$ do:

1. Sort the values of $b_{m,k}$, deleting duplicated elements. The resulting list, r, represents all the possible values that can be assigned to b_k.

2. For each element $r_i \in r$, calculate the sum of the number of bits per symbol that the different clients would obtain in the considered carrier if r_i is finally used as the number of transmitted bits. This magnitude can be denoted by B_k and is obtained by multiplying r_i by the number of clients with $b_{m,k} >= r_i$, which is denoted by $N(r_i)$. It should be taken into account that $\rho_{n,k} = 0$ if $r_i > b_{m,k}$, i.e., the mth client will not use carrier k.

3. Select the value of r_i that provides the highest B_k.

An example is given below to illustrate the procedure. For simplicity, only three carriers, denoted as k_0, k_1, k_2, are considered in an scenario with $M = 4$ clients. The single-user tone map of the different users are $b_{1,k} = [3,4,6]$, $b_{2,k} = [6,5,9]$, $b_{3,k} = [6,2,7]$, $b_{4,k} = [9,5,9]$. Hence, for k_0, $r = [3,6,9]$ and the following results are obtained when the second and third steps of the algorithm are executed,

- $r_1 = 3 \Rightarrow B_{k_0} = 3 \cdot N(3) = 3 \cdot 4 = 12$,
- $r_2 = 6 \Rightarrow B_{k_0} = 6 \cdot N(6) = 6 \cdot 3 = 18$,
- $r_3 = 9 \Rightarrow B_{k_0} = 9 \cdot N(9) = 9 \cdot 1 = 9$.

Since the highest bit rate is achieved when client 1 does not use carrier k_0, it results that $\rho_{m,k_0} = [0,1,1,1]$. The number of bits that the clients would extract from each multicast symbol is $b_{n,k_0} \cdot \rho_{m,k_0} = [0,6,6,6]$.

In the same way, for k_1, the obtained results are:

- $r_1 = 2 \Rightarrow B_{k_1} = 2 \cdot N(2) = 2 \cdot 4 = 8$,
- $r_2 = 4 \Rightarrow B_{k_1} = 4 \cdot N(4) = 4 \cdot 3 = 12$,
- $r_2 = 5 \Rightarrow B_{k_1} = 5 \cdot N(5) = 5 \cdot 2 = 10$.

Therefore, $b_{n,k_1} \cdot \rho_{m,k_1} = [4,4,0,4]$. Finally, using the same procedure, $b_{n,k_2} \cdot \rho_{m,k_2} = [6,6,6,6]$.

With these results, the number of bits per symbol obtained for each client is:

- $b_{1,k} = [0,4,6] = 10$,
- $b_{2,k} = [6,4,6] = 16$,
- $b_{3,k} = [6,0,6] = 12$,
- $b_{4,k} = [6,4,6] = 16$,

If the GCT algorithm is applied in the same scenario, the results would be $b_{1,k} = b_{2,k} = b_{3,k} = b_{4,k} = [3,2,6] = 11$. As expected, with the AMBM algorithm the clients with the best channel conditions obtain better results at the expense of reducing the bitrate of clients with bad conditions. This is in contrast to the results obtained with the GCT algorithm, where all the clients obtain the same bitrate to the detriment of clients with good SNR. On the other hand, the AMBM algorithm usually leads to different physical bit rates for each multicast client. As a consequence, a higher layer coding must be used to manage this asymmetry. Different alternatives can be used to this end, but the most well-known are the MDC (Multiple Description Coding) [Goyal, 2001] and the Fountain codes.

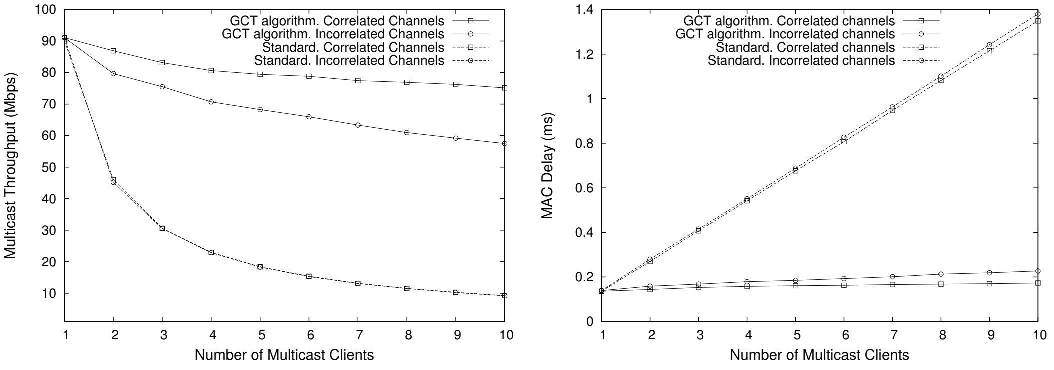

(a) Throughput

(b) Delay

Figure 6.1: Throughput and delay obtained with the standard HPAV algorithm and the GCT based version

MDC is a source coding technique used to separate a media stream into multiple substream called descriptors. The reception of only one of these descriptors is enough to decode and show the original audio or video but, the higher number of descriptors are received, the higher quality is obtained. The disadvantage of MDC is that it introduces a significant overhead, which for a video source is usually about 44% [Li and Liu, 2003].

On the other hand, the most popular Fountain codes nowadays are the Raptor codes, which introduce an overhead of about 4-5% [Luby et al., 2007]. Hence, this seems to be the most suitable alternative to be used in conjunction with the AMBM algorithm.

6.3 Evaluation

In this section, the presented multicast algorithms are evaluated using the simulation presented in chapter 3. Firstly, the influence on the throughput and the delay of the correlation among the channels of a given network is assessed. To this end, both the HPAV standard and the modified version that includes the GCT algorithm are evaluated. Secondly, the AMBM and the GCT techniques are compared. Finally, the performance of a video streaming service using the standard HPAV and the GCT based HPAV version is assessed.

6.3.1 Effect of the correlation among channels

This subsection analyzes the influence of the correlation among the channels of each in-home network. To this end, the standard HPAV and the GCT based version are compared in two scenarios. In one of them, the channels of each in-home network are uncorrelated. In the other, correlated channels are generated using the second version of the channel generator. Saturated conditions are assumed in both cases. Figure 6.1 depicts the mean throughput and the MAC delay experienced by the multicast clients as a function of the multicast group size.

Figure 6.1(a) shows that, as expected, the correlation among channels has nearly no effect when the multicast is implemented as point-to-point transmissions. On the other hand, when the GCT algorithm is used, discarding the correlation leads to an underestimation of the performance, ranging from about 8% for two users to about 23% for ten users.

It is worth noting that the GCT algorithm significantly outperforms the point-to-point solution for any number of multicast clients. Moreover, the improvement increases with the number of clients.

The GCT algorithm has been discarded as a multicast solution in other OFDM systems such as the 802.11 family standards. This conclusion has been traditionally extrapolated to PLC without taking into account the particularities of this environment. However, the obtained throughput results show that it is a simple and effective solution for in-home PLC networks.

Regarding the MAC delay, it can be seen that with the strategy used in the standard, it grows linearly with the number of clients. This is because between the transmission of two frames to a particular client, the transmissions to the rest of multicast clients should be made. On the contrary, this does not happen with the GCT algorithm, since all the transmissions are simultaneously received by all the group members. In this case, the delay increment is only caused by the decrease of the overall multicast capacity that occurs when the number of clients increases.

All the channels used in the simulations of the subsequent sections have been obtained using the correlated version of the channel generator.

6.3.2 Performance of the AMBM algorithm

As mentioned, the AMBM algorithm is intended to increase the multicast performance in scenarios with a high number of users. Figure 6.2(a) shows the multicast physical bit rate (C_M) obtained by the AMBM and the GCT for various multicast group sizes. Each curve has been obtained by averaging the results of 200 simulations. The AMBM algorithm always provides better results than the GCT algorithm. As expected, the obtained gain increases with the number of multicast client.

To clearly assess the gain of the AMBM with respect to the GCT, the average bit rate gain of the former with respect to the latter is depicted in Figure 6.2(b). As seen, the gain increases with the number of multicast clients, leading to 10% for multicast groups with 10 members. The reason for this behavior is that the probability of having one user with bad channel conditions increases with the size of the multicast group. This limits the multicast bit rate attained by users with good channel conditions when the GCT algorithm is used, but has very little effect when the AMBM is used.

Up to now, only the physical bit rate has been explored. However, the AMBM algorithm requires the use of high layer coding to allow proper decoding of the information by users with different physical bit rates. As previously mentioned, around 4-5% of overhead is introduced when raptor codes are used. Hence, according to Figure 6.2, the AMBM algorithm outperform the GCT solution only when the number of clients exceeds five, since the bit rate gain is higher than the coding overhead only from this point on. However, the introduction of a raptor encoder/decoder adds more complexity and resource consumption

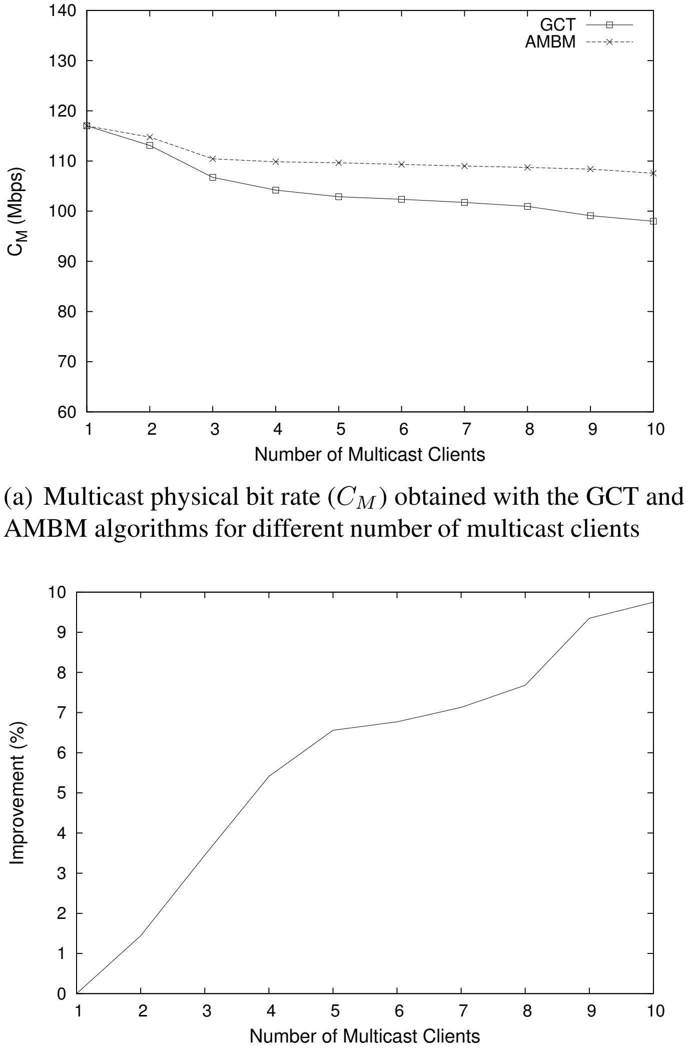

(a) Multicast physical bit rate (C_M) obtained with the GCT and AMBM algorithms for different number of multicast clients

(b) Average bit rate gain of the AMBM algorithm with respect to the GCT one

Figure 6.2: Comparison between AMBM and GCT algorithms

to the system, thus the use of AMBM algorithm is only recommended when a significant gain is obtained. The extrapolation of Figure 6.2 for larger multicast group sizes indicates that significant gains can be obtained for groups with more than 15 clients, where gains higher than 10% will be obtained.

6.3.3 Video streaming evaluation

This section assesses the performance of the standard HPAV and the modified version with the GCT algorithm, when they are used to deliver MPEG-2 video. The QoS requirements for this service are summarized in table 6.1. Since this is not a real-time service, it does not have any jitter or delay requirements.

Figure 6.3(a) depicts the obtained throughput as a function of the multicast group size

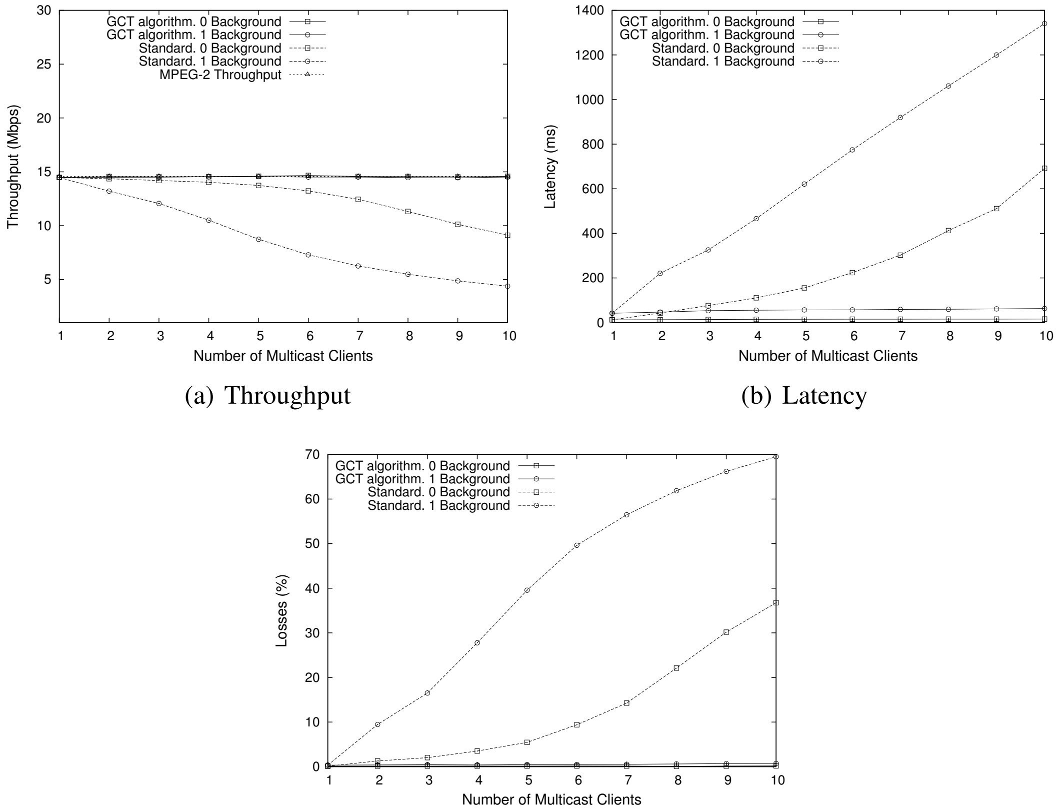

(a) Throughput

(b) Latency

(c) Losses

Figure 6.3: MPEG-2 throughput, latency and packet losses obtained with the standard HPAV and the GCT based version, with and without background traffic

when the multicast video server is transmitting to the clients with and without sharing the channel with another station that is performing a data transmission (background traffic). Figure 6.3(b)(c) shows the latency and data loss in the same scenario.

It can be seen that the GCT based version offers much better performance than the standard HPAV for this multimedia service. Without other traffic is present in the network, the point-to-point solution currently implemented in the HPAV can be used to transmit multicast video to a maximum of four clients. At this point, the packet loss reaches 5.46%. From this value on, the throughput decreases and packet loss increases in such way that the service performance is severely degraded. When the channel is shared with a background data transmission, the concatenated point-to-point solution used in the standard leads to bad results even with only two multicast clients (9.46% of the pack-

Table 6.1: QoS requirements for an MPEG-2 streaming service

Throughput	Packet loss	Latency
≈ 15 Mbps	5%	<4-5 seconds

ets are lost). On the other hand, the modified HPAV that includes the GCT algorithm achieves good performance in both cases (with and without background traffic) with up to ten multicast clients. In the figure, it can be seen that the results offered by this algorithm perfectly fits with the traffic offered by the MPEG-2 encoder.

6.4 Publications

The work developed in this chapter has been partially published in the following references:

- P.J. Piñero, J.A. Cortes, J. Malgosa, F.J. Ca nete, P. Manzanares, L. Diez, *Analysis and improvement of multicast communications in HomePlug-AV based in-home networks*, Computer Networks, Vol 62, pp. 89-100, 2014
- P.J. Piñero, J. Malgosa, P. Manzanares, J.P. Muñoz, *Evaluation of a New Proposal for Efficient Multicast Transmission in HomePlug-AV Based In-Home Networks*, Lecture Notes of the Institute for Computer Sciences, Social Informatics and Telecommunications Engineering, Vol. 82, pp. 58-70, 2012.

Chapter 7

Cross-Layer extension of HPAV CSMA/CA algorithm

Abstract- This chapter proposes a cross-layer extension of the CSMA/CA protocol used in HPAV. The objective is to allocate more bandwidth to nodes with QoS needs by giving them more channel access opportunities. An easy way to do this is by appropriately modifying the contention window size of the participants considering both the QoS requirements of the upper-layer services and the physical layer restrictions. The presented algorithm has been mathematically modeled and evaluated by means of simulation. Furthermore, the issues related to its implementation in real HPAV devices are addressed.

7.1 Introduction

As said in previous chapters, most commercial HPAV modems only implement a contention based service based on CSMA/CA at MAC layer. Therefore, when the number of stations present in the network is high, an excessive degradation of the QoS can be perceived by the end user. In the last years, several papers have been published that try to improve this aspect of HPAV networks. For example, in [Yoon et al., 2008] [Kriminger and Latchman, 2011], the CSMA/CA contention window size is optimized in order to obtain better QoS results. In addition, in mediums like PLC, cross-layer techniques have recently elicited much interest in the scientific community. These techniques allow the use of information of different layers (physical layer or upper layers) at MAC layer to improve the network performance. For example, [Papaioannou and Pavlidou, 2008] proposes a cross-layer optimization in the TDMA slots assignment procedure. However, to the best of our knowledge, there are not any publications about the application of cross-layer techniques to HPAV CSMA/CA protocol.

This chapter addresses the design and evaluation of a cross-layer extension for the HPAV CSMA/CA algorithm. It modifies the contention window size of the different clients using both physical layer information and the QoS requirements of the upper-layer services, obtaining in this way better results than any previously presented extension of the HPAV CSMA/CA standard version. The performance of this optimization technique has been evaluated with the HPAV simulator presented in chapter 3. This simulation tool implements both physical and MAC layers of the standard, which makes it ideal for evaluating cross-layer protocols.

7.2 Optimal HPAV CSMA/CA contention window size

7.2.1 Overview

Based on the Markovian model of the HPAV CSMA/CA protocol described in chapter 4, [Kriminger and Latchman, 2011] proposes an optimization of the contention window size (W) that improves the protocol performance for a large number of users[1]. To maximize the throughput, it is presented a constant contention window based scheme in which W must grow linearly with the number of stations present in the network (n) while the DC counter should always be initialized to a constant value. The constants which determine the linear relation between W and n will depend on the value selected for the DC counter. Different combinations of these values are tested in the referenced paper, being the best results obtained with values shown in eq. (7.1).

$$W(n) = 5 \cdot n + 10 \qquad for \quad DC = 3 \tag{7.1}$$

It is necessary to remark that the approximations taken to obtain this algorithm are only valid for a large number of active stations. Therefore, it is important to corroborate the exact number from which this algorithm obtains good results. To that end, both algorithms, the original an the optimal contention window size extension, are compared using the previously presented simulator. Figure 7.1 shows the evolution of the total network throughput under saturation conditions as the number of active stations increases. As can be seen, the reference algorithm outperforms the standard version of the protocol for a number of users higher than four. Since the number of active stations in a home network is usually higher than this value, it will be the starting point for the cross-layer extension proposed in this paper. However, it could also be applied to the standard CSMA/CA algorithm without any problem.

Both, this algorithm and the cross-layer extension proposed in this chapter are managed by the network Central Coordinator (CCo). According to HPAV standard, this node has a complete knowledge of the network and controls different aspects, such as the time allocated for CSMA/CA use or the TDMA scheduling. Hence, it should also manage the contention window of the different nodes.

7.2.2 Analysis

As it will be explained later, to adequately execute the presented algorithm it is needed an estimation of the QoS perceived by the upper layer service depending on the physical layer bitrate. The throughput could be used in this purpose but, to accurately calculate it,

[1] From now on we shall refer to the HPAV CSMA/CA algorithm as standard and to the extension proposed in [Kriminger and Latchman, 2011] as reference.

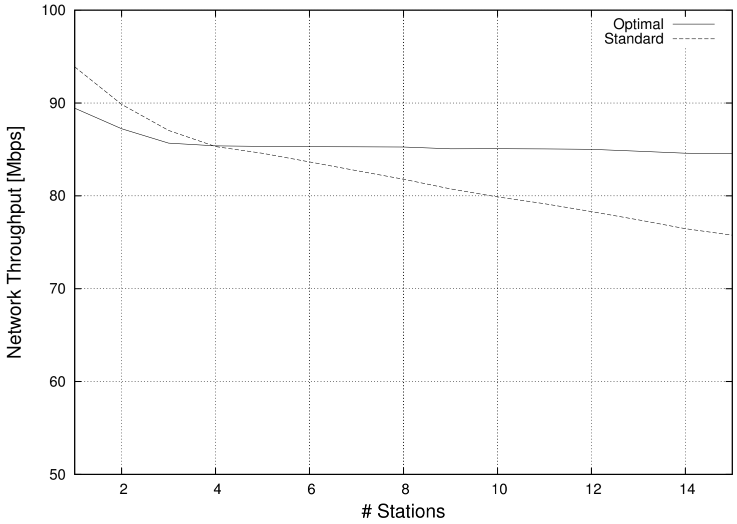

Figure 7.1: Throughput obtained with the original HPAV CSMA/CA algorithm and with the optimal contention window extension versus the number of active stations in the network

an estimation of the overhead introduced by the MAC layer in the reference algorithm is needed.

Firstly, it is important to remark that the overhead calculation has been performed under saturation conditions because it is the worst possible scenario. The overhead can be obtained through simple mathematical calculations and some simulations. It can be divided into three different terms, the "Fixed Overhead" (O_f), which is inherent to the protocol, the "Variable Overhead" (O_v), which depends on the number of contending stations (n) and the "Physical Block Overhead" (O_h), due to headers associated to the Physical Blocks:

$$O = O_f + O_v(n) + O_h \tag{7.2}$$

The former term can be obtained from the figure 2.5, where it can be extracted that O_f is approximately:

$$O_f = PRS0 + PRS1 + RIFS + ACK + CIFS \tag{7.3}$$

where these parameters have the values indicated in chapter 3.

On the other hand, the O_v term, which depends on the number of contending stations, includes the effects of the backoff and the collisions:

$$O_v = \sigma \cdot W_{BO}(n) + C(n) \tag{7.4}$$

where σ is the length of an idle slot ($35.84\mu s$) and $W_{BO}(n)$ is the mean window size chosen by a node when it achieves to transmit a frame. Therefore, the product of these two terms represents the mean backoff (BO) time. Finally, $C(n)$ represents the collisions effect.

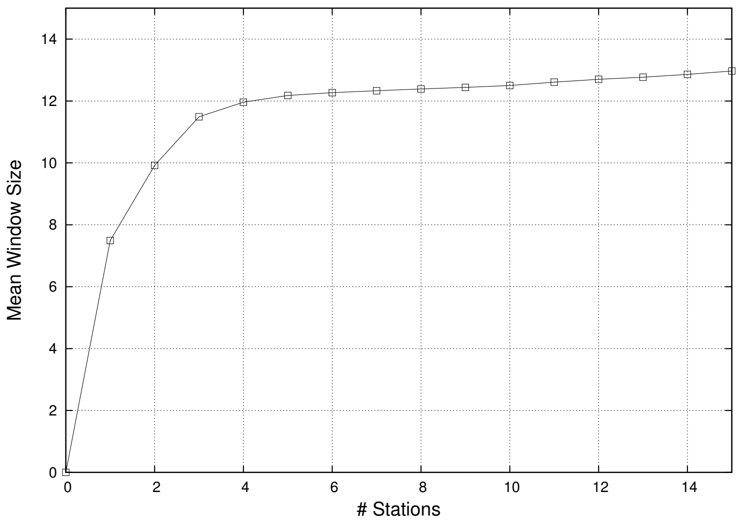

Figure 7.2: Mean contention window size selected for a successful transmission versus number of contending stations

A representative value for O_v can be extracted from Figure 7.1. It can be seen that with the optimal protocol the throughput decrement is very low for a number of clients between 4 and 15, which is a valid range for our purposes (below 4 clients is very unlikely that the cross-layer algorithm has to be launched. On the other hand, a HPAV network with more than 15 stations is also improbable due to the PHY layer constraints). For this range of stations, the network throughput drop is about 1 Mbps and, as it will be shown below, it is mainly caused by variations in the mean backoff time. Therefore, in this case, the overhead caused by collisions can be neglected ($C(n) = 0$).

Regarding the mean backoff time, the mean window value selected by a node when achieves to transmit its information versus the number of contending stations has also been calculated using the simulator. The results are shown in Figure 7.2. As can be seen, the mean window size ranges approximately from $W = 12$ ($n = 4$) to $W = 13$ ($n = 15$). This increment explains the small throughput loss shown in the previous figure. To obtain a general value for the protocol overhead, the worst case has been considered ($W = 13$).

Finally, the effect of the headers in the physical blocks (O_h) should also be included. The total length of these blocks is 520 bytes and their header length is 8 bytes. Hence, this overhead value can be easily calculated as follows:

$$O_h(\%) = \frac{8}{512 + 8} \cdot 100 = 1.5\% \tag{7.5}$$

Assuming the worst case in which the node is able to use the entire data transmission time (Maximum Frame Length, MAX_{FL}, is $2501.12\mu s$ including the RIFS in HPAV), the time spent in the transmission of these headers is:

$$O_h = (2501.12\mu s - 30.72\mu s) * 0.015 = 37.05\mu s \tag{7.6}$$

With the obtained values, the overhead introduced by the “Fixed Overhead” (O_f) and the “Variable Overhead” (O_v) terms in each frame transmission can be calculated as follows:

$$O = O_f + O_v(n) + O_h = PRS0 + PRS1 + RIFS + ACK + CIFS + 13 \cdot \sigma + 37.05 = 35.84 + 35.84 + 30.72 + 140.48 + 100 + 13 \cdot 35.84 + 37.05 = 845.95\mu s \tag{7.7}$$

As before, assuming the worst case, the overhead percentage can be calculated as follows:

$$O(\%) = \frac{845.95}{845.95 + MAX_{FL} - RIFS} \cdot 100 = \frac{845.95}{845.95 + 2501.12 - 30.72} \cdot 100 = 25.50\% \tag{7.8}$$

Then, by applying a security factor, the total overhead is approximately a 26%. Hence, the MAC throughput of a node when the optimal algorithm is used can be calculated using the following expression:

$$S_i \sim (1 - 0.26) \cdot \frac{C_i}{n} = 0.74 \cdot \frac{C_i}{n} \qquad \forall i \in 1...K \tag{7.9}$$

where C_i is the physical bitrate of the considered node and n is the number of active stations in the network.

Finally, to check that all the assumptions are adequate for a generic case, Figure 7.3 shows the evolution of the throughput under saturated conditions of one station as a function of the number of contending stations. It shows both the results obtained by simulation and the estimated values obtained from the deduced expression, supposing that all the stations have a physical layer capacity of 116 Mbps (Mean PHY bitrate of the stations after averaging 50 simulations according to Figure 3.7). As can be seen, it has been obtained a good estimator of the station throughput in the range of 4 to 15 stations, while the error obtained for a smaller number of stations is not very high.

7.3 Cross-layer protocol extension

7.3.1 Protocol overview

The main idea behind this cross-layer extension of the HPAV CSMA/CA protocol is the regulation of channel access through the modification of the contention window size of a set of stations. In other words, it reduces the window size of the stations with QoS problems, while it increases the window size of the rest of the stations. In this way, the resources can be more fairly distributed, giving more channel-access possibilities to stations with QoS problems. It is performed completely at MAC layer, but it needs the QoS requirements of the upper layer services and the physical layer capacity.

The protocol starts when a node suffers a QoS degradation, which can be caused by a drop of its physical capacity or because a new node has arisen to compete for the channel. In order to detect this degradation, the nodes define a lower and an upper threshold of the maximum admissible values for latency and jitter in different application layer services.

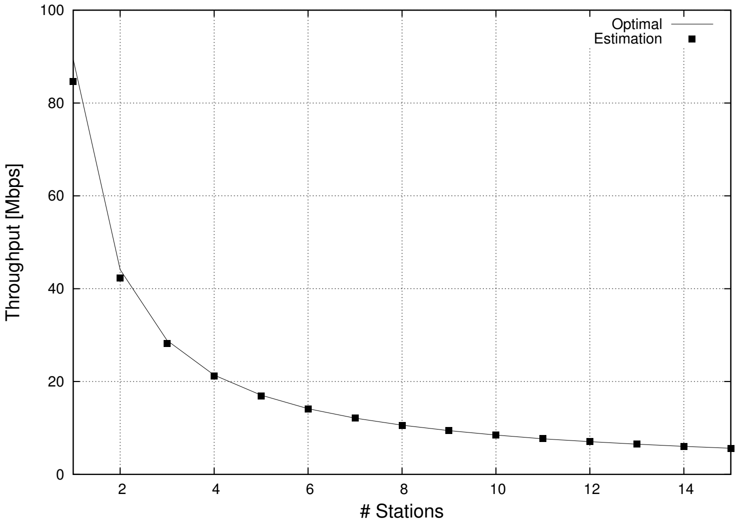

Figure 7.3: MAC throughput estimator evaluation

These maximum values are passed to the MAC layer when the service starts using the HPAV M1 interface, already defined for this purpose. When a node detects that more than 1% of MAC frames have been transmitted with a latency or jitter over the upper threshold, it is inferred that the service is close to fail, and it informs the CCo about it, using a new message called *alarm*. In that moment, the CCo starts the algorithm described in Section 7.3.3 and it asks all the nodes for the following three parameters: their physical bit rates (C_i), the bandwidth required by their services (SBW_i), and if the number of frames transmitted with a latency or jitter located between both thresholds is over 1%. The way of transmitting this information to the CCo will depend on the particular implementation of this protocol extension, but it could be done using new defined messages. From these parameters, the CCo classifies the nodes as follows:

- *Critical nodes*. Nodes with QoS problems that have launched the alarm. The objective is to increase their channel access opportunities to improve their performance.

- *Safe nodes*. Those that have a good QoS and may increase their contention window size to share some bandwidth with the critical nodes. They have more than 99% of frames below the lower threshold and fulfill Eq. (7.10), which as explained before, roughly estimates the QoS in the stations that do not launch an alarm.

$$SBW_i < 0.74 \cdot \frac{C_i}{n} \qquad \forall i \in 1...n \tag{7.10}$$

- *Border nodes*. The rest of the nodes. The service in these nodes is close to fail. Therefore, they should maintain their channel access opportunities.

7.3.2 Modeling the Effect of the Contention Window Size Modification

With the goal of accurately determining how to modify the contention window size of the safe and critical nodes, a mathematical model has been designed. The gain G, defined as the increase (or decrease) in the probability to win a channel access in a node due to the decrease (or increase) of its contention window size will be obtained. Consider a network of K stations, each one with a contention window size W_i. The U_i variable maintains the BC counter value that each station obtains for a particular channel access. Therefore, $U_i \in [1, W_i]$ with $P(U_i) = 1/W_i$ (for convenience, we will use the interval $[1, W_i]$ instead of $[0, W_i - 1]$). After the random backoff procedure, the channel access is obtained by the node with the lowest U_i value. Taking station 1 as reference, and without loss of generality, its channel access probability $P(win)$ can be calculated as follows:

$$P(win) = P(U_1 < min(U_2, ..., U_K)) \tag{7.11}$$

For simplicity, we define $m = min(U_2, ..., U_K)$. Applying the Total Probability law in (7.11),

$$\begin{aligned} P(win) = \sum_{i=2}^{W} P(win|m = i) \cdot P(m = i) = \\ \sum_{i=2}^{W} \frac{i-1}{W} \cdot P(m = i) = \frac{E[m]-1}{W} \end{aligned} \tag{7.12}$$

The same analysis can be made when the reference node decreases its contention window size by one. In this case $U_1 \in [1, W-1]$ and $U_i \in [1, W]$ $\forall i \geq 2$. Thus,

$$\begin{aligned} P(win) = \sum_{i=2}^{W} P(win|m = i) \cdot P(m = i) = \\ \sum_{i=2}^{W} \frac{i-1}{W-1} \cdot P(m = i) = \frac{E[m]-1}{W-1} \end{aligned} \tag{7.13}$$

The gain G obtained when a node decreases its contention window size can be easily calculated by dividing (7.12) by (7.13):

$$G = \frac{W}{W-1} = 1 + \Delta G \Rightarrow \Delta G = \frac{1}{W-1} \tag{7.14}$$

obtaining a positive increase ΔG which is inversely proportional to the new window size. On the other hand, the gain obtained when the reference node increases its contention window size can be calculated similarly (in this case the gain is negative):

$$G = \frac{W}{W+1} = 1 + \Delta G \Rightarrow \Delta G = -\frac{1}{W+1} \tag{7.15}$$

It is necessary to consider that the gains have been obtained assuming that, excepting the reference node, the rest of the nodes have the same $W_i = W$ $\forall i \neq 1$. However, it

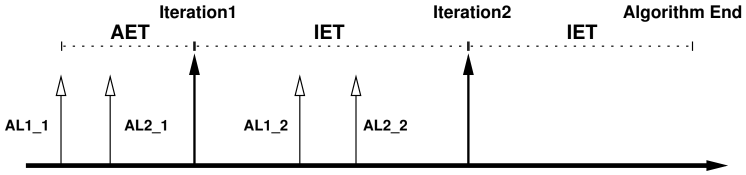

Figure 7.4: Algorithm timing sequence

is possible that, after more than one alarm has been processed, this uniformity no longer holds. But if K and W are large enough, $E[m]$ barely varies for large values of U_i and therefore (7.14) and (7.15) can still be considered true.

7.3.3 Proposed algorithm

The proposed algorithm is executed by the CCo after receiving the notification of a QoS degradation (e.g. alarm AL1_1 in Figure 7.4) and it works as follows:

1. Wait during *Alarm Evaluation Time* (AET) for other notifications of QoS degradation (e.g. alarm AL2_1 in Fig.2). This waiting time is needed because of a network performance drop usually affects to more than one node at the same time. This amount of nodes is referred as K_{crit}.

2. Decrease by one the contention window size of the *critical* nodes.

3. Select the minimum amount of safe nodes (K_{safe}) that better approximate Eq. (7.16), beginning with those which have a lower W_i.

$$\sum_{i=1}^{K_{safe}} |\Delta G_i| = \sum_{i=1}^{K_{safe}} \frac{1}{W_i + 1} \approx \sum_{i=1}^{K_{crit}} \frac{1}{W_{crit} - 1} \tag{7.16}$$

4. Increase by one the contention window size of each *safe* node selected in the previous step.

5. Evaluate the network behavior during *Iteration Evaluation Time* (IET). If in this period the alarms persist, or new alarms are launched (see Figure 7.4), the algorithm goes back to step 2. Otherwise, the algorithm ends.

In the case of Figure 7.4, the algorithm obtains a correct solution after two iterations. As can be seen in the figure, the procedure time T_{proc} of the proposed solution can be calculated using the expression $T_{proc} = AET + n_{iter} \cdot IET$. Note that both evaluation times (IET and AET, which are set in this work to 1 and 5 seconds respectively) are selected by the CCo depending on the involved services, considering that they have to be long enough to be able to detect the possible alarms.

In addition, a node that has triggered an alarm should inform the CCo when its service ends or when a predefined time has passed without any frame over the lower threshold (in this work this time has been set to 10 seconds, but it will depend on the specific

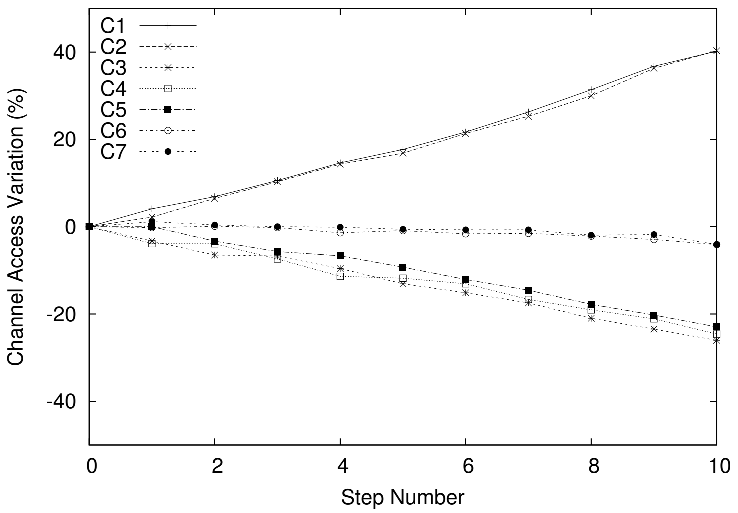

Figure 7.5: Channel access rate variation for the different nodes

application). After receiving this notification, or simply when the algorithm is not able to solve the problem after a predefined number of iterations, the CCo should restore the system to the previous state. In this last case, if the problem was caused by the arising of a new node to compete for the channel, it could be rejected by the CCo using the already implemented admission control functionality.

Fig. 7.5 represents the channel access rate variation as a function of the number of applied iterations in a scenario where seven nodes compete for the channel: two of them are *critical* (C1 and C2), other two are *border* (C6 and C7) and the rest are *safe* nodes (C3, C4 and C5). As can be seen, the channel access probability of the *border* nodes remains nearly constant. This figure can also help us to define the maximum number of iterations of the algorithm. In this case a maximum number of five iterations is chosen. A considerable gain for the *critical* nodes (approximately 20%) is obtained after five iterations, in a reasonable time.

Finally, it is necessary to talk about the selected values for the upper and lower thresholds used to classify the nodes. The upper threshold is used to predict that a service is close to fail. Hence, it should be strictly lower but simultaneously close to the maximum admissible value for the evaluated parameter. It is widely used in the literature values like 90% or 95%. We choose 90% value to have a little more time to ensure smooth implementation of our proposal.

On the other hand, the lower threshold is used to prevent the *safe* nodes to become *critical* nodes during the algorithm execution due to the decrement in their channel access rates. This fact should be avoided because it can cause the algorithm to deteriorate the whole system performance. By this reason, the lower threshold value should be far enough of the upper threshold. However, it must be also large enough to guarantee that there are enough *safe* nodes. To obtain the dominant condition, it is necessary to study first the amount of *safe* nodes needed by the algorithm. The window size in the reference algorithm is $5n + 10$ (where n is the number of contending stations) and substituting the obtained values for $4 <= n <= 15$ in eq. 7.16 during five iterations of the algorithm, the number of *safe* nodes is the same as the number of *critical* nodes. Therefore, if at an instant of time there are two or maybe three *critical* nodes, it will be required no more than two or three *safe* nodes. On the other hand, nodes transmitting raw data from services without QoS have not restrictions and can be always selected as *safe* nodes. Accordingly, the number of *safe* nodes needed with QoS restrictions is very small. Therefore, the restriction that the lower threshold should be far enough of the upper threshold dominates to the restrition of that it must be also greater enough to guarantee that there will be enough *safe* nodes.

There are many possibilities for the lower threshold value, but 70% satisfies the above restrictions. Using this value we have checked in our simulations that no *safe* nodes become *critical* during the algorithm execution and simultaneously there are always enough *safe* nodes to guarantee that the algorithm works fine. However, it is necessary to remark that different values can be selected depending on the evaluated system or the expected algorithm behavior.

Furthermore, to consider that a station is over a threshold, the 1% of frames should be over it. This 1% value was selected because in most of the QoS related literature [Szigeti and Hattingh, 2005], it is considered that the service fails when more than 1% of frames are above their corresponding QoS maximum admissible value (for example when more than 1% of frames have a latency over 150 ms for a real time service). Therefore, we consider this 1% adequate to evaluate when a parameter is above a predefined threshold.

7.4 Implementation challenges

The issues related to the implementation of this algorithm in a real HPAV device will be addressed in this section. They can be divided into two different aspects:

- *Computational complexity*. Evaluation of the complexity of the algorithm, checking if it can be executed in real time mode.
- *Standard modifications*. Required changes in the HPAV standard to implement the algorithm. This is an important consideration because if major changes are required the algorithm implementation could be unfeasible.

7.4.1 Computational complexity

To evaluate the computational complexity of the proposed cross-layer mechanism, a particular implementation will be chosen, demonstrating that it could be executed in real time in a embedded system. It is important to remark that embedded software development is out of the scope of this thesis. The proposed solution may not be the optimal one, but is a possible one, and it is enough to test the feasibility of the algorithm implementation.

During the AET time period, the CCo is waiting for alarms (step 1 of the procedure):

```
for each received($Alarm_i$) do
    $MAC_i \in C$
    $\Delta G_{crit}$ += $1/(W_i + 1)$
```

```
end for
```

The MAC address of the alarm's issuer is added into the C set and the accumulated gain obtained by reducing its windows size is calculated. Here, the complexity of the algorithm is mainly due to the arithmetic division. The most common algorithms to divide a couple of numbers in real microprocessors are the Newton-Raphson, Goldschmidt and SRT [Soderquist and Leeser, 1997]. The first two are in fact equivalents and have quadratic convergence (which means that the number of accurate digits in the estimation of quotient doubles at each iteration) and SRT exhibits only linear convergence. However, SRT allows to overlap the components of the division step. In addition, it is also possible to substitute multiplications by logical mask and shifting bits. The algorithm election is not easy since it is an architecture decision. An in depth study about the complexity of these algorithms can be found in [Oberman and Flynn, 1997]. Looking carefully table 2 of that reference, it can be inferred that, for a very cheap hardware (embedded systems are), a good approximation of the number of machine cycles needed for a division is 25. However, a real implementation of our design could assume that since the amount of values for W_i is small (from 5 up to 100), it could be feasible to pre-calculate all possible $1/(W_i - 1)$ and store them in ROM. In this case, the complexity of the division is reduced to the cost of a single memory access.

When the AET period has finished, it is time to classify the rest of the terminals according to their QoS:

```
for $i \leftarrow 1$ to $K - C$ do
  RequestFor$(C_i, SBW_i, 1\%)$
  if $1\% \mid SBW_i > 0.74C_i/K$ then
    $MAC_i \in B$
  else
    $MAC_i \in S$
    putInOrderedTable$(W_i)$
  end if
end for
```

The subroutine $putInOrderedTable(W_i)$ stores W_i in ascendant order, and also stores the values $1/(W_i - 1)$ and the accumulated gain of *safe* nodes. The table can be easily implemented using linked chains. In this case, the computational complexity is mainly due to the sorting algorithm. This complexity is well studied in [Knuth, 1998]. The easiest sorting algorithm consists of comparing the new value with the first one, next with the second one, and so forth until a location is found. If the location is not found, the new value goes to the last position. Therefore, in the worst case, the classification algorithm requires as many comparisons as the number of contending stations. Another good solution for sorting is the Binary Search, due to it presents a logarithmic convergence. Since the number of contending station in a PLC in-home network will be around ten, the first algorithm is extremely simple to implement and in our case, and it has not real complexity.

The next steps of the algorithm (steps 2 to 5) do not have any operator with a remark complexity:

```
for $i \leftarrow 1$ to 5 do
    for $j \leftarrow 1$ to $C$ do
        $W_i - -$
    end for
    for $m \leftarrow 1$ to sizeOf(OrderedTable) do
        if $\Delta G_{crit} >$ GetTableValue($\Delta G_{safe}$) then
            $W_m + +$
        end if
    end for
end for
for $i \leftarrow 1$ to $C \cup S$ do
    SendTo($W_i$)
end for
```

Hence, the proposed algorithm has a type P computational complexity (deterministic polynomial time). That is, if the number of contending stations is n, its execution time is $O(n^x)$, for some x. Assigning a weight to each type of operation, it is possible to calculate it. In the worst case (all stations generate an alarm), the first set of instructions is $O(n)$. The second set is $O(n^2)$ since although the function $PutInOrderedTable$ has linear complexity ($O(n)$), it is inside of a loop of size n. Finally, the last sets of instructions are serialized loops of size n (assuming always the worst case), so the complexity is $O(n)$. As a consequence, the overall algorithm has $O(n^2)$ complexity. In conclusion, from these results, there is not any reason why the proposed procedure can not be run in real-time mode within a PLC modem, since in our case the value of n will be small in most cases.

7.4.2 Standard modifications

As said in previous sections, the proposed cross-layer algorithm is performed completely at MAC layer. Hence, it is important to find out how the information required by the algorithm can be available in this layer in a real HPAV device. This information basically consists on the physical layer bitrate and the QoS requirements of the upper-layer services, and can be passed to the MAC layer using the following mechanisms already defined in HPAV standard:

- When the upper layer starts an application, the convergence layer of HPAV identifies the type of service and opens a connection in the MAC layer using the HPAV M1 interface. During the connection opening procedure, it is exchanged a parameter called CSPEC, which contains information related to the QoS parameters of the service. This parameter can be used to transmit the QoS limits required by the proposed cross-layer algorithm.

- The PHY layer interface has a function to launch a channel estimation procedure. Through this procedure, the parameters of this particular channel are calculated and returned to the MAC layer, which can use them to determine the physical bitrate.

On the other hand, as described in the protocol overview, when the CCo receives an alarm and the algorithm starts, it asks the involved nodes for some required parameters.

Then, the needed modification is only the adding of some new control messages to launch the alarms and to communicate this information to the CCo. However, this modification does not involve important changes in the MAC layer, so we consider that it can be applied without major compatibility issues.

7.5 Evaluation

For purposes of evaluation, a typical in-home scenario composed of seven HPAV stations is assumed. Two stations run TCP data transmissions, two other stations run a HDTV MPEG-2 video streaming service, two others run an MPEG-4 HDTV service, and the last one runs a VoIP service. The parameters to evaluate the QoS for these services are shown in Table 7.1. They are used to define the thresholds of the stations. TCP data transmission service has no QoS limits since it is a best-effort service, not generating any alarm.

Two different scenarios are evaluated. In the first one, a station suddenly comes to compete for the channel. Concretely, one of the stations running a TCP service is not present at the start of the simulation, appearing at second 100, causing a performance degradation and consequently the start of the proposed cross-layer mechanism. Figure 7.6 shows the instantaneous latency and jitter of the VoIP and the two MPEG-4 stations, respectively. The whole system starts with the reference algorithm. Then, at $t = 100s$, the joining of the station causes a QoS deterioration in the MPEG-4 services. After that, the system runs for 100 seconds without the cross-layer mechanism. The values of the evaluated parameters before solving the degradation can be observed in this interval. Then, at $t = 200$ s, the proposed algorithm is activated. After four iterations (approximately 40 seconds), a good solution for all the stations is achieved. Note that the two MPEG-4 stations are the *critical* nodes and the VoIP service is considered a *border* node. At $t = 300$ s, the TCP session finishes. Consequently, after 10 seconds without any packet over the lower threshold, the algorithm should restore the initial conditions. However, this event has been delayed to $t = 400$ s to better show the results.

In this point, it is interesting to evaluate how the end-user perceives these changes. To this end, the QoE can be a very useful metric. Assuming that the packets received with a latency or jitter over the QoS requirements are considered lost, the evolution of the packet losses can be seen in Figure 7.7. In this case, only the MPEG-4 services are represented since VoIP service does not lose any packet. As can be seen, after the arriving of the new station, the losses in the MPEG-4 services increase considerably, but they are reduced

Table 7.1: Service parameter limits for good QoS (from [Szigeti and Hattingh, 2005])

Service	Latency	Jitter	Estimated Bandwidth	Packet Loss Probability
VoIP	150 ms	10 ms	8 Kbps	1%
MPEG-4	150 ms	30 ms	5 Mbps	1%
MPEG-2	3 s	-	12 Mbps	1%

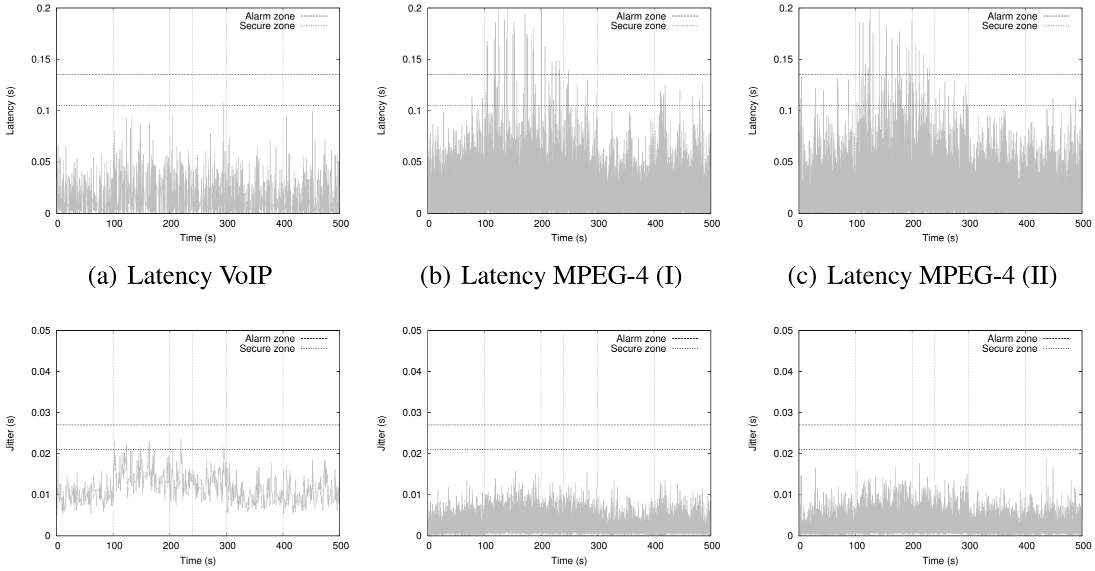

(a) Latency VoIP (b) Latency MPEG-4 (I) (c) Latency MPEG-4 (II)

(d) Jitter VoIP (e) Jitter MPEG-4 (I) (f) Jitter MPEG-4 (II)

Figure 7.6: Latency and jitter evolution for different stations of the evaluation scenario along with their corresponding thresholds. Vertical lines represent the changes in the network configuration indicated in Section 7.5.

when the algorithm is activated, disappearing after the algorithm execution.

The relation between these losses and the video PSNR is given in [Frnda et al., 2013] [Rozhon et al., 2014]:

$$PSNR = a + b \cdot Ln(X) \tag{7.17}$$

where X represent the packet loss in % and a, b are variable parameters which depend on the evaluated service ($a = 22.19$, $b = -2.29442$ for MPEG-4). As can be seen, this equation cannot evaluate PSNR when there are no packet losses. The PSNR evolution calculated using the previous expression is shown in Figure 7.8 (a). When losses are 0, the PSNR value is considered 40 dB, which is a typical value for standard MPEG-4 videos and enough to obtain a high reference QoE.

Table 7.2: MOS estimation from video PSNR for MPEG-4 services

PSNR (dB)	MOS
> 37	5 (Excellent)
$31 - 37$	4 (Good)
$25 - 31$	3 (Fair)
$20 - 25$	2 (Poor)
< 20	1 (Bad)

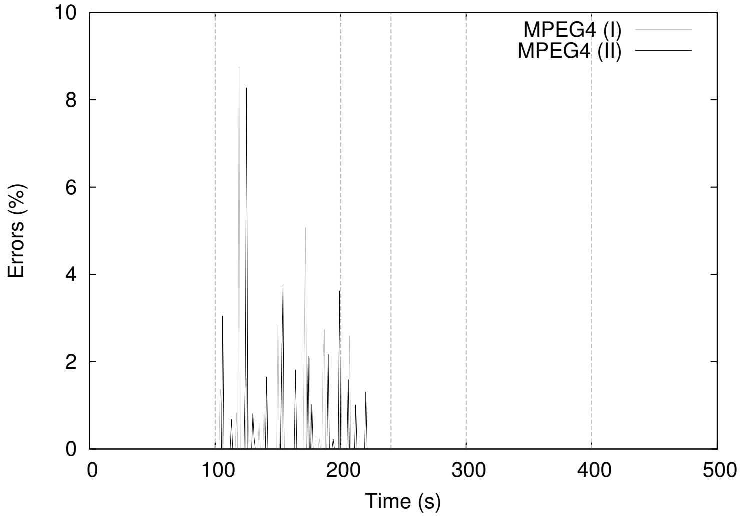

Figure 7.7: Packet losses percentage evolution for MPEG-4 stations

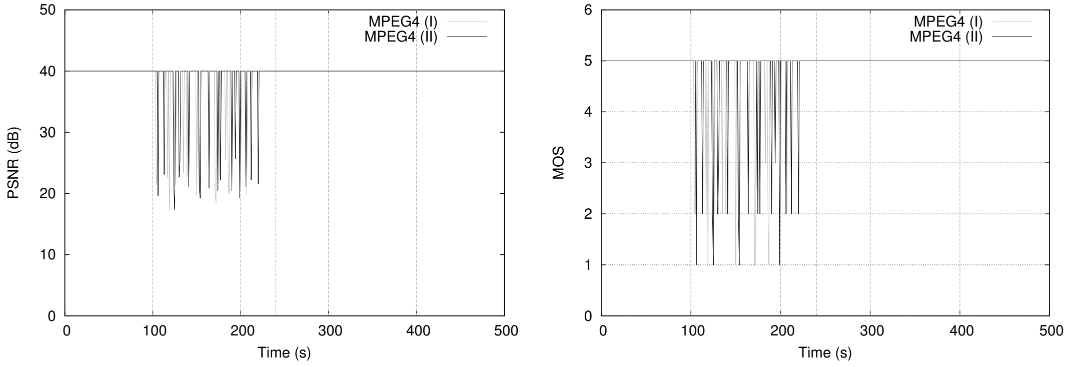

(a) Video PSNR

(b) MOS

Figure 7.8: PSNR and MOS for MPEG-4 services estimated from the packet losses

Finally, from [Gross et al., 2004] a relation between the PSNR and MOS (Mean Opinion Score) can be considered (see Table 7.2). MOS is one of the most extended methods to evaluate user QoE. By translating the previously obtained PSNR values to MOS Figure 7.8 (b) is obtained. As can be seen, the appearing of the new station in t=100s clearly degrades both the QoS and the QoE. Then, after the algorithm application, both terms are clearly improved.

The second scenario evaluates the performance of the proposed mechanism facing a channel capacity drop suffered by a node. This drop can be due to a noise increment or to an impedance mismatch caused for example by the connection/disconnection of a home appliance. In this case, it is evaluated how much channel degradation, in terms of physical bitrate, is able to tolerate the stations running the MPEG-4 services. We obtained that, without the proposed algorithm, these stations can tolerate a maximum channel degradation corresponding to a physical bitrate of 44 Mbps. However, with the proposed algorithm, the tolerance to the channel degradation increases. These stations run correctly the services with a physical bitrate of only 33 Mbps, that corresponds to an increase of the tolerated degradations of a 25%.

7.6 Publications

The work developed in this chapter has been partially published in the following references:

- P.J. Piñero, J. Malgosa, P. Manzanares, J.P. Muñoz, *Homeplug-AV CSMA/CA Cross-layer Extension for QoS Improvement of Multimedia Services*, IEEE Communications Letters, 2014

Chapter 8

Conclusions

Abstract- This chapter summarizes the main conclusions obtained during the realization of this thesis and outlines some issues which can be addressed in future related works.

8.1 Conclusions

As said in the beginning of this thesis, in-home networks are key to the adequate development of the Future Internet (also known as Internet of Things). One of the most important factors to ensure the pervasiveness of these infrastructures is the existence of adequate technologies that facilitate their installation and maintenance. Among the different alternatives present on the market nowadays, this work has been centered on PLC (PowerLine Communications), analyzing its main drawbacks and proposing, as far as is possible, solutions to them.

The first part of the thesis consists of a detailed evaluation of the HomePlug AV standard, which is the most popular PLC technology at present. This analysis comprises two steps: Real Measurements and Simulation. In the first part, real modems were used to evaluate the performance of the standard for unicast and multicast communications in different network configurations. The second part of this analysis consists of a vast set of simulations performed with the simulation tool that is presented in chapter 3. This tool includes a realistic PLC channel generator and considers the physical and the MAC layers defined in the standard. Hence, the performance of the HPAV MAC layer can be accomplished over realistic channel conditions. The proposed simulator has been employed to evaluate the performance of in-home networks as a function of the number of active stations. The throughput of each station and the overall network throughput, the delay, the jitter and the number of collisions per seconds have been obtained. The first main conclusion of this work is that the developed simulator can be used as a tool for in-home network planning. As an example, it has been used to planning high and standard definition TV services over the in-home network.

Other conclusion was the high influence of the PHY layer bitrate over the MAC layer performance. To our best knowledge this fact was not adequately studied in the PLC bibliography. In fact, the models of MAC layer published in the literature assume that the PHY transmission rate of all the pairs is equal to the maximum transmission rate allowed by the medium. At the end of chapter 4, it is presented an extension of one of the more accepted models of the HPAV CSMA/CA algorithm, which considers real physical capacities for the different stations in the network. This model was also validated using the simulator.

Furthermore, it was decided from the results that there were three areas in HPAV standard that could be improved: problems in unicast communications under congestion conditions, the performance of multicast communications and the implementation of cross-layer protocols to build a MAC layer aware of the particular characteristics of the PHY and upper-layer services. These problems are addressed in chapters 5, 6 and 7 respectively.

The first improved aspect is related to unicast communications. As can be extracted from the results presented in chapter 4, PLC technology presents some particularities that can significantly reduce the TCP protocol performance. To solve these problems, the use of Fountain codes was proposed. The characteristics of these codes make them ideal for PLC environments. Therefore, a protocol based on Fountain codes to achieve reliable data transmission over PLC networks was implemented. The results obtained in this experiments were positive, showing that the implemented protocols offered better performance than TCP protocol in raw data transmission.

In addition, the properties of the Fountain Codes also make them ideal to aggregate different communication flows into one flow with a better performance. This idea was very interesting for one of the main objectives of this thesis, the evolution of the HPAV CCo to an in-home network coordinator able to manage interfaces of different technologies. To this end, a linux driver that permits the aggregation of heterogeneous in-home interfaces was developed. This driver employs a bandwidth estimation procedure based on packet dispersion and uses Fountain codes to overcome the problems generated by variable-capacity technologies like PLC. It was evaluated by combining a PLC modem and an Ethernet interface, showing that the aggregated interface offered better performance than the other two interfaces when used separately.

The HPAV multicast problems are addressed in chapter 6. The developed simulator is firstly used to assess the performance of standard HPAV multicast communications. Since the standard HPAV transforms a IP multicast transmission into consecutive point-to-point transmissions, the attained bitrate decreases very rapidly as the number of users increases. Presented results show that this poor performance can be notably increased with the quite simple strategy of using a common tone map for all the different multicast clients. This technique has been traditionally discarded because of the poor performance it achieves in wireless scenarios. However, the correlation among the power line channels established in a given network makes it useful for in-home PLC networks. Moreover, another technique based in the aggregated multicast bitrate maximization is also proposed and evaluated. This technique, combined with Fountain codes, was found as a good solution for large multicast group sizes, like hotels or offices. Finally, the common tone map technique was also compared to the standard for a video steaming service delivery, offering much better results.

The use of cross-layer techniques to improve the HPAV MAC layer performance is evaluated in chapter 7. These techniques have been traditionally used in the TDMA service, but in this work, a cross-layer extension of the CSMA/CA algorithm is presented. It uses information from both the physical and the upper-layer services to adapt the contention window size of the different clients when there are QoS problems. The presented protocol has been evaluated in two in-home scenarios, where the appearance of a new station or a bitrate drop (due to a change in the noise conditions) may cause QoS problems in some nodes. In both cases, the presented cross-layer extension shows good results, clearly outperforming any previously presented extension of the HPAV CSMA/CA standard version.

8.2 Future work

The results obtained in this thesis point to several interesting directions for future work:

- *Algorithms implementation*. Since during this thesis we have collaborated with Broadcom corporation, it may be possible to implement some of the algorithms proposed in real devices. Concretely, the most interesting alternatives are Multicast techniques and the CSMA/CA cross-layer extension.
- *TDMA*. The simulation tool developed in this work only implements CSMA/CA service at MAC layer. Nowadays, however, the TDMA service is implemented in most commercial modems, being very useful to assure QoS of very restrictive applications. One obvious future work is the implementation of this service in the simulator. With it, some algorithms related to TDMA slot assignments can be developed.
- *In-home network coordinator*. The ultimate aim of this work is the design of a in-home network coordinator. This device should be able to manage interfaces of different technologies, assuring the end-to-end QoS. In the PLC interface, it would act as the CCo with all the features developed in this thesis. Some preliminary steps toward the design of this device have been taken in this thesis, but it is still a lot of work to do in this area.

Appendix A

HPAV Simulator Software Description

A.1 Introduction

In this appendix it is explained in more detail the software architecture of the HPAV simulator described in chapter 3. Basically, this simulator is divided into two parts: PHY and MAC layers. The former includes both the channel generator and the modulator module. It outputs the PHY layer bitrate for each pair of the stations of the network. On the other hand, the MAC layer module performs an event-driven simulation of the HPAV CSMA/CA protocol, also including all the functionality related to traffic generation.

A.2 PHY Layer

The PHY layer module has been developed under Matlab environment. It is mainly divided into two separated submodules: channel generator and OFDM modulator (information about its structure can be found in [PLC, 2014]). In order to use this module, a configuration file should be created. Through this file, some important parameters, like the frequency range, the number of points of the generated channel response (N), the impedance of the transmitter and the receiver, etc. are configured. In our case, the output of this module will be composed of N=2048 points in the frequency range from 0.1 to 37.5 MHz. An impedance of 50Ω were selected for both, the transmitter and the receiver. For the rest of parameters, the default values are chosen (see channel generator user-guide in [PLC, 2014]).

As described in chapter 3, two versions of channel generator submodule were employed in this thesis. The first one was able to simulate long-term variations in one station's channel. It is called through the following function:

[H,f,net,dist]=PLC_channel_generator_MAC(M)

As can be seen, the number of long-term variations (M) should be indicated as input. On the other hand, the outputs of the function are:

- *H (NxM)*. Complex frequency response of the generated channels.

- *f*. Frequency vector.
- *net*. Data structure that contains the network topology, including the selected impedance and the length of the wires.
- *dist*. Link distance between transmitter and receiver nodes.

As example, Figure 3.3 shows the result of generating a channel with $M = 4$ long-term variations. These results can be interpreted as the channel responses of a particular station when there are four changes in the network topology (caused for example by a home appliance connection/disconnection).

With the second version, the correlation existing among the channels established in a home scenario can be modeled. Up to n channels (for n different stations) inside the same *"home"* can be generated by using the following function:

[H,f,net,dist]=PLC_channel_generator_MAC(n)

The outputs of this function are similar to those obtained in the first channel generator version. The only difference is the *dist* variable, which in this case is a (1xn) vector, including the different distances obtained for the n channels. Figure 3.4(c) shows the result of generating $n = 4$ correlated channels, which can correspond to the channel responses observed by four different stations placed in the same home scenario.

Regarding the OFDM modulator submodule, it obtains the PHY layer bitrate of a station from its channel response and its noise. As said in chapter 3, three noise profiles have been defined: heavily, medium and weakly disturbed. To obtain this PHY bitrate the following function should be used:

[R,b] = simulador_OFDM_conform_envent(H,Noise,BER)

The inputs for this function are the channel response (H) of the evaluated channel, the noise profile (*"baj"*, *"med"* or *"alt"*) options and the BER required by the system, which in HPAV is 10^{-5}. The outputs are the PHY bitrate (R) and the bit loading algorithm (b), which is a vector containing the number of bits assigned for each HPAV carrier.

For example, to obtain a ten-clients scenario using the second version of the channel generator, the following pseudo-code can be used, where the noise profile is randomly selected for each channel:

```
$n\_stations = 10$
$config$
$[H, f, net, dist] = PLC\_channel\_generator\_MAC(n\_stations)$
for $i \leftarrow 1$ to $n\_stations$ do
  $n\_r = ceil(3 \cdot rand())$
  if $n\_r == 1$ then
    $[R, b] = simulador\_OFDM\_conform\_envent(H, baj, 10^{-5})$
  else if $n\_r == 2$ then
    $[R, b] = simulador\_OFDM\_conform\_envent(H, med, 10^{-5})$
  else
```

```
        $[R, b] = simulador\_OFDM\_conform\_envent(H, alt, 10^{-5})$
    end if
end for
```

A.3 MAC Layer

The MAC layer module is a C-based program which performs an event-driven simulation of the HPAV CSMA/CA. It takes as input the PHY bitrates of the different stations and the scenario description, and generates a detailed report for each of these stations with the evolution of the main parameters related to the service QoS.

The program structure overview can be seen in Figure A.1, where the different program modules and the interconnection between them are presented. The functionality associated to each of these modules is:

- *Events*. Event types definitions and event list management.
- *Buffer*. Generic buffer implementation.
- *Rand*. Random number generation. The supported distribution and the methods used to generate the random variables is described in Appendix B.
- *Frame_Generator*. Traffic generation module which contains models for the services most commonly found in a home network.
- *Station*. Functionality related to the HPAV stations, like the management of the data frames.
- *Sim_csma*. Auxiliar functions needed in the main program, like file initialization or CSMA/CA counters management.
- *HPAV_simulator*. Main program.

To launch a simulation, the main program should be called with the following input parameters:

HPAVSimulator –length SIM_TIME –file PHY_FILES –time TIME_FILE –n_sim NSIM

The meaning of these parameters is:

- *SIM_TIME*. Total simulation time.
- *PHY_FILE*. Text file containing the paths to the files containing the PHY bitrate of the different stations.
- *TIME_FILE*. Text file containing the limits of the different time regions if long-term variations in the channels are considered.

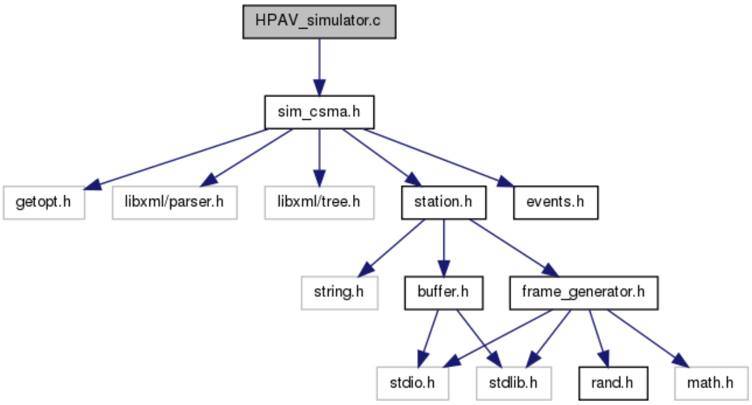

Figure A.1: MAC module software structure

- *NSIM*. Simulation number for batch executions.

In addition, if a point-to-point multicast simulation is performed, the number of multicast clients and the path to their PHY bitrate files should be introduced using the *–n_multicast* and *-file_multicast* parameters.

As output, the program generates a text file called "*(NSIM)_(NCLIENT).out*" for each station, which contains the station throughput, delay, latency and jitter as a function of the simulation time. The outputs for the different simulations can be analyzed with a script to obtain the desired statistic values.

Finally, the complete procedure to launch a simulation is composed of the following steps:

1. Generate the PHY bitrates for the stations and save them into different files. Generate the input text file with the paths to them.

2. Configure the Client.xml file with the desired scenario configuration. It should be indicated the number of stations and the service characteristics. The available services can be found in frame_generator.h file.

3. Create the TIME_FILE with the adequate time regions. Note that if no long-term variations in the channel are simulated, this file only contains a time region which limit should be equal or higher than the simulation time.

4. Launch the MAC layer simulator. This could be done using a launcher script with the following functionality:

```
sim_time=200
for $i \leftarrow 1$ to $n\_sim$ do
    HPAVSimulator –length $\$sim\_time$ –file $simulation\$i\_files.txt$
    –time $timeRegions.txt$ –n_sim $\$i$
    mv *.out ./Resultados
end for
./AnalyzeResults ./Resultados
```

Appendix B

Random Variate Generation

B.1 Introduction

Different traffic models for the most common services used in a domestic environment were presented in chapter 3. However, generating a random variable with a specific probability distribution sometimes is not a trivial task.

Random variable generators invariably use as their starting point a random number generator $U(0,1)$, which distribution is shown in eq. B.1. The objective is to transform one or more uniform random variables in an efficient way to obtain a variable with the desired distribution. The methods used in this work to generate the models are presented in this appendix.

$$F_U(u) = \begin{cases} 0 & \text{if } x \leq 0 \\ u & \text{if } 0 < x < 1 \\ 1 & \text{if } x \geq 1 \end{cases} \tag{B.1}$$

B.2 Exponential Exp(a)

The exponential distribution (whose distribution function is shown in eq. B.2) is used to generate the time separation between frames when the Poisson traffic model is used.

$$F(x) = \begin{cases} 1 - e^{\frac{-x}{a}} & \text{if } x \geq 0 \\ 0 & \text{if } x < 0 \end{cases} \tag{B.2}$$

The way of generating a exponentially distributed random variables is widely presented in related bibliography, since it is one of the classic examples for the well-known Inverse Transform technique [Cheng, 1998]. A random variable with this distribution can be obtained by solving $u = F(x)$ for x:

$$x = F^{-1}(u) = -a \cdot ln(1-u) \tag{B.3}$$

where u is the random number generator $U(0,1)$.

B.3 Normal N(μ,σ^2)

The well-known Normal distribution with mean μ and variance σ^2 has the following PDF:

$$f(x) = \frac{1}{\sqrt{2\pi\sigma^2}} \cdot e^{\left[-\frac{(x-\mu)^2}{2\sigma^2}\right]} \tag{B.4}$$

while it does not have a closed form for the CDF.

Since this is a very used distribution, there are lots of methods to generate Normally distributed variables. In this work, the polar version of the Box-Muller algorithm proposed in [Box and Muller, 1958] was selected, because it is very simple and fast:

```
while True do
  Generate $U_1, U_2$, $U(0,1)$ variates
  Let $V_1 = 2 \cdot U_1 - 1$, $V_2 = 2 \cdot U_2 - 1$, $W = {V_1}^2 + {V_2}^2$
  if $W < 1$ then
    Let $Y = \left(\frac{-2 \cdot ln(W)}{W}\right)^{1/2}$
    return $X_1 = \mu + \sigma \cdot V_1 \cdot Y$ and $X_2 = \mu + \sigma \cdot V_2 \cdot Y$
  end if
end while
```

As can be seen, each time the method is executed it returns a pair of independent Normal variates. If only one is needed, just X_1 can be returned.

B.4 Beta B(p,q)

Although the Beta distribution does not appear in the traffic models description, it is needed to generate Gamma distributed variates as it will be shown below. The PDF of this distribution is:

$$f(x) = \begin{cases} \frac{x^{p-1} \cdot (1-x)^{q-1}}{B(p,q)} & \text{if } 0 < x < 1 \\ 0 & \text{otherwise} \end{cases} \tag{B.5}$$

where B(p,q) is the Beta function and $p, q > 0$ are shape parameters:

$$B(p,q) = \int_0^1 z^{p-1} \cdot (1-z)^{q-1} \mathrm{d}z \tag{B.6}$$

There are different methods to generate Beta distributed variables depending on the values of the shape parameters. For the required case ($p, q < 1$), the following method proposed in [Cheng, 1998] was selected:

```
repeat
  Generate $U, V$, $U(0,1)$ variates
  Let $Y = U^{1/p}$, $Z = V^{1/q}$
until $Y + Z > 1$
return $X = \frac{Y}{Y+Z}$
```

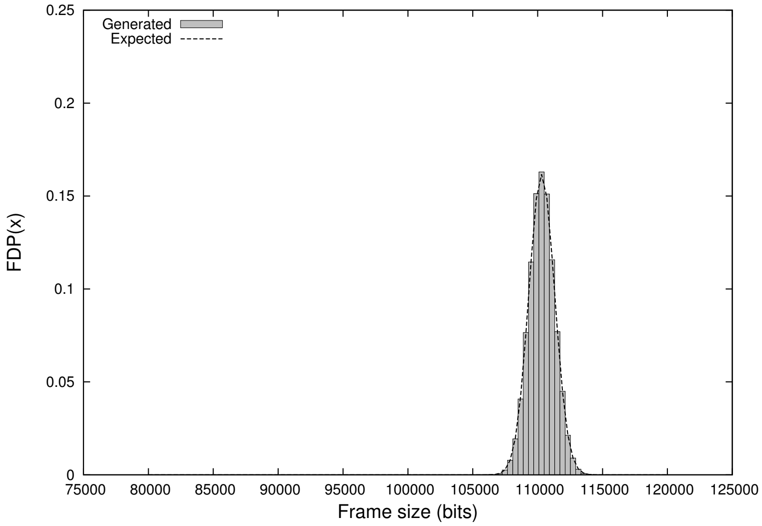

Figure B.1: Gamma variate generator evaluation

B.5 Gamma GAM(k,θ)

The Gamma distribution, whose PDF was previously presented in eq. 3.3, is used in this work to generate the size of the MPEG-4 service frames. The method selected to generate the Gamma variates was proposed in [Jain, 1991] and it makes use of the Beta distribution:

```
Let $gamma_1 = -\theta \cdot ln[\prod_{i=1}^{k} U(0,1)]$
Let $x = Beta(k - \lfloor k \rfloor, 1 - (k - \lfloor k \rfloor))$
Let $y = Exponential(1)$
Let $gamma_2 = \theta \cdot x \cdot y$
return $gamma_1 + gamma_2$
```

In this case, it is interesting to evaluate the results generated with this algorithm to validate Gamma and Beta variates generators. To this end, 50000 MPEG-4 type I frames were generated (θ = 9.013 and k = 12240). The obtained histogram is shown in Figure B.1, where it is compared to the expected result obtained with Matlab. In addition, according to [Montgomery and Runger, 2003], the mean and variance of a gamma distributed variable are $k \cdot \theta$ and $k \cdot \theta^2$ respectively. Hence, the expected values are $E[X]$ = 110319.12 $bits$ and $V[X]$ = 994306.23 $bits^2$. By analyzing the results, the values for the generated frames were $E[X]$ = 110318.23 and $V[X]$ = 998683.350 $bits^2$. Therefore, both Gamma and Beta random variate generators have been validated.

B.6 Extreme EXT(a,b)

The Extreme distribution is used in the network gaming traffic model. Its PDF was shown in eq. 3.4, while its CDF has the following form:

$$F(x) = e^{-e^{-\frac{x-a}{b}}} \tag{B.7}$$

To obtain an algorithm to generate random variates that follow this distribution, the inverse transform method can be applied. The result in this case is:

$$x = F^{-1}(u) = -b \cdot ln[-ln(U)] + a \tag{B.8}$$

B.7 Lognormal LN(θ, τ^2)

The sizes of the frames in the MPEG-2 service follows a Lognormal distribution, whose PDF was presented in eq. 3.2. To generate random variables which follow this distribution, it could be used the property that if Y is normally distributed $N(\mu, \sigma^2)$, then $X = e^Y$ is lognormally distributed $LN(\mu, \sigma^2)$. Hence, the following algorithm could be applied:

```
Let $Y = N(\mu, \sigma)$
return $X = e^Y$
```

Note that μ and σ^2 are related to the mean and variance of the lognormal, θ and τ^2 respectively, by the formulas:

$$\mu = ln\frac{\theta^2}{\sqrt{\theta^2 + \tau^2}} \tag{B.9}$$

$$\sigma^2 = ln\frac{\theta^2 + \tau^2}{\theta^2} \tag{B.10}$$

Therefore, μ and σ should be calculated before using the previously presented algorithm.

Appendix C

List of Acronyms

ADTDM	Advanced Dynamic Time Division Multiplexing
AFE	Analog Front End
AGC	Automatic Gain Control
AMBM	Aggregated Multicast Bitrate Maximization
AVLN	In-home AV Logical Network
AWGN	Additive White Gaussian Noise
BC	Backoff Counter
BER	Bit Error Rate
BPC	Backoff Procedure Counter
BPL	Broadband PLC
BSC	Backoff Stage Counter
BTC	Backoff Time Counter
CCo	Central Coordinator
CDF	Cumulative Distribution Function
CEA	Consumer Electronics Association
CIFS	Contention InterFrame Space
CL	Convergence Layer
CM	Connection Manager
CPE	Customer Premise Equipment

CSMA/CA	Carrier Sense Multiple Access/Collision Avoidance
CSPEC	Connection Specification
DC	Deferral Counter
DNL	Discovered Networks List
DSL	Discovered Stations List
DVB	Digital Video Broadcasting
EMC	Electromagnetic compatibility
FEC	Forward Error Correction
GCT	Greatest Common Tonemap
HE	Head End
HLE	Higher Layer Entity
HPAV	HomePlug Audio-Video
HPNA	Home Phoneline Networking Alliance
ILP	Integer Linear Programming
ISP	Inter-System Protocol
ITU	International Telecommunication Union
LDPC	Low Density Parity Check
LP	Linear Programming
MAC	Medium Access Control
MDC	Multiple Description Coding
MIMO	Multiple Input Multiple Output
MoCA	Multimedia over Coax Alliance
MPDU	MAC Protocol Data Unit
NB-PLC	Narrowband PLC
NEK	Network Encryption Key
NID	Network Identifier
OFDM	Orthogonal Frequency Division Multiplexing

PB	Physical Block
PDF	Probability Density Function
PHY	Physical
PLC	Power line communications
PLCP	Physical Layer Convergence Protocol
PLR	Packet Loss Ratio
PPDU	PHY Protocol Data Unit
PRS	Priority Resolution Slot
PSD	Power Spectral Density
QoS	Quality of Service
RIFS	Response InterFrame Space
RLC	Random Linear Codes
ROBO	Robust Modulation
RTT	Round Trip Time
SAP	Service Access Point
SME	Small-Medium Enterprises
SNR	Signal-To-Noise Ratio
TCC	Turbo Convolutional Coding
TCM	Trellis Coded Modulation
TDMA	Time Division Multiple Access
TM	Tone Map
UPA	Universal Powerline Alliance
VoIP	Voice Over IP

Bibliography

[IEE, 1997] (1997). IEEE standards for local and metropolitan area networks. *IEEE Std 802.3x-1997 and IEEE Std 802.3y-1997 (Supplement to ISO/IEC 8802-3: 1996; ANSI/IEEE Std 802.3, 1996 Edition)*, pages 0–324.

[Hpa, 2007] (2007). HomePlug AV standard. HomePlug power line alliance.

[bro, 2014] (2014). Broadcom power line communications solutions. http://www.broadcom.com/products/Broadband-Carrier-Access/Powerline-Communications-Solutions/. Accessed: March 2014.

[HDP, 2014] (2014). HD-PLC alliance. http://www.hd-plc.org/. Accessed: March, 2014.

[Hpn, 2014] (2014). Home phoneline networking alliance. http://www.homepna.org/. Accessed: March, 2014.

[Pro, 2014] (2014). Homeplug certified products. http://www.homeplug.org/certified_products/. Accessed: March, 2014.

[Hpa, 2014] (2014). HomePlug powerline alliance. http://www.homeplug.org/. Accessed: March, 2014.

[imp, 2014] (2014). Implementation of online codes. http://sourceforge.net/projects/onlinecodes/. Accessed: March, 2014.

[kti, 2014] (2014). Linux cross reference. source code of the header containing ktime. http://www.lxr.free-electrons.com/source/include/linux/ktime.h,. Accessed: March 2014.

[afp, 2014] (2014). Linux cross reference. source code of the linux raw socket family. http://lxr.free-electrons.com/source/net/packet/af-packet.c. Accessed: March 2014.

[bon, 2014] (2014). The linux foundation: Bonding. http://www.linuxfoundation.org/collaborate/workgroups/networking/bonding. Accessed: March, 2014.

[Moc, 2014] (2014). Multimedia over coaxial alliance. http://www.mocalliance.org/. Accessed: March, 2014.

[PLC, 2014] (2014). PLC working group of the university of malaga. http://www.plc.uma.es. Accessed: March, 2014.

[wir, 2014] (2014). Wireshark network protocol analyzer. http://www.wireshark.org/. Accessed: March, 2014.

[Afkhamie et al., 2005a] Afkhamie, K., Katar, S., Yonge, L., and Newman, R. (2005a). An overview of the upcoming HomePlug AV standard. In *Power Line Communications and Its Applications, 2005 International Symposium on*, pages 400–404.

[Afkhamie et al., 2005b] Afkhamie, K., Latchman, H., Yonge, L., Davidson, T., and Newman, R. (2005b). Joint optimization of transmit pulse shaping, guard interval length, and receiver side narrow-band interference mitigation in the HomePlug AV OFDM system. In *Signal Processing Advances in Wireless Communications, 2005 IEEE 6th Workshop on*, pages 996–1000.

[Atzori et al., 2010] Atzori, L., Iera, A., and Morabito, G. (2010). The Internet of Things: A survey. *Comput. Netw.*, 54(15):2787–2805.

[Bakanoglu et al., 2010] Bakanoglu, K., Mingquan, W., Hang, L., and Saurabh, M. (2010). Adaptive resource allocation in multicast OFDMA systems. In *Wireless Communications and Networking Conference (WCNC), 2010 IEEE*, pages 1–6.

[Berrou and Glavieux, 1996] Berrou, C. and Glavieux, A. (1996). Near optimum error correcting coding and decoding: Turbo-codes. *Communications, IEEE Transactions on*, 44(10):1261–1271.

[Box and Muller, 1958] Box, G. E. P. and Muller, M. E. (1958). A note on the generation of random normal deviates. *Annals of Mathematical Statistics*, 29:610–611.

[Canete et al., 2011] Canete, F., Cortes, J., Diez, L., and Entrambasaguas, J. (2011). A channel model proposal for indoor power line communications. *Communications Magazine, IEEE*, 49(12):166–174.

[Cheng, 1998] Cheng, R. (1998). Random variate generation. In Banks, J., editor, *Handbook of Simulation*, pages 139–172. Wiley.

[Chung et al., 2006] Chung, M. Y., Jung, M.-H., Lee, T.-J., and Lee, Y. (2006). Performance analysis of HomePlug 1.0 MAC with CSMA/CA. *Selected Areas in Communications, IEEE Journal on*, 24(7):1411–1420.

[Chung and Goldsmith, 2001] Chung, S. T. and Goldsmith, A. (2001). Degrees of freedom in adaptive modulation: A unified view. *IEEE Trans. Commun*, 49:1561–1571.

[Cortes et al., 2014] Cortes, J., Canete, F., Diez, L., and Torres, L. (2014). Oriented comparison of indoor plc channel models. *In preparation*.

[Färber, 2002] Färber, J. (2002). Network game traffic modelling. In *Proceedings of the 1st workshop on Network and system support for games*, pages 53–57.

[Ferreira et al., 2011] Ferreira, H., Lampe, L., Newbury, J., and Swart, T. (2011). *Power Line Communications: Theory and Applications for Narrowband and Broadband Communications over Power Lines*. Wiley.

[Francis et al., 2012] Francis, B., Narasimhan, V., Nayak, A., and Stojmenovic, I. (2012). Techniques for enhancing tcp performance in wireless networks. In *Distributed Computing Systems Workshops (ICDCSW), 2012 32nd International Conference on*, pages 222–230.

[Frnda et al., 2013] Frnda, J., Voznak, M., Rozhon, J., and Mehic, M. (2013). Prediction model of QoS for triple play services. In *Telecommunications Forum (TELFOR), 2013 21st*, pages 733–736.

[Goyal, 2001] Goyal, V. (2001). Multiple description coding: compression meets the network. *Signal Processing Magazine, IEEE*, 18(5):74–93.

[Gross et al., 2004] Gross, J., Klaue, J., Karl, H., and Wolisz, A. (2004). Cross-layer optimization of OFDM transmission systems for MPEG-4 video streaming. *Computer Communications*, 27:1044–1055.

[Harfoush et al., 2009] Harfoush, K., Bestavros, A., and Byers, J. (2009). Measuring capacity bandwidth of targeted path segments. *IEEE/ACM Trans. Netw.*, 17(1):80–92.

[Hassan H., 2005] Hassan H., Garcia J.M., B. O. (2005). Generic modeling of multimedia traffic sources. In *3rd International Working Conference on Performance Modelling and Evaluation of Heterogeneous Networks*.

[Jacobson, 1988] Jacobson, V. (1988). Congestion avoidance and control. *SIGCOMM Comput. Commun. Rev.*, 18(4):314–329.

[Jain, 1991] Jain, R. (1991). *Art of Computer Systems Performance Analysis Techniques For Experimental Design Measurements Simulation And Modeling*. John Wiley & Sons.

[Kim et al., 2007] Kim, J., Kwon, T., and Cho, D.-H. (2007). Resource allocation scheme for minimizing power consumption in OFDM multicast systems. *Communications Letters, IEEE*, 11(6):486–488.

[Kim et al., 2008] Kim, M.-S., Son, D.-M., Ko, Y.-B., and Kim, Y.-H. (2008). A simulation study of the PLC-MAC performance using Network Simulator-2. In *Power Line Communications and Its Applications, 2008. ISPLC 2008. IEEE International Symposium on*, pages 99–104.

[Knuth, 1998] Knuth, D. E. (1998). *The Art of Computer Programming, Volume 3: (2nd Ed.) Sorting and Searching*. Addison Wesley Longman Publishing Co., Inc., Redwood City, CA, USA.

[Koumaras et al., 2005] Koumaras, H., Skianis, C., Gardikis, G., and Kourtis, A. (2005). Analysis of H. 264 video encoded traffic. In *Proceedings of the 5th International Network Conference (INC2005)*, pages 441–448.

[Kriminger and Latchman, 2011] Kriminger, E. and Latchman, H. (2011). Markov chain model of homeplug CSMA MAC for determining optimal fixed contention window size. In *Power Line Communications and Its Applications (ISPLC), 2011 IEEE International Symposium on*, pages 399–404.

[Krunz and Hughes, 1995] Krunz, M. and Hughes, H. (1995). A traffic model for MPEG-Coded VBR streams. In *In Proc. of the ACM Sigmetrics/Performance Conference*, pages 47–55.

[Latchman et al., 2005] Latchman, H., Afkhamie, K., Katar, S., Mashburn, B., Newman, R., and Yonge, L. (2005). High speed multimedia home networking over powerline. *NCTA technical papers*, pages 9–22.

[Li and Liu, 2003] Li, B. and Liu, J. (2003). Multirate video multicast over the internet: an overview. *Network, IEEE*, 17(1):24–29.

[Liu et al., 2008] Liu, J., Chen, W., Cao, Z., and Letaief, K. (2008). Dynamic power and Sub-carrier allocation for OFDMA-based wireless multicast systems. In *Communications, 2008. ICC '08. IEEE International Conference on*, pages 2607–2611.

[Luby, 2002] Luby, M. (2002). LT codes. In *Proceedings of the 43rd Symposium on Foundations of Computer Science*, pages 271–280.

[Luby et al., 2007] Luby, M., Watson, M., Gasiba, T., and Stockhammer, T. (2007). High-quality video distribution using power line communication and aplication layer forward error correction. In *Power Line Communications and Its Applications, 2007. ISPLC '07. IEEE International Symposium on*, pages 431–436.

[MacKay, 2005] MacKay, D. J. C. (2005). Fountain codes. *Communications, IEE Proceedings*, 152(6):1062–1068.

[Maiga et al., 2010] Maiga, A., Baudais, J., and Helard, J. F. (2010). Subcarrier, bit and time slot allocation for multicast precoded OFDM systems. In *Communications (ICC), 2010 IEEE International Conference on*, pages 1–6.

[Maymounkov and Mazieres, 2003] Maymounkov, P. and Mazieres, D. (2003). Rateless codes and big downloads. In *Peer-to-Peer Systems II*, volume 2735 of *Lecture Notes in Computer Science*, pages 247–255.

[Miras, 2002] Miras, D. (2002). Network QoS Needs of Advanced Internet Applications: A Survey. Technical report.

[Montgomery and Runger, 2003] Montgomery, D. C. and Runger, G. C. (2003). *Applied Statistics and Probability for Engineers*. John Wiley and Sons.

[Montoro et al., 2011] Montoro, D., Malgosa, J., Piñero, P. J., Muñoz, J. P., and Manzanares, P. (2011). Accurate packet timestamping on linux platforms for precise capacity estimation - an implementation of a highly accurate timestamping system embedded in the linux kernel and its application to capacity estimation. In *International Conference on Software and Data Technologies (ICSOFT)*, pages 137–142.

[Muñoz et al., 2011] Muñoz, J., Piñero, P., Malgosa, J., Manzanares, P., and Sanchez, J. (2011). Rateless codes for reliable data transmission over HomePlug AV based in-home networks. In *Software and Data Technologies: 4th International Conference, ICSOFT 2009. Revised Selected Papers*, volume 50 of *Communications in Computer and Information Science*, pages 181–191. Springer Berlin Heidelberg.

[Oberman and Flynn, 1997] Oberman, S. F. and Flynn, M. J. (1997). Division algorithms and implementations. *IEEE transactions on computers*, 46(8):833–854.

[Papaioannou and Pavlidou, 2008] Papaioannou, A. and Pavlidou, F.-N. (2008). A cross-layer scheduling scheme for multimedia services over power line networks. In *Power Line Communications and Its Applications, 2008. ISPLC 2008. IEEE International Symposium on*, pages 58–63.

[Pinero et al., 2011a] Pinero, P., Cortes, J., Canete, F., Diez, L., Manzanares, P., and Malgosa, J. (2011a). A realistic HomePlug-AV simulator for in-home network services planning. In *Global Telecommunications Conference (GLOBECOM 2011), 2011 IEEE*, pages 1–5.

[Pinero et al., 2011b] Pinero, P., Malgosa, J., Manzanares, P., and Munoz, J. (2011b). Homeplug-AV CSMA/CA evaluation in a real in-building scenario. *Communications Letters, IEEE*, 15(6):683–685.

[Pinero et al., 2014] Pinero, P., Malgosa, J., Manzanares, P., and Munoz, J. (2014). Homeplug-AV CSMA/CA cross-layer extension for qos improvement of multimedia services. *Communications Letters, IEEE, Accepted for publication*.

[Piñero et al., 2014] Piñero, P., Cortés, J., Malgosa, J., Cañete, F., Manzanares, P., and Díez, L. (2014). Analysis and improvement of multicast communications in HomePlug AV-based in-home networks. *Computer Networks*, 62(0):89 – 100.

[Piñero et al., 2012] Piñero, P., Malgosa, J., Manzanares, P., and Muñoz, J. (2012). Evaluation of a new proposal for efficient multicast transmission in HomePlug AV based in-home networks. In *IT Revolutions*, volume 82 of *Lecture Notes of the Institute for Computer Sciences, Social Informatics and Telecommunications Engineering*, pages 58–70. Springer Berlin Heidelberg.

[Piñero et al., 2011] Piñero, P. J., Montoro, D., Malgosa, J., Manzanares, P., and Muñoz, J. P. (2011). Rateless codes for heterogeneous in-home interfaces aggregation. In *Power Line Communications and Its Applications (ISPLC), 2011 IEEE International Symposium on*, pages 243–248.

[Rozhon et al., 2014] Rozhon, J., Rezac, F., Slachta, J., and Voznak, M. (2014). Voice and image quality prediction in IP networks. *International Journal of Communication Networks and Information Security. Under Review*.

[Schulzrinne et al., 2003] Schulzrinne, H., Casner, S., Frederick, R., and Jacobson, V. (2003). RFC 3550: RTP: A Transport Protocol for Real-Time Applications. Technical report.

[Shokrollahi, 2006] Shokrollahi, A. (2006). Raptor codes. *Information Theory, IEEE Transactions on*, 52(6):2551–2567.

[Soderquist and Leeser, 1997] Soderquist, P. and Leeser, M. (1997). Division and square root: choosing the right implementation. *Micro, IEEE*, 17(4):56–66.

[Stockhammer et al., 2011] Stockhammer, T., Heiles, J., and Lüken, J. (2011). DVB-IPTV content download services–overview and use cases. *Multimedia Tools Appl.*, pages 533–555.

[Suh and Mo, 2008] Suh, C. and Mo, J. (2008). Resource allocation for multicast services in multicarrier wireless communications. *Wireless Communications, IEEE Transactions on*, 7(1):27–31.

[Szigeti and Hattingh, 2005] Szigeti, T. and Hattingh, C. (2005). *End-to-End QoS Network Design: Quality of Service in LANs, WANs, and VPNs*. Cisco Press.

[Wu et al., 2010] Wu, B., Shen, J., and Xiang, H. (2010). Resource allocation with minimum transmit power in multicast OFDM systems. *Systems Engineering and Electronics, Journal of*, 21(3):355–360.

[Yonge, 2013] Yonge, L. (2013). An overview of the HomePlug AV2 technology. *Journal of Electrical and Computer Engineering*, 2013.

[Yoon et al., 2008] Yoon, S.-G., Jeongkyun, Y., and Bahk, S. (2008). Adaptive contention window mechanism for enhancing throughput in HomePlug AV networks. In *Consumer Communications and Networking Conference, 2008. CCNC 2008. 5th IEEE*, pages 190–194.

[Zahariadis, 2003] Zahariadis, T. (2003). *Home Networking Technologies and Standards*. Artech House Inc.